

From the Institute of Physical and Theoretical Chemistry of the University of Regensburg

IN VITRO AND IN VIVO CHARACTERIZATION OF ALGINATE  
BASED ANISOTROPIC CAPILLARY HYDROGELS TO GUIDE  
DIRECTED AXON REGENERATION

**Doctoral Thesis**

To obtain the Academic Degree 'Doctor rerum naturalium'

(Dr. rer. nat.)

From the Faculty of Chemistry and Pharmacy

University of Regensburg



Presented by

Kiran Chandrakantrao Pawar

Born 15 June 1980 in Loha-Nanded, India

Regensburg, August 2010

This work was conducted in the Institute of Physical and Theoretical Chemistry and Department of Neurology in the University of Regensburg from April 2007 to August 2010 under supervision of Dr. Rainer Mueller and Prof. Dr. Norbert Weidner.

<b>Official registration:</b>	15/06/2010
<b>Defence:</b>	20/09/2010
<b>Ph.D. supervisor:</b>	PD Dr. Rainer Mueller
<b>Adjudicators:</b>	Prof. Dr. Norbert Weidner Prof. Dr. Armin Goepferich
<b>Chair:</b>	Prof. Dr. Werner Kunz

***Dedicated to my family***

# Contents

1 Introduction and goal of thesis.....	1
1.1 Principles of regenerative medicine.....	3
1.2 Biomaterials for regenerative medicine.....	5
1.3 Goals of the thesis.....	8
References.....	10
2 Fundamentals.....	13
2.1 Principles of regenerative medicine and tissue engineering.....	15
2.2 Nervous system.....	16
2.2.1 Central nervous system.....	18
2.2.2 Peripheral nervous system.....	19
2.3 Injury to the nervous system.....	19
2.4 Strategies to overcome failure of regeneration after nerve injury.....	20
2.5 Scaffold material to enhance nerve regeneration after injury.....	21
2.5.1 Hydrogels made from synthetic polymers.....	23
2.5.1.1 Poly(2-hydroxyethyl methacrylate) (pHEMA) and copolymers.....	24
2.5.1.2 Poly(2-hydroxypropyl methacrylamide) (pHPMA).....	25
2.5.1.3 Poly(ethylene glycol) (PEG).....	26
2.5.2 Hydrogels made from natural polymer.....	27
2.5.2.1 Agarose.....	28
2.5.2.2 Hyaluronan.....	30
2.5.2.3 Methylcellulose.....	31
2.5.2.4 Chitosan.....	32
2.5.2.5 Collagen.....	32
2.5.2.6 Matrigel.....	33
2.5.2.7 Fibrin.....	34

2.5.3 Hydrogels exhibiting anisotropic structure.....	35
2.5.3.1 Alignment of fibers.....	36
2.5.3.2 Oriented channel by molding/templating techniques.....	37
2.5.3.3 Oriented channels by freeze drying.....	38
2.5.4 Alginate based anisotropic capillary hydrogels.....	38
2.5.4.1 Preparation of alginate based anisotropic capillary hydrogels.....	40
2.5.4.2 Alginate capillary hydrogels for nerve regeneration.....	42
2.6 Relevance of in vitro assay with spinal cord injury.....	43
2.6.1 Dorsal root ganglia.....	43
2.6.2 Entorhinal cortex slice culture.....	44
2.6.3 Spinal cord slice culture.....	45
References.....	46
3 Materials and methods.....	57
3.1 Chemicals.....	59
3.1.1 Hydrogel preparation and characterisation.....	59
3.1.2 Dorsal root ganglion culture.....	59
3.1.3 Entorhinal cortex and spinal cord slice cultures.....	60
3.1.4 <i>In vivo</i> experiments.....	60
3.1.4.1 Anaesthetic.....	60
3.1.4.2 Perfusion and spinal cord tissue preparation.....	60
3.1.4.3 Animals.....	61
3.2 Methods.....	62
3.2.1 Preparation of alginate based capillary hydrogels.....	62
3.2.1.1 Characterisation of alginate hydrogels.....	63
3.2.2 In vitro model of regeneration: Isolation of dorsal root ganglia.....	66
3.2.2.1 Immunohistochemical analysis.....	67

3.2.3 In vitro models: Central nervous system slice culture model.....	69
3.2.3.1 Entorhinal-hippocampal slice culture.....	69
3.2.3.2 Spinal cord slice culture.....	69
3.2.3.3 Morphological analysis of <i>in vitro</i> slice cultures.....	69
3.2.4 Spinal cord injury <i>In vivo</i> model.....	70
3.2.4.1 Surgical procedure.....	70
3.2.4.2 Processing of spinal cord tissue.....	71
3.2.4.3 Nissl staining.....	71
3.2.4.4 Morphological analysis of spinal cord tissue.....	72
3.2.5 Statistical analysis.....	72
References.....	73
4 Results.....	75
4.1 Structure of alginate based capillary hydrogels.....	77
4.1.1 Ion exchange.....	79
4.1.2 Stabilisation of alginate based capillary hydrogels.....	79
4.1.3 Determination of gelatin constituent.....	81
4.2 Oriented outgrowth of DRG axons guided by anisotropic capillary hydrogels in vitro.....	82
4.2.1 Influence of capillary diameter and gelatin constituent on axonal outgrowth.....	83
4.2.2 Influence of capillary diameter and gelatin constituent on Schwann cell migration.....	86
4.3 Oriented outgrowth of entorhinal axons guided by anisotropic capillary hydrogels in vitro.....	88
4.3.1 Influence of capillary diameter and gelatin constituent on axonal outgrowth.....	89

4.3.2 Influence of capillary diameter and gelatin constituent on astrocyte migration.....	91
4.4 Oriented axonal outgrowth of spinal cord slice cultures into ACH.....	93
4.4.1 Influence of capillary diameter and gelatin constituent on axonal outgrowth from spinal cord slice culture.....	94
4.4.2 Influence of capillary diameter and gelatin constituent on astrocyte migration.....	97
4.5 anisotropic alginate-based gels enhance directed axon regrowth following spinal cord injury in vivo.....	98
4.5.1 Integration of alginate gels.....	99
4.5.2 Influence of capillary diameter and gelatin constituent on axonal outgrowth in vivo.....	100
References.....	103
5 Discussion and conclusion.....	105
5.1 Discussion.....	107
5.2 Conclusion.....	114
References.....	116
Appendix.....	121
Curriculum vitae.....	127
Acknowledgement.....	131

# **Chapter 1**

## **Introduction and Goal of Thesis**





## 1.1 Principles of regenerative medicine

Regenerative medicine is the process of creating living, functional tissue to repair or replace tissue or organ function lost due to damage, disease, age or hereditary defect. Regenerating damaged tissue or organs in the body can be achieved by stimulating the previously irreparable organs to heal on their own. This approach is envisioned for patients that require life saving organ implants which often are not available due to a deficit in appropriate donor organs. The vision of regenerative medicine is to grow various tissue or organs in the laboratory to implant them thereafter. There are several approaches within the concept of regenerative medicine which involve the use of stem cell therapy, biomaterial scaffolds, drug based strategies using biologically active molecules, and transplantation of *in vitro* grown organs or tissues commonly known as tissue engineering (Langer R *et al.* 1993). The organs or tissues regenerated by tissue engineering and regenerative medicine are used in breast reconstruction, angioplasty, blood vessel, heart valve, cornea, pancreas, liver, genitourinary tissue, bone, cartilage, tendon and ligament, periodontal and nerve regeneration.

The human body has a unique capacity to regenerate damaged tissue and aged cells. However after traumatic injury and severe disease the regenerative capacity of host tissue is often not sufficient to cope with the tissue damage. In the following, the most important examples of tissue engineering and regenerative medicine strategies are briefly summarized.

There is a significant need for breast reconstruction due to cancer. The current approach to reconstruct breast tissue includes reconstructive surgery utilizing autologous tissue flaps, or implants of synthetic materials such as silicone. The particular tissue engineering approach for breast reconstruction uses a combination of patients own cells with polymeric scaffolds (Kim BS *et al.* 1998). Within angioplasty, as a second example, endovascular stents were currently used to widen or re-open narrowed or occluded blood vessels, which typically result from atherosclerosis. Three basic types of stents have been designed: balloon-expandable stents, self-expanding stents and thermal-expanding stents (Mueller HS *et al.* 1998). Tissue engineering of blood vessel attempts to regrow cellular vessels, which involves seeding the lumen of an artificial graft made from natural biologic and /or synthetic materials with endothelial cells (Herring MB *et al.* 1987, Weinberg CB *et al.* 1986). Also the heart valve leaflet can be grown *in vitro* seeding fibroblasts and endothelial cells derived from human, bovine and ovine sources on biodegradable poly(glycolic acid) meshes (Zund G *et al.* 1997).

The development of optic material has a long history. In particular the cornea is an excellent candidate for application of tissue engineering strategies. In previous attempts glass and various polymer materials have been used and now the most commonly used materials are poly(methyl methacrylate) (PMMA) and synthetic or natural hydrogels. For soft contact lenses poly(2-hydroxyethyl methacrylate) (pHEMA) has been used extensively (Chirila TV *et al.* 1994). Due to donor shortage for human pancreases, the immediate alternative is to use nonhuman donor islets in case of pancreatic diseases like diabetes mellitus. In tissue engineering strategies insulin producing cells can be implanted after encapsulation in a matrix made of synthetic or biological polymers by which cell survival and functionality can be prolonged (Lanza RP *et al.* 1995). Also in case of liver diseases tissue engineering may provide a therapeutic concept by combining the physical architecture of a biomaterial scaffold with cellular components. Biodegradable polymers provide a surface for the adhesion of hepatocytes in a three dimensional structure, which is important for cell interaction and tissue specific gene expression. Their porous structure allows sufficient nutrient delivery, waste removal and gas exchange, and ingrowth of host tissue (Vacanti CA *et al.* 1994). In genitourinary tissue engineering one of the challenges is to expand a small number of genitourinary associated cells to a clinically useful cell mass. Tissue engineering has been applied experimentally for the reconstruction of several urologic tissues and organs, including bladder, ureter, urethra, kidney, testis, and genitalia. Scaffolds for engineering genitourinary tissues have been fabricated from naturally derived materials, synthetic polymers, and acellular tissue matrices (Atala A *et al.* 1993, Atala A *et al.* 2004).

Another challenge for regenerative medicine and tissue engineering strategies is their application in the damaged nervous system. After traumatic injury in the nervous system nerves become transected. After transection, the axon distal to the lesion becomes disconnected from its neuronal cell body and degenerates so called Wallerian degeneration. This occurs after nerve injury in both the central nervous system (CNS) and peripheral nervous system (PNS). Following spinal cord injury spinal cord parenchyma including glial and neuronal cells is lost. Long descending projection axons from the motorcortex (corticospinal tract) and subcortical regions, ascending sensory projections and projections spanning a shorter distance get transected more or less completely depending on the lesion severity. Ultimately a cystic lesion defect develops. The spinal cord lacks the intrinsic capacity to replace organotypic tissue, which, besides expression of growth inhibitory factors

and lack of growth promoting factors, represents the major factor contributing to the failure of (CNS) axons to regenerate (Tuszynski MH *et al.* 1999). Substantial progress in replacing the lesion defect and subsequently promoting axonal regeneration has been achieved through cell transplantation strategies. Specific primary cell populations replace lost spinal cord parenchyma and provide a growth permissive substrate for regenerating axons (Reier PJ *et al.* 2004). However, cell transplantation approaches either do not promote axon regeneration in a directed rostro-caudal fashion for proper reconnection of disrupted axon pathways with their target neurons located caudal to the spinal cord lesion site.

It is the aim of tissue engineering to substitute a damaged tissue, for example neural tissue, with a temporary scaffold guiding cells to reorganize the structure and the function of the tissue lost by trauma or disease. Such a temporary scaffold is thought to act as a mimic of the original extracellular matrix generating a physical environment exerting chemical and biological cues conducive for the cells, which are seeded within the scaffold or located in the boundary area of the residual tissue.

## **1.2 Biomaterials for regenerative medicine:**

It is difficult to define the term biomaterial still more widely working definitions of biomaterials are “A biomaterial is any material natural or synthetic, which comprises the entire or a fraction of living structure or it represents a biomedical device which performs, augments, or replaces a natural function.” as well as “A biomaterial is a nonviable material used in medical devices, so it is intended to interact with a biological system.” From clinical point of view biomaterials comprise a large spectrum of materials and devices developed and optimized for long term application such as permanent and non-degradable artificial joints as well as for short term application such as degradable soft hydrogels for cell and drug delivery or tissue engineering (Williams DF 1987, Park JB *et al* 1992).

Biocompatibility must account for a host response to a material, as well as the physiological effects of the environment on the material itself. Independent of the origin of materials they build up interface with the living tissues as soon as they are implanted into the body. This interface between the foreign, man-made, non-living material and living tissue defines its biocompatibility. Current material development needs to rely upon engineering or design approach considering the functional requirements, environmental conditions, and tissue regenerative processes at the interface between the living and the prosthetic material at molecular level. The ultimate goal of biomaterial research must be to replace lost organ or

tissue function without introducing detrimental side effects (Black J 1992).

Biomaterials used in the context of tissue engineering should act as mimic of the extracellular matrix (ECM). The dynamics of cell-ECM interactions contribute to cell migration, proliferation, differentiation and programmed cell death as well as modulation of the activities of cytokines and growth factors, and directly activating intracellular signaling all of which are important parameters to consider when preparing and using tissue analogs. The ECM is a complex insoluble polymer network structure containing as basic components collagens and other glycoproteins, hyaluronic acid, proteoglycans, glycosaminoglycans, and elastins. Moreover, ECM consists of soluble molecules such as growth factors, cytokines, matrix-degrading enzymes, and their inhibitors (Wessells NK *et al.* 1968). The distribution of these molecules is not fixed but varies to a certain extent from tissue to tissue and during development. Many studies showed the direct participation of the ECM in cell adhesion and migration in gastrulation, migration of neural crest cell, angiogenesis, and epithelial organ formation. Also cell proliferation, differentiation and maintenance of tissue specific gene expression is modulated by cell-ECM interaction (Erickson CA *et al.* 1993). From a colloid chemical point of view the ECM can be considered as a hydrogel, since the ECM of native tissues is composed of a variety of hydrophilic macromolecules, all of which are cross-linked to a three-dimensional network,.

In this context, artificial hydrogels made from hydrophilic polymers of natural or synthetic origin have received special attention for the application as temporary guiding structures in soft tissue regeneration, especially in spinal cord repair. The implantation of hydrogels into the injured spinal cord attempts to replace degenerated tissue. Furthermore, hydrogels can be combined with soluble factors such as specific receptor ligands and neurotrophic or growth factors, which induce cell repair mechanisms and provide a growth-permissive environment. The porous structure of the hydrogels allows the incorporation of assisting cells and provides room for the sprouting axons. Hydrogels exhibiting some kind of anisotropy are able to physically or biochemically direct the regrowing axons toward their distal targets (Petit-Zeman S 2001, Gosh K *et al.* 2007).

Biomaterials play an important role in regenerative medicine and tissue engineering as potential carrier systems for various drug molecules or cell types. The numerous biomaterials used in the majority of applications are biodegradable natural and synthetic polymers. Some of the natural polymers are polysaccharides and proteins which are mostly hydrophilic but

synthetic biodegradable polymers such as poly( $\alpha$ -hydroxy acids), poly(glycolic acid) (PGA), poly(lactic acid) (PLA), and poly (lactide-co-glycolide) (PLGA) are rather hydrophobic and often need modification to make them suitable for living cells. Most of the biomaterial scaffolds are designed to carry mechanical load and to exert appropriate degradation characteristics. Modification with additional functionalities for example to attract specific cell types by incorporation of natural ECM molecules like collagen or fibronectin is a possibility to make biomaterial scaffolds more suitable for the tissue designed to regenerate and therefore more biocompatible.

From a biological point of view, hydrogels are similar to soft tissues in their macroscopic structure and mechanical properties. By controlling the cross-link density, several parameters, such as pore size and elasticity, can be adjusted fitting the requirements of the tissue to be regenerated. Due to their hydrophilic properties, hydrogels exhibit low interfacial tensions allowing cells to migrate into the artificial structure, which makes them more advantageous over alternative scaffold materials (Nisbet DR *et al.* 2008, Nomura H *et al.* 2006).

Hydrogels have often been applied in strategies for peripheral nerve regeneration using so-called nerve guidance tubes or channels (Yannas IV *et al.* 2004). The gels were filled into the lumen confined by the semi-permeable membranes of the artificial conduit. Several types of hydrogel fillings, mostly components of the natural ECM, enhanced the regeneration capacity of this kind of biomaterial-based strategy in comparison to empty or fluid-filled conduits (Williams LR *et al.* 1987, Chen YS *et al.* 2000, Bailey SB *et al.* 1993).

In case of central nervous system cases of spinal cord injury are accompanied by cavity formation and, therefore, repair strategies will not only require neuronal survival and axonal growth but also reconnection across the cavity by means of a bridging graft. Hydrogels seem to be an ideal artificial substrate for bridging spinal lesions because they are advantageous for filling in small areas and their structural, mechanical, and biochemical properties are modifiable (Geller HM *et al.* 2002, Novikova LN *et al.* 2003). The perception that three-dimensional structures provide a better contact guidance for regenerating axons as compared to empty guidance tubes has led to an increase in the use of hydrogels and porous polymer scaffolds for nerve repair strategies. Biomaterial based approaches are surgical suture, use of nerve guidance channel, fibrin glue, poly(ethylene glycol) fusion. Tissue engineering approaches include delivery of neurotrophic factors, use of functionalized gels, seeding with Schwann cells and use of genetically engineered cells. The advantage of these types of

hydrogel tube fillings or scaffolds is that their mechanical and biodegradation properties can be adjusted more easily compared to gels derived from ECM proteins. Furthermore, some specialized sorts of hydrogels provide the opportunity to create anisotropic structures which are assumed to further enhance the regeneration capacity of tissue engineering based strategies. Alginate hydrogels are one example of these specialized hydrogels which under specific conditions form structures of highly oriented, parallelly aligned circular capillaries.

### **1.3 Goals of the thesis:**

This thesis is focused on the preparation and characterization of alginate based anisotropic capillary hydrogels (ACH) for nerve regeneration. We studied the effect of the capillary diameter and gelatin incorporation as an example of ECM modification on nerve regeneration *in vitro* and *in vivo*. For *in vitro* analysis we used central nervous system models as well as a peripheral nervous system model. In the peripheral nervous system model we assessed a dorsal root ganglion outgrowth assay while in the central nervous system models entorhinal cortex slice cultures and spinal cord slice cultures were applied. Furthermore we did the *in vivo* study we implanted the alginate based anisotropic capillary hydrogels into rat spinal cord lesions.

The first aim of this thesis was to prepare anisotropic capillary hydrogels with different capillary diameter. This goal was achieved by using different divalent metal ions for ionotropic gel formation. Capillary structure could be varied by controlling the parameters within the ion diffusion and complexation process leading to gels exhibiting a wide range of capillary diameters between 10 and 200  $\mu\text{m}$ . The capillary structures were stabilized by chemical crosslinking to decelerate the degradation period. The stability tests *in vitro* proved its stability over several weeks time period. Metal cations which were used to create the capillary structure were removed by an ion exchange process. To improve biocompatibility of ACH we started to incorporate gelatin (gACH) to modify the alginate hydrogels (pACH).

As a result from the DRG assay, the length of re-grown axons increased with increasing capillary diameter as well as after gelatin modification. The axon density showed also the same trend like axon length in that the axons grew in form of bundles within wider capillary unlike single axons in small capillary hydrogels. Also the Schwann cell density increased with increasing capillary diameter and after gelatin modification.

As the main results for CNS slice cultures axon density increased with increasing capillary

diameter and after gelatin modification of alginate based capillary hydrogels. The axons passed through the whole capillary distance of 300  $\mu\text{m}$  more often in wider capillaries than in gels of smaller capillary diameter. The astrocyte density in capillary hydrogels increased with increasing in capillary diameter and after gelatin modification. Therefore the migration of astrocytes into capillaries showed the same trend like the axon density.

A preliminary *in vivo* examination of implanting different capillary hydrogels into the rat spinal cord was achieved. The hydrogels with different capillary diameter were well integrated into the spinal cord lesion. Axon density increased with increasing capillary diameter and after gelatin modification of alginate based capillary hydrogels.



## References:

- Atala A. Tissue engineering for the replacement of organ function in the genitourinary system. *Am J Transplant* 2004;4 Suppl 6:58-73.
- Atala A, Freeman MR, Vacanti JP, Shepard J, and Retik AB. Implantation *in vivo* and retrieval of artificial structures consisting of rabbit and human urothelium and human bladder muscle. *J Urol* 1993;150:608-12.
- Bailey SB, Eichler ME, Villadiego A, Rich KM. The influence of fibronectin and laminin during Schwann cell migration and peripheral nerve regeneration through silicon chambers. *J Neurocytol* 1993;22:176-84.
- Black J. Biological performance of materials: fundamentals of biocompatibility, 2<sup>nd</sup> ed. New York: Marcel Dekker; 1992.
- Bellamkonda R, Aebischer P. Tissue engineering in the nervous system. *Biotech Bioeng* 1994;43:543-54.
- Chen YS, Hsieh CL, Tsai CC, Chen TH, Cheng WC, Hu CL, et al. Peripheral nerve regeneration using silicone rubber chambers filled with collagen, laminin and fibronectin. *Biomaterials* 2000;21:1541-7.
- Chirila TV. Modern artificial corneas; the use of porous polymers. *Trends Polym Sci* 1994;2: 296-300.
- Dörfler HD. Grenzflächen und kolloid-disperse Systeme: Physik und Chemie Berlin Germany: Springer, 2002.
- Erickson CA, Perris R. The role of cell-cell and cell-matrix interactions in the morphogenesis of the neural crest. *Dev Biol* 1993;159:60-74.
- Furnish EJ, Schmidt CE. Tissue engineering of the peripheral nervous system. In: Patrick Jr CW, Mikos AG, McIntire LV, editors. *Frontiers in tissue engineering*. New York, NY: Pergamon Press; 1998. p. 514-35.
- Geller HM, Fawcett JW. Building a bridge: engineering spinal cord repair. *Exp Neurol* 2002; 174:125-36.
- Ghosh K. and Ingber DE. Micromechanical control of cell and tissue development: Implications for tissue engineering. *Adv Drug Deliv Rev* 2007;59:1306-18.
- Herring MB, Gardner AL, and Glover JA. Single-staged technique for seeding vascular grafts with autogenous endothelium. *Surgery* 1987;84:498-502.
- Kim BS, and Mooney DJ. Development of biocompatible synthetic extracellular matrices for tissue engineering. *Trends Biotechnol* 1998;16:224-30.

Langer R. and Vacanti JP. Tissue engineering. *Science* 1993;260:920-6.

Lanza RP, and Chick WL. Encapsulated cell therapy. *Sci Am Sci Med* 1995;2:16.

Mueller-Huelsbeck S, Schwarzenberg H, Wesner F, Drost R, Gliher CC, and Heller M. Visualization of flow patterns from stents and stent-grafts in an *in vitro* flow-model. *Invest Radiol* 1998;33:762-70.

Nisbet DR, Crompton KE, Horne MK, Finkelstein DI, Forsythe JS. Neural tissue engineering of the CNS using hydrogels. *J Biomed Mater Res B* 2008;87:251-63.

Nomura H, Tator CH, Shoichet MS. Bioengineered strategies for spinal cord repair. *J Neurotrauma* 2006;23:496-507.

Novikova LN, Novikov LN, Kellerth JO. Biopolymers and biodegradable smart implants for tissue regeneration after spinal cord injury. *Curr Opin Neurol* 2003;16:711-5.

Park JB, Lakes RS. *Biomaterials: An introduction*, 2<sup>nd</sup> ed. New York: Plenum Press;1992.

Petit-Zeman S. Regenerative medicine. *Nat Biotechnol* 2001;19:201-6.

Reier PJ. Cellular transplantation strategies for spinal cord injury and translational neurobiology. *Neuro Rx* 2004;1:424-51.

Tuszynski MH, Kordower J. *CNS Regeneration*. San Diego: Academic Press;1999.

Vacanti CA, Vacanti JP, and Langer R. Tissue engineering using synthetic biodegradable polymers. In *polymers of biological and biomedical significance*. W. Shalaby, Am Chem Soc Washington DC: vol.540,pp.16-34;1994.

Valentini RF, Aebischer P, Winn SR, Galletti PM. Collagen- and laminin-containing gels impede peripheral nerve regeneration through semipermeable nerve guidance channels. *Exp Neurol* 1987;98:350-6.

Williams DF (Ed.) *Definitions in biomaterial: proceedings of a consensus conference of the European society for biomaterial*, Chester England. Amsterdam: Elsevier;1987.

Williams LR, Danielsen N, Muller H, Varon S. Exogenous matrix precursors promote functional nerve regeneration across a 15-mm gap within a silicone chamber in the rat. *J Comp Neurol* 1987;264:284-90.

Weinberg CB, Bell E. A blood vessel model constructed from collagen and cultured vascular cells. *Science* 1986;231:397-99.

Wessells NK, Cohen JH. Effect of collagenase on developing epithelia *in vitro*: Lung, ureteric bud, and pancreas. *Dev Biol* 1968;18:294-309.

Yannas IV, Hill BJ. Selection of biomaterials for peripheral nerve regeneration using data from the nerve chamber model. *Biomaterials* 2004;25:1593-600.

Zund G, Breuer CK, Shinoka T, Ma PX, Langer R, Mayer JE and Vacanti JP. The *in vitro* construction of a tissue engineered bioprosthetic heart valve. Eur J Cardiothorac Surg 1997;11:493-97.

# **Chapter 2**

## **Fundamentals**



## **2.1 Principles of regenerative medicine and tissue engineering**

Regenerative medicine is the process of creating living, functional tissue to repair or replace tissue or organ function lost due to age, disease, damage, or congenital defects. The main focus of regenerative medicine is to understand the regeneration processes occurring in nature and to re-establish and to apply this knowledge for developing new strategies for tissue regeneration in humans. This emerging field utilizes tools from research in human development, stem cell biology, genetics, material science, bioengineering, and tissue engineering. The human body has the capacity of regeneration during lifetime: skin and blood for example renovate continuously, however some organs or body parts like liver, bones, muscles, and blood vessels have limited capacity of self-renewal. After injury or degeneration, multicellular organisms try to re-establish homeostasis by two processes: The first process is to restore both physical and physiological integration of the injured organ by forming cellular matrix or a patch representing the process of scar formation. The second process is reiteration of the developmental processes created due to injury which is the process of regeneration. When organs or tissues are irreparably damaged they may be replaced with an artificial device or donor organ. Regenerative medicine also empowers scientists to grow tissues and organs in the laboratory and safely implant them when the body can not heal itself. Importantly regenerative medicine has the potential to solve the problem of the shortage of organs available for donation compared to the number of patients that require life saving organ transplantation. William Haseltine was not only among the first ones to invent the term “regenerative medicine” but also believes that regenerative medicine will arrive in four phases. The first phase is to stimulate the body’s own renovation mechanisms by the action of growth factors. The second is implanting tissues or organs grown outside the body. The third is rejuvenating old tissues, by resting cell’s biological clock. The final phase is science of nanotechnology and material science (Petit-Zeman S 2001, Geoffrey C *et al.* 2007).

Tissue engineering combines the principles of biology and engineering to the development of functional substitutes for damaged tissue. Tissue engineering can be used to restore, maintain, or enhance tissues or organs. In the future, engineered tissues could reduce the need for organ replacement. Three general strategies exist for treating diseased or injured tissues in patients. The first strategy is implantation of freshly isolated or cultured cells into the site of injury. Its limitation could be failure of the infused cells to maintain their function in the patient or

immunological rejection. The second strategy is implantation of tissue assembled *in vitro* from cells and scaffolds. The success of this approach is depending on appropriate signal molecules such as growth factors and development of methods to deliver these molecules to their targets. The third strategy is *in situ* tissue regeneration. A scaffold designed to mediate the healing and tissue regeneration process is implanted into the body in the site from which the tissue was lost. Unlike in the *ex vivo* tissue engineering technique cells cultured with scaffold for regeneration of the tissue outside of the body, and then implanted the engineered tissue into the defect. For strategies 2 and 3 biomaterial scaffolds are required which implanted directly into the injured tissue stimulate the body's own cells to promote local tissue repair. Impressive advances have been made in the fabrication of biocompatible and biodegradable scaffolds, cell seeding techniques, and implantation protocols. For clinical application, the scaffolds used must be not cytotoxic and should act as a template for 3D tissue growth as well as support for various tissue types like fibrous, vascular and organ specific cells. For scaffolds containing cells into the recipients injured tissue seeded and *in vitro* precultured, it is assumed that after implantation cells into the recipients injured tissue seeded cells proliferate and integrate into the host tissue bed. The scaffold will degrade, finally dissolve completely and leave a mature construct behind which is identical to the surrounding tissue. The most commonly used matrices have been formed from natural materials such as collagen or from synthetic polymers. (Langer R *et al.* 1993, Linda G *et al.* 2002).

## **2.2 Nervous system**

The nervous system is an organ system containing a network of specialized cells called neurons that coordinate the actions of an animal and transmit signals between different parts of its body. The nervous system is divided into two parts, the central nervous system (CNS) and the peripheral nervous system (PNS).

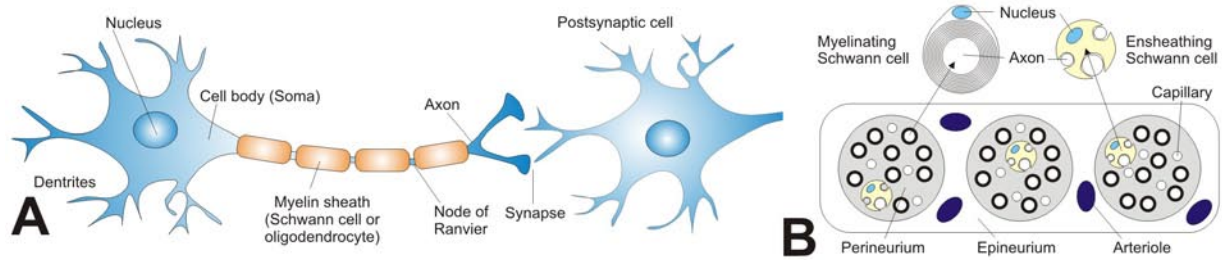


**Figure 2.1: (A) Schematic drawing of a neuron and its connection to a postsynaptic cell; (B) anatomy of the peripheral nerve.**

Neurons are the basic structural and functional elements of the nervous system and consist of a cell body, termed soma, and its extensions, the axons and dendrites. Neurons send signals to other cells as electrochemical waves travelling along thin fibers called axons, which cause chemicals called neurotransmitters to be released at junctions called synapses (Figure 2.1A). A cell that receives a synaptic signal may be excited, inhibited, or otherwise modulated. Sensory neurons are activated by physical stimuli impinging on them and send signals that inform the central nervous system of the state of the body and the external environment. Motor neurons situated either in the central nervous system or in peripheral ganglia connect the nervous system to muscles or other effector organs. Central neurons, which in vertebrates greatly outnumber the other cell types, make all of their input and output connections with other neurons. Neurons can be distinguished from other cells in a number of ways; their communication with other cells via synapses is the fundamental property, rapid transmission of electrical and chemical signals via membranes. Many types of neurons possess an axon, a protoplasmic protrusion that can extend to distant parts of the body and make thousands of synaptic contacts. In the body axons frequently travel in bundles called nerves. These nerves include sensory and motor neurons that transfer physical stimuli into neural signal and neural signal into activity respectively. The neurons receive their input from other neurons and give their output to other neurons.

Along with neurons, the nervous system contains supporting cells so called glia, which provide structural and metabolic support. In the central nervous system they are called astrocytes, oligodendrocytes, ependymal cells and radial glia and in the peripheral nervous system there are Schwann cells and satellite cells. In the human brain the functions of glial cells are to give support and provide nutrition, maintain homeostasis, form myelin and take part in transmission of signals in the nervous system. Many axons are covered with a myelin



sheath. It is a many layered coating which produces wraps around the axon and efficiently insulates it. At a so-called Node of Ranvier, the axonal membrane is uninsulated and can generate electrical activity (Figure 2.1A). In the central nervous system oligodendrocytes form the myelin sheath while in the peripheral nervous system Schwann cells execute this function (Figure 2.1B). Glial cells are non-neuronal and roughly equal the number of neurons. One of the most important functions of glial cells is to destroy pathogens and remove dead neurons. Important types of glial cells generate the so-called myelin sheath around axons which acts as electrical insulation and helps to transmit action potential more efficiently and rapidly.

### **2.2.1 Central nervous system (CNS)**

The central nervous system contains the brain, spinal cord, optic, olfactory and auditory systems. The central nervous system is enclosed within the dorsal cavity with the brain in the cranial cavity and the spinal cord in the spinal cavity. The brain is protected by the skull while the spinal cord is protected by the vertebrae.

The brain is a centralised mass of nerve tissue with a jelly-like substance and a typical mass of about 1.5 kg. The vertebrate brain is divided into three main parts referred as the hindbrain, midbrain, and forebrain. The hindbrain develops to form the cerebellum, pons, and medulla oblongata. The cerebellum coordinates complex muscular movements, the medulla oblongata controls functions like breathing and blood circulation. The midbrain controls many important functions such as eye movement, visual and auditory system. The substantia nigra is part of the midbrain and involved in the control of body movement. The substantia nigra contains a large number of dopaminergic neurons. The degeneration of these neurons leads into Parkinson's disease. The forebrain is the largest portion of the brain. It includes the cerebral hemispheres, the thalamus, hypothalamus and the limbic system (the corpus callosum, hippocampus, and amygdala). The function of the forebrain controls sensory and motor functions, temperature regulation, reproductive functions, eating and sleeping. The brain is surrounded by a connective tissue called the meninges. It is a membrane that separates the brain from the skull. This three layered covering is made up of the dura mater, the arachnoid mater, and the pia mater. The brain is bathed in a fluid called cerebrospinal fluid (CSF). This fluid protects the brain from mechanical shocks, is also important for metabolism and helps the brain to float.

The second very important part of the CNS is the spinal cord. The spinal cord is a long, thin, tubular bundle of nervous tissue that extends from the medulla of the brain. It is shorter than the spinal column; it ends between the first and second lumbar vertebrae. The length of the spinal cord is around 45 cm in male and 43 cm in female. The primary function of the spinal cord is the transmission of neural signals between the brain and the body. The cross section of the spinal cord shows a white matter tract in the peripheral region which contains myelinated axons of sensory and motor neurons. The inner part of the peripheral region is grey, butterfly-shaped and consists of motoneurons, neuroglia cells and unmyelinated axons. The spinal cord has three important functions: It carries motor information travelling down the spinal cord from the brain to body parts, it carries sensory information travelling up the spinal cord towards the brain and it serves as centre for coordinating certain reflexes.

### **2.2.2 Peripheral nervous system (PNS)**

The PNS is a collective term for the nervous system structures that do not lie within the CNS. The main function of the PNS is to connect the CNS to the limbs and organs. Unlike the central nervous system, the PNS is not protected by bone or by the blood-brain barrier, leaving it exposed to toxins and mechanical injuries. The large majority of the axon bundles called nerves are considered to belong to the PNS, even when the cell bodies of the neurons to which they belong reside within the brain or spinal cord. The peripheral nervous system consists of 12 cranial nerves and 31 pairs of spinal nerves. Ten out of 12 cranial nerves originate from the brain stem and mainly control the function of the anatomic structure of the head. The spinal nerves originate from the spinal cord and control the function of the rest of the body. The PNS is divided into a somatic and a visceral part. The somatic part consists of the nerves that innervate the skin, joints, and muscles. The cell bodies of somatic sensory neurons are located in the dorsal root ganglia of the spinal cord. The visceral part, also known as the autonomic nervous system, contains neurons that innervate the internal organs, blood vessels, and glands.

### **2.3 Injury to the nervous system**

The nervous system can be injured due to mechanical, chemical and thermal damage. It can also be affected because of inherited genetic abnormalities. Mechanical injuries can be take place due to traction and compression forces. Also injury can happen due to fracture or displacement of bone and ligament injuries. After nerve injury in the CNS, motor and/or

sensory function of lower extremities can be impaired which is called paraplegia. After complete transection at the cervical level the four limbs can be paralyzed, which is called tetraplegia. After nerve injury, axons get disrupted and damage of blood vessels and cell membranes occurs. The complete transection of a nerve is the most severe injury. After complete transection, the distal part of the nerve rapidly starts to degenerate because of the disturbed cytoskeleton and damaged cell membranes. Phagocyte cells such as macrophages (CNS) and Schwann cells (PNS) clear myelin and axonal debris of the detached nerve. After injury, the distal end generally increases major damage while the proximal end often is only minimally damaged and can further regenerate towards the distal end. Damaged axons form growth cones and are guided by soluble signal molecules like the nerve growth factor (NGF). In the PNS, Schwann cells proliferate and migrate forming cellular bridges which are called bands of Buengner and serve as a guiding structure for regenerating axons. Furthermore, Schwann cells are responsible for myelination of the regenerated axons (Furnish EJ *et al.* 1998, Tuszynski MH *et al.* 1999, Schmidt CE *et al.* 2003, Ide C 1996).

Spinal cord injury can be caused due to traffic accidents, sports accidents, and violence acts. After spinal cord injury, spinal cord parenchyma is lost which includes glial cells and neural cells. The spinal cord lacks the intrinsic capacity to replace organotypic tissue due to formation of growth inhibitory factors and a lack of growth promoting factors (Sofroniew MV *et al.* 1999, Aigner L *et al.* 1995). After CNS injury, astrocytes and inflammatory cells activate and proliferate to form a collagen type IV fibrous scar which will restrict further damage to the tissue, but it also inhibits axonal regrowth. Several weeks after injury, macrophages migrate and clear tissue debris at the lesion site, which results in fluid filled cysts surrounded by scar tissue (Klapka N *et al.* 2006, Schwab ME *et al.* 2002). Glial scar made up of myelin and cellular debris blocks the few neurons as well as astrocytes, oligodendrocytes, and microglia that survived from axotomy to reach their synaptic target (Fitch MT *et al.* 1999).

## **2.4 Strategies to overcome failure of regeneration after nerve injury**

Until few years back, it has been thought that the adult mammalian CNS cannot regenerate after injury or disease. In recent years after the discovery of stem cells existing in the adult rat brain, it was shown that the CNS has some capacity for self repair and regeneration. After spinal cord injury, there is currently no clinically effective therapy available to restore nerve

function. Within eight hours after trauma, treatment with high dose of anti-inflammatory agents such as minocycline showed some reduction in swelling and tissue loss as well as restored partial nerve function (Reynolds B *et al.* 1992, Bracken MB *et al.* 1990, Lee SM *et al.* 2003, Weidner N *et al.* 2002).

Depending on the extent of the injury, the clinical treatment for peripheral nerve injury consists of reconnecting the nerve by microsurgery with end-to-end suturing or introducing autologous nerve graft. Several cutaneous nerves can serve as an autologous nerve graft with a length up to 40 cm and a diameter of 2-3 mm. Current surgical techniques provide sensory and motor recovery of about 80%. The major disadvantages of the nerve graft concept are the need of several surgical interventions and the loss of function at the donor site (Midha R 2006).

## **2.5 Scaffold material to enhance nerve regeneration after injury**

Certain cellular, molecular and biomaterial based strategies have already become partially included into clinical therapies. These approaches are intended to bridge the gap between disrupted nerve ends or in spinal cord injury using some growth permitting substances which will help the axons to regenerate and reach their targets (Potter W *et al.* 2008, Bunge MB *et al.* 2001).

As an alternative to the autologous nerve graft for peripheral nerve regeneration, biomaterial-based strategies using artificial guidance channels have been introduced. The major benefit of artificial conduits is that no secondary injury is created to repair the primary one. The nerve guides serve to physically direct axons regrowing from the proximal nerve end. It has been shown that length, diameter, rigidity, permeability, degradability, interior surface, and luminal constitution are primary properties of the artificial guidance structure which are decisive for successful nerve regeneration. For this purpose, many natural-based and synthetic materials have been used for the manufacture of nerve conduits such as autologous veins and arteries, collagen, proteoglycans, glycosaminoglycans, polysaccharides, polyhydroxyacids, polyphosphoesters, polyorganophosphazenes, polytetrafluoroethylene, or silicone (Midha R 2006, Belkas JS *et al.* 2004, Ciardelli G *et al.* 2006, Hudson TW *et al.* 1999).

A major disadvantage of common guiding tubes is that their lumen does not have any sub-compartmentation. Sprouting axons, whose diameters are magnitudes smaller than those of

the artificial tubing, have no guiding structure available and, thus, cannot regenerate in a directed rostro-caudal fashion within the interior space of the tube. Therefore, aside from the aforementioned physical properties of nerve guidance tubes, the creation of internal substructures that mimic the microarchitecture of native neural tissue has to be taken into consideration in the manufacturing of an optimized nerve conduit. For this purpose, biologically active polymer networks have been incorporated into guiding tubes, thus mimicking the native extracellular matrix and substantially improving neural regeneration (Schmidt CE *et al.* 2003).

As a result of biomaterials research hydrogels have been proposed as potential candidates for various drug delivery and tissue engineering applications. From a colloid chemical point of view, hydrogels exhibit some very special properties in that they depict a transition state between liquids and solids whose structure is hard to define. They are elastic coherent colloid-disperse systems consisting of at least two components, a dispersed component and water as the dispersion medium. These two components are spread throughout the gel continuously penetrating each other. The dispersed component forms a three-dimensional network establishing hollow sites that are filled with the dispersion medium. Gels are heterogeneous on a microscopic scale but in most instances isotropic on a macroscopic scale. Common hydrogels often contain very little amounts of the gelling agents (commonly not more than 2%) and consist mainly of water. The macroscopic mechanical properties of a gel are determined by the concentration and the molecular weight of the polymer molecules as well as the number and the rigidity of the linkages between the polymers (Dorfler HD 2002).

The extracellular matrix (ECM) of the nervous tissue is composed of a variety of macromolecules belonging to the classes of proteins, proteoglycans, and glycosaminoglycans. These molecules can exert inhibitory as well as promoting effects on axon regeneration. The chondroitin sulfate proteoglycans such as aggrecan, versican, neurocan, and brevican have been identified as a major class of inhibitory molecules. The major promoter molecules of the neural ECM are the laminins, which have been found to play an important role in cell attachment and proliferation, axonal growth, and guidance in the developing nervous systems (Grimpe B *et al.* 2002). Exemplary studies of bridging gaps in the PNS by nerve guidance tubes showed that intraluminal fillings consisting of hydrogels of either laminin, collagen, or fibronectin improved axon regeneration as assessed by the increased number of myelinated axons within those conduits. Additionally, a greater influx of Schwann cells migrating into

the regeneration zone was observed (Chen YS *et al.* 2000, Bailey SB *et al.* 1993). Also fibrin and Matrigel, which is a solubilized basement membrane preparation extracted from mouse sarcoma cells and composed of a variety of extracellular matrix constituents and growth factors, were shown to increase the total axon density within nerve guidance tubes (Tsai EC *et al.* 2006). However, in some cases, and more pronounced for collagen, intraluminal hydrogel fillings have been shown to hinder nerve regeneration, whereby limited molecular diffusion and cellular migration were proposed to be responsible for the negative outcome. Based on these findings, the importance of identifying the proper concentration and physical conditions for the intraluminal gel has been strongly advocated (Valentini RF *et al.* 1987).

In the following subsection, the most interesting types of hydrogels which have been examined on their capability to be used in nerve regeneration therapies are summarised (Mueller R *et al.* 2009).

### **2.5.1. Hydrogels made from synthetic polymers**

The most commonly used hydrogels from synthetic polymers are based on poly(ethylene glycol) (PEG) and methacrylates. The hydrogels based on PEG are biodegradable (Livnat M *et al.* 2005, Wechsler S *et al.* 2008). The hydrogels based on methacrylate polymers get degraded slowly or are non-biodegradable (Mabilleau G *et al.* 2004). The water soluble methacrylate polymers i.e. poly(2-hydroxyethyl methacrylate) (pHEMA) and poly[N-(2-hydroxypropyl) metacrylamide] (pHPMA) are non toxic and biocompatible and have been used for repairing spinal cord injury. The chemical structure of the basic polymer components are shown in Figure 2.2.

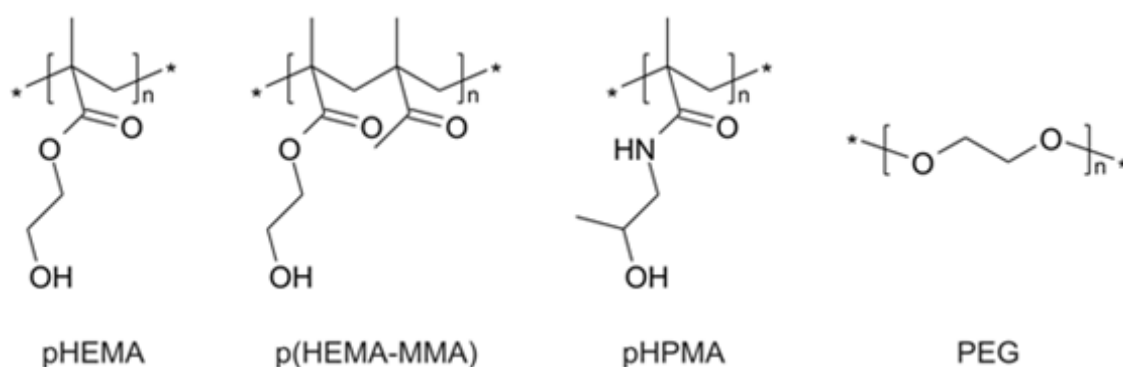


**Figure 2.2: Chemical structures of synthetic polymers used in hydrogel-based repair strategies for spinal cord injury.** [pHEMA = poly(2-hydroxyethyl methacrylate); p(HEMA-MMA) = poly(2-hydroxyethyl methacrylate-co-methyl methacrylate); pHPMA = poly[N-(2-hydroxypropyl) methacrylamide]; PEG = poly(ethylene glycol)].

### 2.5.1.1 Poly(2-hydroxyethyl methacrylate) (pHEMA) and copolymers

pHEMA is a linear hydrophilic macromolecule which can be cross-linked by using dimethacrylate monomers during polymerization. In spinal cord injury repair, pHEMA and its copolymer p(HEMA-MMA) have been used for manufacturing porous hydrogel scaffolds or hydrogel tubes. (Giannetti S *et al.* 2001, Dalton PD *et al.* 2002). The mechanical properties of hydrogel tubes made of p(HEMA-MMA) are similar to the ones of spinal cord. The morphology shows a gel like outer layer and a macroporous inner layer. These mechanical and morphological properties can be varied by changing the monomer composition and the surface chemistry of the molds used to prepare the tubes (Andac M *et al.* 2008).

The stability of pHEMA against degradation in physiological environment has been investigated in a number of studies. Macrophages increase their production of lysosomal enzymes and release large amounts of reactive oxygen species with micro beads of pHEMA. The macrophages degraded linear pHEMA faster than the pHEMA cross-linked by ethylene glycol dimethacrylate (Mabilleau G *et al.* 2004). The pHEMA gels when crosslinked with degradable crosslinker agents or such as dextran or disulfide containing molecules gets degraded by enzymes cleaved under reducing conditions (Andac M *et al.* 2008). The hydrogels which degrade in physiological environment are considered as non toxic (Montheard JP *et al.* 1992).

The effectiveness of the different kinds of pHEMA has been examined in different studies. Tubes of p(HEMA-MMA) were implanted into adult rat spinal cord (complete transected

model), leading to axon growth and tissue bridge formation into the tube. But the axons didn't cross the whole tube length and astroglia did not enter the tube but only surrounded the tube. Moreover, the locomotor function of the animals didn't improve compared to the control group (Tsai EC et al. 2004). In experiments where pHEMA sponges saturated with collagen were implanted into dorsal column transection sites of adult rats, it was shown that just few axons entered the implant covering only a short distance (Giannetti S *et al.* 2001). Impregnation of the pHEMA hydrogels with collagen type IV lead to Schwann cell survival in a large number. After implanting in lesioned rat optic tract, regenerating axons travelled a distance up to 450  $\mu\text{m}$  into the hydrogel (Plant GW *et al.* 1998).

To investigate the optimal intraluminal filling the following studies have been conducted. The hydrogel guiding channels of pHEMA were filled with different matrices such as Matrigel<sup>TM</sup>, collagen, fibrin, either alone or in combination with the neurotrophic factors neurotrophin-3 (NT-3), and fibroblast growth factor-1 (FGF-1), and implanted into complete thoracic spinal cord transection sites. After 8 weeks, the tubes filled with Matrigel<sup>TM</sup> showed a prominent effect on axonal ingrowth (neurofilament staining). The combination with neurotrophic factors did not increase axon ingrowth. Retrograde labeling of brainstem nuclei revealed that Matrigel<sup>TM</sup> filled tubes did not promote the regrowth of the respective axon projections. This suggests that the majority of neurofilament positive fibers within Matrigel<sup>TM</sup> filled hydrogels were not descending motor projections. In contrast to the observed structural changes, locomotor assessments using the BBB score revealed functional improvement only with fibrin or collagen filled tubes (Tsai EC et al. 2006).

#### **2.5.1.2. Poly(2-hydroxypropyl methacrylamide) (pHPMA)**

The second methacrylate polymer, which was found to be more biocompatible than the pHEMA, is pHPMA and has received great attention in the context of nerve regeneration. (Lesny P *et al.* 2002). In similarity to pHEMA, it can be synthesized in form of linear macromolecules or as a cross-linked polymer network. pHPMA has been commercialized under the brand NeuroGel<sup>TM</sup> and is a cross-linked, viscoelastic hydrogel which has similarity to neural tissue in mechanical properties. The hydrogel displays an open porous structure with interconnecting pores of about 10  $\mu\text{m}$  in size. It is considered as not degradable shown to be stable for up to 21 months in spinal cord defects (Woerly S *et al.* 1998).

The pHPMA hydrogel was implanted into acute and chronic spinal cord lesions in complete transection injuries at midthoracic level of adult rats and cats. After 5 months of implantation



modest axonal ingrowth (neurofilament immunoreactive axons, detection of biotinylated dextran amine (BDA)/horseradish peroxidase (HRP) labeled propriospinal projections) has been reported (Woerly S *et al.* 1999, 2001a, 2001b, 2004). However, the provided data do not give a clear picture of the extent of axon regeneration into the implants. The functional recovery was shown by improved locomotor function after the implantation of pHPMA hydrogel into the chronically transected rat spinal cord after 3 months post injury.

To enhance the tissue regeneration capacity of pHPMA hydrogels covalent immobilization of arginine-glycine-aspartic acid (RGD) cell adhesive oligopeptides to the pHPMA backbone was performed. After implanting into complete thoracic spinal cord transections, the RGD modified hydrogels formed a more effective tissue-bridge with axon ingrowth and remyelination than the unmodified pHPMA hydrogels were able to form (Woerly S *et al.* 2001c). In another experiment, pHPMA was covalently modified with the neurite promoting sequence isoleucine-lysine-valine-alanine-valine (IKVAV) and implanted into an adult rat frontal cortex lesion cavity. The provided data did not show superior effects of the modified pHPMA compared to the unmodified pHPMA (Cui FZ *et al.* 2003). Another alternative to modify the growth promoting effects of pHPMA was investigated by coupling amino group containing carbohydrates to the hydrogel backbone. This type of modification did not show any advantage compared to the other conditions, when implanted into fimbria-fornix lesion cavities in adult rats (Duconseille E *et al.* 1998). Furthermore it was tried to incorporate neurotrophic factor producing fibroblasts within pHPMA hydrogels in order to release brain derived neurotrophic factor (BDNF) and ciliary neurotrophic factor (CNTF). This strategy showed enhanced axon regrowth into the implant after optical tract lesion in postnatal day 18-21 rats. As a control pHPMA hydrogels filled with unmodified fibroblasts showed no axon ingrowth (Loh NK *et al.* 2001).

#### **2.5.1.3. Poly(ethylene glycol) (PEG)**

Poly(ethylene glycol) (PEG) is a linear hydrophilic polymer which has very low binding affinity to proteins and cells. PEG hydrogel can be prepared by cross-linking of terminal hydroxyl groups substituted by functional groups reactive for cross-linking. As one approach, lactic acid (LA) units were coupled to terminal hydroxyl groups, and then followed by modification with acrylic acid. An aqueous solution of these acrylated PLA-PEG-PLA macromers was transferred into a cross-linked hydrogel by applying photoinitiation (Burdick JA *et al.* 2006, Piantino J *et al.* 2006). By using the same procedure, neurotrophic factors

(BDNF, CNTF, NT-3) were successfully integrated within microspheres or films of the PEG hydrogel.

In CNS injury, hydrogels prepared from acrylate PLA-PEG-PLA macromers were assessed for delivery of trophic factors. PEG hydrogels loaded with CNTF showed enhanced neurite outgrowth in postnatal mouse retinal explants. The degradation components of this hydrogel did not display any cytotoxic effects (Burdick JA *et al.* 2006). In another study, hydrogels containing NT-3, which were photoinitiated *in situ* after incomplete thoracic spinal cord transections in adult rats, promoted more likely collateral sprouting rather than true axon regeneration of raphespinal and corticospinal axons. Modest recovery of locomotor function was reported. To which extent raphespinal and corticospinal axon sprouting contributed to the observed functional improvement remained unclear (Piantino J *et al.* 2006). In a very meticulous study, BDNF-containing poly(D,L-lactic acid) macroporous guidance scaffolds, prepared by a thermally induced polymer-solvent phase separation process generating longitudinally oriented macropores connected to each other by a network of micropores, were implanted into the completely transected rat spinal cord (Patist CM *et al.* 2004). Compared to hydrogels without BDNF, axon ingrowth and the survival of adjacent neurons in the rostral and caudal host spinal cord were increased. In none of the reported experiments astroglia was found to enter the scaffold. Locomotor function has not been improved. In a subsequent study identical poly(D,L-lactic acid) based hydrogels seeded with Schwann cells overexpressing a bifunctional neurotrophin with BDNF and NT-3 activity yielded similar results, which was attributed to the poor survival rate of seeded Schwann cells (Hurtado A *et al.* 2006).

In another study, three different peptides conjugated to PEG-hydrogels were compared. Photopolymerizable PEG hydrogels were conjugated with adhesion peptides derived from fibronectin (RGD) and laminin (IKVAV and tyrosine-isoleucine-glycine-serine-arginine, YIGSR) to enhance outgrowth of neurites. Neurite extension from PC12 cells was increased in RGD-conjugated hydrogels more than in IKVAV hydrogels, whereas YIGSR-conjugated hydrogels did not promote axon ingrowth (Gunn JW *et al.* 2005).

### **2.5.2. Hydrogels made from natural polymers**

Carbohydrates, glycosaminoglycans and proteins have been used to prepare hydrogels for spinal cord repair therapies. In Figure 2.3 the chemical structures of the carbohydrate-based polymers are depicted.

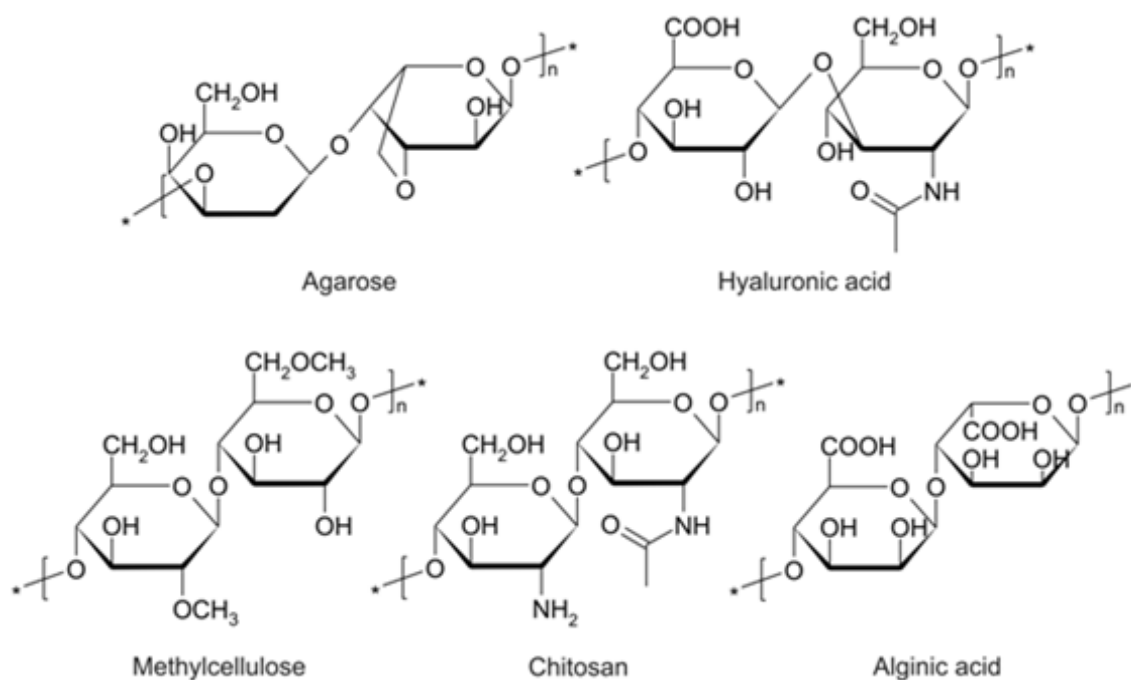


**Figure 2.3: Chemical structures of carbohydrate-based polymers used in hydrogel-based repair strategies for spinal cord injury.**

### 2.5.2.1 Agarose

Agarose is a linear polysaccharide, which is built up from alternating units of  $\beta$ -D-galactopyranose and  $\alpha$ -3,6-anhydro-L-galactopyranose coupled by 1,3- and 1,4-galactosidic linkages. It is extracted from the cell walls of red algae. Agarose can be gelled by cooling of heated aqueous solutions. Agarose is non-toxic, non degradable by microorganisms, compatible with many cell types and has therefore often been used as nutrient broth in microbiology or for cell culture applications. Eight months after being subcutaneously implanted into rats, agarose hydrogels are degraded very slowly compared to collagen implants. As the degrading species macrophages have been identified (Fernandez-Cassio S *et al.* 2007). Solutions with agarose concentrations between 0.5 and 2% form gels with isotropic pore structure. The pore radius ranges between 50 and 350  $\mu$ m and decreases with the increase in agarose concentration (Bellamkonda R *et al.* 1995a).

Agarose hydrogels have been optimized for nerve regeneration purposes regarding their physical properties and biocompatibility. An agarose gel of 1% showed to be optimal for neurite extension from chick dorsal root ganglia (DRG). Neurite extension was inversely correlated to the agarose gel stiffness (i.e. agarose concentration) with a 3-dimensional

growing rate of 20  $\mu\text{m/h}$  in 0.75% and 5  $\mu\text{m/h}$  in 2.0% hydrogels (Balgude AP *et al.* 2001). Neurite outgrowth in agarose gels significantly increased with incorporation of the polycationic polysaccharide chitosan compared to the outgrowth in pure agarose gels. In contrast neurite outgrowth significantly decreased with incorporation of the polyanionic polysaccharide alginate (Dillon GP *et al.* 1998). Agarose hydrogels were modified by immobilization of laminin and laminin-derived oligopeptide sequences to enhance nerve regeneration. Incorporation of laminin significantly enhanced neurite extension from three-dimensionally cultured embryonic chick DRG and PC12 cells compared to unmodified agarose gels (Yu X *et al.* 1999). Agarose backbone modified with cell adhesive YIGSR containing laminin oligopeptide sequence dramatically enhanced neurite extension *in vitro* from chick DRG. The data obtained from *in vivo* adult rat dorsal root transection showed similar findings (Borkenhagen M *et al.* 1998).

Agarose hydrogels modified with the outgrowth-promoting IKVAV-oligopeptide showed mixed results: in experiments with chick DRG, neurite extension was significantly reduced, but neurite extension from PC12 cells was enhanced compared to pure agarose gels. Agarose hydrogels loaded with nerve growth factors (NGF) stimulated neurite outgrowth from DRG and PC12 cells (Bellamkonda R *et al.* 1995b). *In situ* gelling agarose hydrogel has been developed for application in the spinal cord. These hydrogels were prepared from hydroxyethylated agarose which forms gels at a temperature of below 17°C and can be used to fill even irregular spinal cord defects. The hydrogel also served as carrier of BDNF and was reported to promote neurite outgrowth far beyond self-assembling agarose hydrogels, which were not combined with BDNF (Jain A *et al.* 2006).

Methylprednisolone has been shown to reduce acute inflammation initiated after spinal cord lesion. However, the current clinical practice for delivering systemic MP is inefficient. Therefore, methylprednisolone-loaded microspheres were embedded in agarose hydrogels with the intention to locally deliver the anti-inflammatory drug. These hydrogels, which were placed next to rat spinal cord contusion sites at thoracic level, significantly reduced the lesion volume compared to control animals (Chavatal SA *et al.* 2008). In summary, agarose gels promoted axonal regeneration in a lesioned spinal cord but some concerns remained due to the fact that the material is not biodegradable.

### 2.5.2.2 Hyaluronan

Hyaluronan (hyaluronic acid) is a linear high molecular-weight glycosaminoglycan. The polymer is composed of alternating units of  $\beta$ -D-glucuronic acid and N-acetyl- $\beta$ -D-glucosamine, which are coupled by 1,4- and 1,3-glycosidic linkages. Hyaluronic acid is an important extracellular constituent of all types of connective tissue, also in the CNS. Because of its high density of negative charges, the sodium salt of hyaluronic acid is water-soluble giving a highly viscous solution. Hyaluronan hydrogels can be prepared by reducing the charge density and hydrophilicity of the macromolecule by partial esterification of the carboxylic groups with hydrophobic alcohols, such as ethanol or benzyl alcohol (Campoccia D *et al.* 1998, Mori M *et al.* 2004).

After esterification of hyaluronic acid, its stability against biodegradation is enhanced significantly. The rate of biodegradation is correlated with the degree of esterification. Some types of benzylated hyaluronans were stable in aqueous solution up to several months. After subcutaneous implantation into rats, the ethylester of hyaluronic acid degraded completely within 20 days while benzylester remained stable after 90 days of subcutaneous implantation (Benedetti L *et al.* 1993). The degradation products of benzylated hyaluronan were found to be non-cytotoxic (Avitabile T *et al.* 2001). Hyaluronan hydrogels can be formed by an alternative method by modifying the polysaccharide backbone with methacrylate groups, which can be further cross-linked by light irradiation. These types of hydrogels have isotropic open porous structures with a pore size of about 50  $\mu\text{m}$  (Weng L *et al.* 2008, Baier LJ *et al.* 2003).

Hyaluronan-based hydrogels have been used in several studies for CNS repair strategies. After implantation of fetal “spinal cord nerve cells” embedded in a hyaluronic acid gel into the completely transected adult rat spinal cord in combination with low-power laser irradiation, axon regrowth and partial recovery of locomotor function have been described (Rochkind S *et al.* 2002). The influence of the hydrogel composition on structure, mechanical properties and neural cell adhesion was investigated with a composite consisting of hyaluronic acid and poly-D-lysine (PDL). The pore diameter of the hydrogel decreased from 230 to 90  $\mu\text{m}$  by increasing the PDL content from 10 to 25%. Hydrogels containing 25% PDL exhibit viscoelastic properties similar to brain tissue, promoted neurite elongation and attachment of neonatal rat cortical neurons *in vitro*. Composite hydrogels replaced the lesion defect after implanting into rat brain contusion site (Tian WM *et al.* 2005).

Hyaluronic acid hydrogels immobilized with cell adhesive oligopeptides enhanced axonal regeneration and tissue repair in the injured brain. Cell adhesive oligopeptides have been immobilized to hyaluronic acid hydrogels to enhance tissue repair and axonal regeneration in the injured brain. After implantation of RGD- or IKVAV-modified hyaluronic acid hydrogels into rat cortical lesions, angiogenesis was supported. (Cui FZ *et al.* 2006, Wei YT *et al.* 2007). Taken together, from the available literature it is not evident that hyaluronic acid based hydrogels promoted significant structural repair in the injured mammalian central nervous system.

### **2.5.2.3 Methylcellulose**

Cellulose is the most abundant biopolymer in nature as it is the major component of plant cell walls.  $\beta$ -D-Glucose units are coupled via 1,4-glycosidic linkages resulting in a conformational structure that strengthens intramolecular hydrogen bondings which enables fibril formation and impedes water solubility methylation parts of the hydroxyl groups results in the formation of methylcellulose which is soluble in cold water but forms gels at temperatures above 50°C. The gel forming temperature can be reduced changing physiological conditions in the formulation by varying the polymer and the salt concentration. Three dimensional network and physical cross-link formation between methylcellulose molecules occurs not only due to hydrophobic association of methoxyl substituents, but also due to the formation of inter-chain hydrogen bonds involving unsubstituted primary hydroxyl groups (Buslov DK *et al.* 2008). Typical gels exhibit an open porous structure with pore sizes between 30 and 50  $\mu$ m and an *in vitro* stability against artificial cerebrospinal fluid or serum-containing medium of longer than 15 days (Tate MC *et al.* 2001).

Methylcellulose based hydrogels are examined in regenerative medicine to tract CNS injuries. A hydrogel composed of methylcellulose and hyaluronic acid was used as drug delivery system. The composite hydrogel was injected intrathecally at spinal level after a compression spinal cord injury in adult rats. The composite hydrogel was identifiable in the subdural space after 4 weeks of survival, however no functional improvement could be observed after 4 weeks post injury. (locomotor function assessed with BBB) (Gupta D *et al.* 2006). Hydrogels loaded with recombinant human epidermal growth factor (rhEGF) injected into intrathecal space after compression of rat spinal cord injury showed identical effects (Shoichet MS *et al.* 2007).

#### **2.5.2.4 Chitosan**

Chitosan is a linear polymer composed of N-acetyl-D-glucosamine and D-glucosamine, which are linked via  $\beta$ -1,4-glycosidic linkages and distributed randomly. Chitin is the second most abundant polysaccharide in nature after cellulose. Chitosan is prepared from chitin by alkaline deacetylation. It is the major component of the exoskeletons of insects and crustaceans (Khor E *et al.* 2003). Strong deacetylation of chitin results in water soluble chitosan which can be converted into hydrogel by re-increasing the acetyl content to a minimum of 80% using acetic acid anhydride (Freier T *et al.* 2005, Vachoud L *et al.* 1997). Lyophilization of chitosan hydrogels revealed an open porous structure with pore sizes ranging between 100 and 500  $\mu$ m (Chow KS *et al.* 2001). The compressive strength of chitosan hydrogels increases with a decrease in the degree of acetylation. Chemical cross-linking and incorporation of a second polymer network penetrating the chitosan network enhances mechanical properties of chitosan based hydrogels (Zan L *et al.* 2006).

The neonatal Schwann cells (mixed with fibroblast) and PC12 cells were readily attached to chitosan fibers or membranes (Yuan Y *et al.* 2004, Crompton KE *et al.* 2007). Chitosan polymers show excellent cell adhesion properties, the cationic nature of the chitosan polymer is considered to be responsible for this. Chitosan polymers lead to a significantly enhanced outgrowth of chick DRG neurites and better cell adhesion compared to chitin films, which shows that the nerve cell affinity depends on the amino content in the polysaccharide (Freier T *et al.* 2005). Immobilization of poly-D-lysine (PDL) or laminin adsorption improved the bioactivity of chitosan hydrogels for neural tissue engineering leading to an enhanced adhesion of fetal mouse derived cortical neurons, viability and neurite outgrowth (Gong HP *et al.* 2000, Yu LM *et al.* 2007). Chitosan hydrogels cross-linked with methacrylate were covalently immobilized with laminin-derived oligopeptides. Both oligopeptides, IKVAV and YIGSR, significantly enhanced rat superior cervical ganglion derived neuronal cell attachment. Neurite elongation from these neurons was also increased in oligopeptide containing chitosan hydrogels. Best results were obtained after both oligopeptides had been immobilized in equal amounts (Zielinski BA *et al.* 1994).

#### **2.5.2.5 Collagen**

Collagen is an important structural protein in the extracellular matrix of mammals. At present 28 different types of collagen molecules are known in humans. It builds up networks and fibers supporting cells and tissues with a physical scaffold and important biochemical cues.

For tissue engineering applications and axonal regeneration in the CNS especially type-I collagen was examined. Collagen gels are formed under defined pH and salt conditions at high temperature using a solution of acid soluble collagen molecules in a self assembling process, which is called reconstitution. For most biomedical applications, collagen gels and scaffolds are cross-linked chemically to decelerate the degradation in the physiological environment. The mechanical properties of the hydrogels are improved after cross-linking (Raub CB *et al.* 2006).

Collagen hydrogels are used to fill lesion defects after spinal cord contusion with following transection in adult rats. Promising results have been observed in that axon grew out into the collagen matrix (de la Torre JC *et al.* 1984). These hydrogels became degraded very quickly (Marchand R *et al.* 1990), but the degradation process could be decelerated by chemical cross-linking of the collagen hydrogel with carbodiimide or by its co-precipitation with chondroitin-6-sulfate. Such modified hydrogels maintained their stability up to 6 months (Marchand R *et al.* 1993). A collagen guidance tube containing a collagen-chondroitin-6-sulfate hydrogel implanted into a 5 mm gap created in the injured midthoracic rat spinal cord was shown to promote the ingrowth of myelinated axons (Spilkar MH *et al.* 1997)). Collagen solution underwent self assembly *in situ* when injected into the mid-thoracic rat spinal cord lesion site. The advantage of this method was shown in another experiment in which the *in situ* self-assembled hydrogel allowed ingrowth of specifically labeled corticospinal axons dissimilar to the pre-assembled collagen hydrogel. Microglial and astrocyte cells were observed in the self-assembling hydrogel (Joosten EA *et al.* 1995). The ingrowth of corticospinal axons was improved after incorporation of neurotrophin-3 into the collagen hydrogel (Houweling DA *et al.* 1998). In another study, a collagen gel was used to prepare a gene-activated matrix and evaluated for the expression of thymidine kinase reporter gene in brain cortex and DRG after implantation into a dorsal column lesion. The encoding gene was detectable in the collagen gel and DRG up to seven weeks after injury. Respective mRNA was found in a variety of cells invading the matrix as well as in DRG neurons (Gonzalez AM *et al.* 2006).

#### **2.5.2.6 Matrigel**

Matrigel<sup>TM</sup> is composed of a variety of extracellular matrix constituents and growth factors. It is a solubilized basement membrane preparation extracted from mouse sarcoma cells. Its major component is laminin, followed by collagen type IV, entactin, heparin sulfate and



several growth factors all of which are effective for attachment and differentiation of many cell types (Kleinmann HK *et al.* 1986). Matrigel has been identified as an excellent cell carrier for Schwann cells, olfactory ensheathing cells and mesenchymal stem cells and it significantly improves neurite outgrowth from embryonic rat DRG. The basement membrane solution is transformed into a hydrogel by temperature increase and can be used as a suitable substrate for cell culture (Reed J *et al.* 2009). A biocompatibility study of Matrigel with human fetal neural stem cells showed poor capacity for viability and differentiation capacity of stem cells in contact with different concentrations of Matrigel were reduced compared to cells cultured as neurospheres (Thonhoff JR *et al.* 2008). Guidance channels made of polyacrylonitrile-poly(vinyl chloride) were filled with Matrigel and loaded with Schwann cells. This construct was implanted into rat spinal cord lesions and thought to act as an effective bridge between the two cord stumps. Many myelinated and unmyelinated axons were found within the guidance channels and few axons were able to cross the graft completely (Xu Xm *et al.* 1999). Infusing the Schwann cell seeded Matrigel matrix with BDNF and NT-3 further improved the axon ingrowth (Bamber NI *et al.* 2001).

#### **2.5.2.7 Fibrin**

Fibrin is a fibrillar protein which is mainly involved in the blood clotting process. In the presence of thrombin and calcium ions fibrinogen coagulates to form fibrils and meshes which results in a plug or clot at a wound site. Using artificial nerve guidance tubes to enhance PNS regeneration processes, it was found that fibrin plays a major role in that fibrin formed a matrix bridge inside a saline filled guidance tube after insertion into rat sciatic nerve defect. This matrix bridge connected both nerve stumps and supported Schwann cell adhesion and guided the axon growth (Williams LR *et al.* 1983).

In other experiments it was shown that neurite outgrowth was promoted from chick DRG on isotropic fibrin hydrogels, but it was also observed that neurite extension was accompanied by fibrin hydrogel degradation. The cells of the DRG contributed to hydrogel fibrinolysis directly by secretion of plasmin or plasmin activators (Dubey N *et al.* 2001). In another study rapid degradation and less stability of fibrin hydrogels was evident during neurite outgrowth from chick DRG (Horn EM *et al.* 2007).

To improve fibrin hydrogel properties the fibrin backbone was modified with linear or cyclic RGD peptides resulting in a concentration dependent influence on neurite outgrowth from DRG. The neurite extension was maximal in the intermediate adhesion site density compared

to the condition of high density of RGD concentration which inhibited neurite outgrowth (Schense JC *et al.* 2000).

Another study could show that the fibrin hydrogels enhanced neurite outgrowth from DRG after the incorporation of heparin binding peptides derived from antithrombin III, neural cell adhesion molecule and platelet factor-4 (Sakiyama SE *et al.* 1999). Fibrin was also covalently bound to heparin which acted as a substrate to which NT-3 can bind by non-covalent interactions. The modified fibrin hydrogel displayed higher efficacy in stimulating neurite outgrowth from chick DRG compared to unmodified gels (Taylor SJ *et al.* 2004). Fibrin hydrogels seeded with Schwann cells and equipped with adenoviral vectors encoding BDNF and NT-3 were reported to have a positive effect on axon regeneration (Taylor SJ *et al.* 2006).

### **2.5.3. Hydrogels exhibiting anisotropic structures**

All of these scaffolds and hydrogel substrates presented in the previous sections have good biological properties promoting axonal outgrowth *in vitro* and *in vivo*. However, in the various three-dimensional preparations in which they have been used so far, they are commonly characterized by a more or less amorphous and isotropic three-dimensional structure, which does not permit longitudinally directed regrowth of individual axons. This drawback is one of the main reasons that nerve regeneration over gaps larger than 10-15 mm is commonly very poor.

Therefore, implant materials with anisotropic features such as an array of parallel aligned cylindrical channels, fibers, or gradients of biochemical factors should be straightforward to guide axons regenerating through an injury site and enhance recovery of the injured nervous system. Hollow, water-filled capillaries within a hydrogel would act as guidance channels for axon growth while the polymer matrix of the hydrogel could be loaded with permissive materials or cells to facilitate this process (Friedman JA *et al.* 2002).

**Table 2.1: Features of anisotropically structured hydrogels.**

Anisotropic feature	Technique	Material	Size of structure
Filaments	Unknown	Collagen	20 $\mu\text{m}$
Fibrils	Magnetic alignment	Fibrin	150-500 nm
Channels	Fiber templating	pHEMA	100-400 $\mu\text{m}$
Channels	Needle templating	Chitosan	150-400 $\mu\text{m}$
Channels	Fiber templating	Agarose	200 $\mu\text{m}$
Channels	Freeze-drying	Agarose	70-190 $\mu\text{m}$
Channels	Ion diffusion	Alginate	25 $\mu\text{m}$
Aligned RGDS peptide	Laser irradiation	Agarose	150-170 $\mu\text{m}$

### 2.5.3.1 Alignment of fibers

Anisotropic scaffolds or hydrogels obtained by alignment of fibers of natural or synthetic polymers can serve as bridge for axonal regrowth in the injured nervous system. Collagen fibers of 20  $\mu\text{m}$  in diameter have been prepared from bovine skin by chemical and enzymatic treatment and stabilized by crosslinking with epoxy compounds. These bundles of collagen filaments were inserted into a 5-mm long thoracic spinal cord contusion injury site in adult rats. Axonal regrowth into and out of the implanted biomaterial as well as functional recovery was reported (Yoshii S *et al.* 2004).

Collagen reconstitution within nerve guidance tubes has been performed In the presence of strong magnetic fields which resulted in the formation of hydrogels with collagen fibrils aligned in a parallel orientation. These anisotropic collagen hydrogels guided neurite elongation from chick and rat neonatal DRG (Dubey N *et al.* 1999). Anisotropic fibrin hydrogels were also prepared using the same technique and the fibrin fibril diameter could be varied by adjusting the calcium concentration. Neurite outgrowth from chick DRG using these hydrogels was supported more effectively by larger fibril diameters of about 500 nm than smaller fibril diameters of 150 nm or isotropic fibril gels (Dubey N *et al.* 2001).

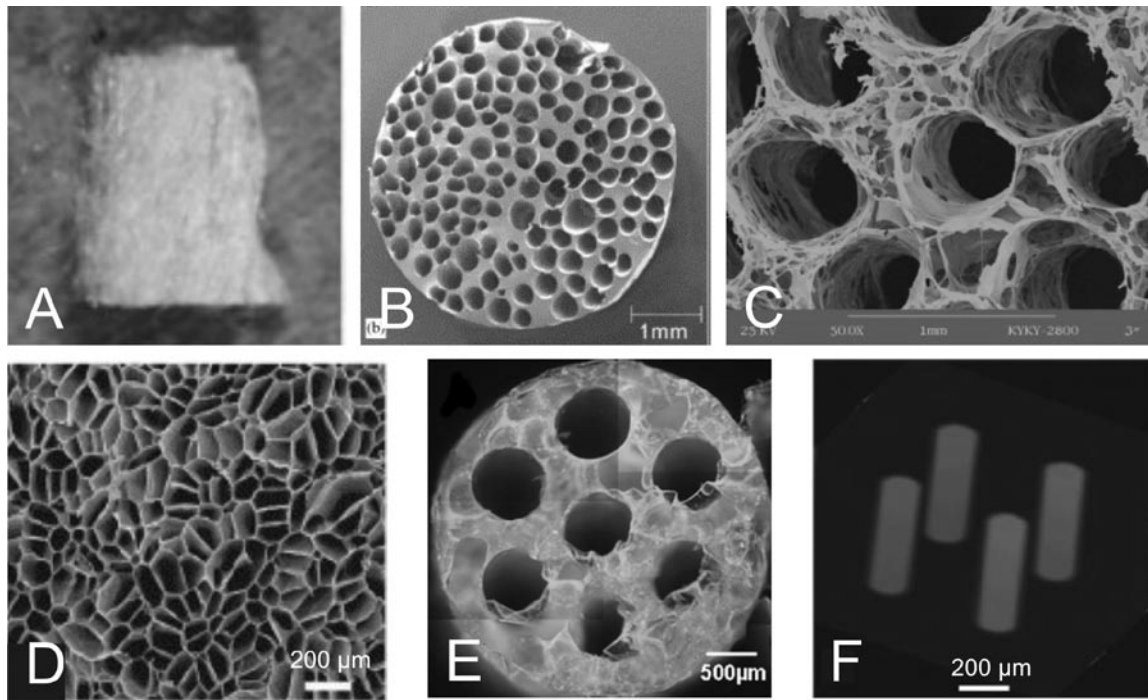


**Figure 2.4: Images of anisotropic structures.** (A) Oriented collagen filaments; (B) channels within pHEMA scaffolds templated by polymer fibers; (C) channels within chitosan hydrogels templated by metal needles; (D) channels within agarose hydrogels created by freeze-drying; (E) channels within PLGA templated by stainless steel wires; (F) channels of bioactive peptides created by photo-immobilization in the line of a laser beam within agarose hydrogels.

### 2.5.3.2 Oriented channels by molding/templating techniques

In this technique, the template materials like metallic needles or fibers of synthetic polymers were arranged in parallel fashion within a tube or other defined volumes. The hydrogel component was injected into the spaces between the template materials. Anisotropic hydrogels of pHEMA have been prepared by polymerization of the monomer solution between fibers of poly( $\epsilon$ -caprolactone), which were removed by dissolution in acetone. Anisotropic gels have been prepared with longitudinally oriented channels with diameters between 100-200  $\mu\text{m}$  or between 300-400  $\mu\text{m}$  (Flynn L *et al.* 2003). pHEMA based anisotropic hydrogels with a maximum of 130 channels and an average channel diameter of 200  $\mu\text{m}$  were modified by covalent immobilization of laminin derived oligopeptide, which enhanced neurite outgrowth from chick DRG (Yu TT *et al.* 2005). Chitosan based anisotropic hydrogels were created with 21 linearly aligned channels by using acupuncture needles of 150-400  $\mu\text{m}$  in diameter. The anisotropic structure helped neuroblastoma cells invade and migrate along the oriented microchannels (Wang A *et al.* 2006). Polystyrene fibers were used

as templates to prepare agarose gels with a 200  $\mu\text{m}$  channel diameter. Templates were dissolved in tetrahydrofuran after gel formation. These anisotropic gels were implanted into gaps of adult rat spinal cord cervical dorsal column transection, showing longitudinally oriented axonal growth along the channels. Axon outgrowth into the hydrogel was significantly enhanced by introduction of brain derived neurotrophic factor (BDNF) overexpressing syngenic mesenchymal stem cells. Astroglia surrounded the implant but did not enter the implant channels however Schwann cells invaded the microchannels which suggests that a significant proportion of the regenerating axons was of DRG origin (Stokols S *et al.* 2006a).

#### **2.5.3.3 Oriented channels by freeze-drying**

Polymer scaffolds with anisotropic structures were created by using a freeze drying method. The temperature gradient applied to a polymer solution determines the direction of growth and the size of ice crystals, which elongate as needles through the polymer solution. The places occupied by ice crystals remain as empty pores after freeze drying and pores become water filled after rehydration of the dried polymer scaffold. Using this method, agarose hydrogels have been prepared which had linearly aligned pores with cross sectional diameters between 71 and 187  $\mu\text{m}$ . In a rat spinal cord injury model it could be shown that axon outgrowth occurred into these anisotropic structures. Scaffolds loaded with recombinant human BDNF enhanced axon outgrowth (Stokols S *et al.* 2006b). Porcine collagen scaffolds with capillary microstructure and pore sizes between 20 and 50  $\mu\text{m}$  have been prepared by freeze drying techniques. These scaffolds were chemically stabilized by carbodiimide crosslinking, which allowed survival and attachment of astrocyte and olfactory ensheathing cells *in vitro*. Neurites from a neuroblastoma cell line readily grew into these hydrogels in an oriented fashion (Mollers S *et al.* 2009).

#### **2.5.4 Alginate based anisotropic capillary hydrogels**

A very specialized type of anisotropic hydrogel, which might be useful for nerve regeneration are ionotropic hydrogels. Alginic acid is also called algin or alginate is a suitable candidate for this purpose. Alginic acid is a linear polysaccharide composed of 1,4-linked  $\beta$ -D-mannuronic acid and  $\alpha$ -L-guluronic acid units, which are arranged in either homopolymeric blocks of one unit or in blocks with alternating residues (Figure 2.6A). The polyuronic acid is the main constituent of brown algae cell walls from which it can be extracted under alkaline conditions to give a water-soluble alkali salt.

Sodium alginate can be transferred into hydrogels from its highly viscous aqueous solution by ionotropic crosslinking with divalent cations. The overall composition and the sequence of the monomers in the alginate molecule will decide the modulus of  $\text{Me}^{2+}$  alginate gels. Alginates with high guluronic acid content form stronger and denser gels than such prepared from mannuronic acid rich alginates (Sabra W *et al.* 2005). Alginate can also form alginic acid gels when the pH of a sodium alginate solution is reduced. Calcium alginate gels are well established in biomedicine, especially in tissue engineering applications (Ehrenfreund-Kleinma T *et al.* 2006, Draget KI *et al.* 1997). Alginate is basically not biodegradable, but in the physiological environment ionic hydrogels are dissolved by exchanging the crosslinking cations by monovalent ions such as sodium or potassium (Shoichet MS *et al.* 1996). In the peripheral and central nervous system alginate hydrogels have been used for nerve regeneration either in an ionically crosslinked form with divalent cations or stabilized by chemical reactions. Neurite outgrowth from chick DRG showed fewer outgrowths in these alginate gels than in the control condition. Neurite outgrowth increased dramatically after Schwann cell seeding (Mosahebi A *et al.* 2001). In another study, pure calcium alginate hydrogels did not support neurite outgrowth from fetal rat DRG until hydrogels were coated with fibronectin or seeded with Schwann cells (Novikova LN *et al.* 2006).

Alginate gels prepared by chemically crosslinking with ethylenediamine and carbodiimide have been implanted into the completely transected postnatal day 30 rat spinal cord. Myelinated and unmyelinated axons, few of which were accompanied by astrocytic processes, have been found to grow into these covalently crosslinked alginate sponges (Kataoka K *et al.* 2004, Kataoka K *et al.* 2001, Suzuki K *et al.* 1999). Neural stem cells derived from fetal hippocampus seeded into chemically crosslinked alginate gels survived after transplantation into the injured spinal cord (Wu S *et al.* 2001). By modifying the hydrogels with laminin or by covalent immobilization of the YIGSR oligopeptide their cell compatibility could be enhanced. Attachment of NB2a neuroblastoma cells and neurite outgrowth was significantly enhanced with calcium gels modified with oligopeptide compared with unmodified gels (Dhoot NO *et al.* 2004). In a different approach, BDNF producing fibroblasts were encapsulated in alginate hydrogels. Under this condition cells survived in the injured spinal cord without immune suppression, they secreted neurotrophic factors and promoted axonal regeneration outside of the implanted hydrogel (Tobias CA *et al.* 2001, Tobias CA *et al.* 2005). Taken together, it can be assumed that chemically cross-linked alginate is more biocompatible than ionically cross-linked alginate because high

concentrations of calcium ions have been identified to exert cytotoxic effects and foreign body reactions (Suzuki Y *et al.* 1998). Because of their negative charge, hydrogels show a reduced cell adhesion, which has to be improved by adding relevant adhesion-promoting proteins, oligopeptides or cells.

All of these applications did not utilize the unique property of the alginate system to produce hydrogels with an oriented capillary structure which seems to be unknown to many research groups.

#### **2.5.4.1 Preparation of Alginate based anisotropic capillary hydrogels**

Alginate has the capacity to produce anisotropic capillary hydrogels by directed ion diffusion. In contrast to the applications summarized above, where ionotropic alginate gels has been prepared by simply mixing alginate solutions with solutions containing divalent cations, hydrogels with anisotropic capillaries are formed when a multivalent cation solution, like e.g.  $\text{Cu}^{2+}$  or  $\text{Ca}^{2+}$ , and a dilute aqueous solution of sodium alginate are superimposed in layers exhibiting one plain inter phase. A membrane-like boundary formation takes place between the two liquids and this membrane consists of non soluble, ionically crosslinked alginate. The electrolyte ions start an oriented diffusion into the solution of the polymer, which results into a continuous gel formation process (Figure 2.5A) and the generation of capillaries which are hexagonally arranged and few centimeters long. The transition from sol to gel is limited by diffusion and proceeds in the propagating front. The lumen of the capillaries is filled with electrolyte solution, while the walls are made up of non soluble metal alginate. The highly oriented structure of the capillaries is loosened up after a certain distance due to a decreased concentration of crosslinking ions in these areas (Thiele H *et al.* 1957, 1958). A dissipative convective process resulting from opposing diffusion gradients and friction of the polyelectrolyte chains is the reason that the ongoing precipitation results in an almost hexagonally structured anisotropic capillary gel (Figure 2.5C) (Thumbs J *et al.* 1996).

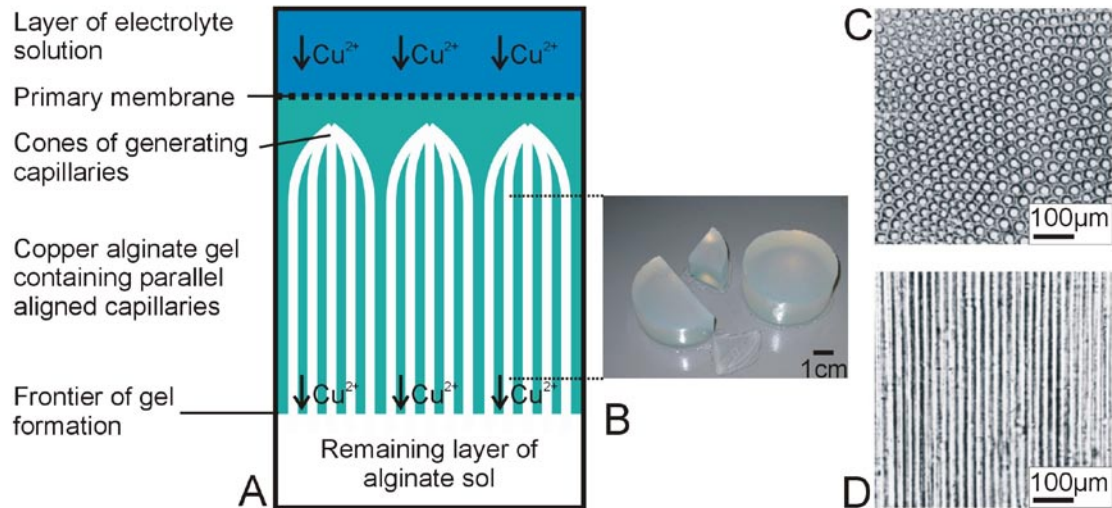


**Figure 2.5: Schematic representation of capillary gel formation after superimposing an alginate sol with an electrolyte solution containing a multivalent cation, e.g.  $\text{Cu}^{2+}$  (A), photograph of a copper alginate gel (B), capillary structure in cross-section (C) and longitudinal section (D).**

The parameters which will affect the degree of regularity within the ionotropic gel are the diffusion potential, the rate of fixation, the rigidity of linkages, the chain length, the degree of dissociation, and the concentration of the solution. In this context the process of ionotropic hydrogel formation has been intensively studied (Thiele H *et al.* 1950, 1955a, 1955b, 1967). The steric arrangement of the carboxylic groups of the G-blocks leads to the formation of cavities which allow a complex formation with divalent cations resulting in ionotropic gel formation (Figure 2.6A). The binding property of  $\text{Ca}^{2+}$  increases when the polyguluronate chain length exceeds a critical value. This is not observed for polymannuronate segments (Rees DA *et al.* 1977).



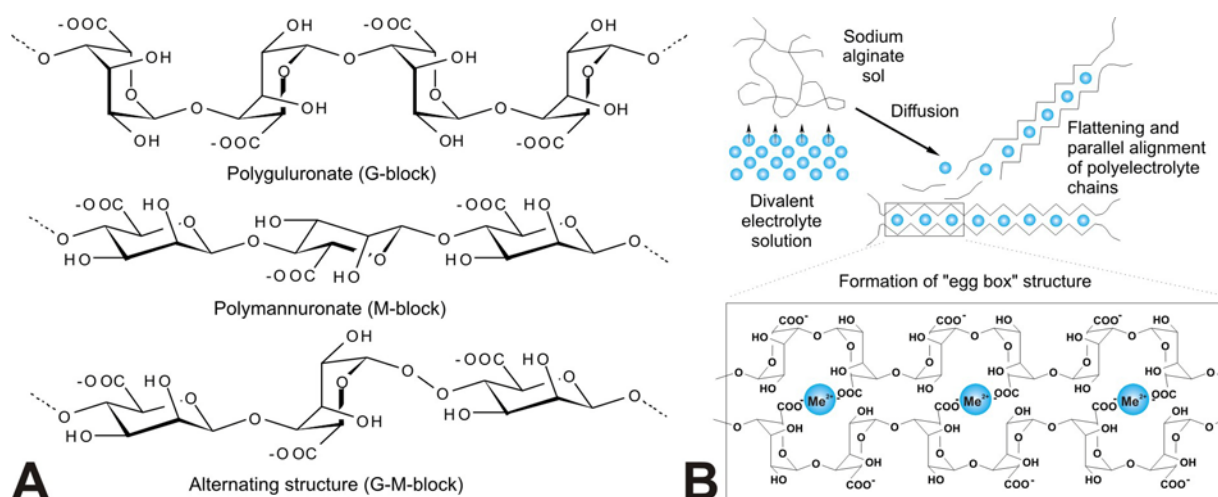


**Figure 2.6: (A) Conformation of the different alginate sequences. (B) Ionotropic gel formation of an alginate sol by diffusion and complexation with divalent cations.**

Thiele et al. (1955) demonstrated that under certain conditions ion diffusion into polyelectrolyte solutions results in structures which have similarities to biological tissues. Using the ion diffusion phenomenon numerous types of natural tissues can be reconstructed, such as skin, blood vessels, bones, teeth, eye lenses, and cornea. Ion diffusion results in an anisotropic structure with highly oriented capillaries which has a very similar structure to that of native dentine (Thiele H *et al.* 1955a,b, Bechhold H *et al.* 1929).

#### 2.5.4.2 Alginate capillary hydrogels for nerve regeneration

Biocompatible and non immunogenic polymers based on calcium alginates were used as injectable scaffold materials for tissue engineering and cell transplantation (Shapiro L *et al.* 1997, Becker TA *et al.* 2001). For nerve regeneration in the central and peripheral nervous system alginates have been used in different forms like hydrogels or freeze-dried sponges, either ionotropically crosslinked with calcium cations or stabilized by chemical reactions. Various studies have shown that alginates are biodegradable without causing inflammatory reactions under cell culture conditions or after transplantation into the mammalian CNS (Suzuki K *et al.* 1999, Orive G *et al.* 2002). Alginate based sponges prepared by covalent crosslinking have been implanted into rat spinal cord lesions and ingrowth of myelinated and unmyelinated axon could be shown. When implanted in 50 mm gaps of the sciatic nerve of cats, an ingrowth of axons and Schwann cells into chemically crosslinked alginate sponges could be seen (Hashimoto T *et al.* 2005). Furthermore, it was found that neural stem cells

seeded into alginate gels survived (Wu S *et al.* 2001) and incorporated growth factors such as TGF- $\beta$  remained bioactive (Milella E *et al.* 2001). Within these isotropic gels, some axonal regeneration occurred, but never in a completely rostro-caudally directed fashion, thus preventing re-connection with the caudal spinal cord.

In preliminary experiments of our groups using copper ions for gel formation resulted in the creation of alginate hydrogels with capillaries of 25  $\mu\text{m}$  in diameter. In transected entorhinohippocampal slice cultures, these highly anisotropic hydrogels elicited robust longitudinally oriented axonal regeneration from the entorhinal cortex with appropriate target reinnervation in the hippocampus. This could be replicated *in vivo*, where identical hydrogels promoted oriented axon regeneration following a cervical dorsal column transection in adult rats. To further augment the regenerative capacity, these hydrogels can be seeded with adult neural progenitor cells (Prang P *et al.* 2006).

## **2.6 Relevance of *in vitro* assay with the spinal cord injury**

The main aim of this thesis was to investigate the axon regeneration after spinal cord injury by using alginate based anisotropic capillary hydrogels. Before going to *in vivo* model we tested these gels in some *in vitro* assay. We selected *in vitro* model from peripheral nervous system like dorsal root ganglia and from central nervous system like entorhinal cortex slice culture and spinal cord slice culture. These *in vitro* assays have relevance to the spinal cord injury model which is mentioned below.

### **2.6.1 Dorsal root ganglia**

A dorsal root ganglion (or spinal ganglion) is a nodule on a dorsal root that contains cell bodies of neurons in afferent spinal nerves. The dorsal root ganglia lie along the vertebral column by the spine. The sensory neurons that convey information from the skin, muscles, and joints of the limbs and trunk to the spinal cord are clustered together in dorsal root ganglia.

The somas of sensory neurons (blue) are found in the dorsal root ganglia. Sensory axons enter the spinal cord through the dorsal root and often synapse on interneurons (green) in the gray matter. Motor neuron cell bodies are located in the gray matter and the axons leave the spinal cord through the ventral root. Spinal nerves are formed when the dorsal and ventral roots join together.

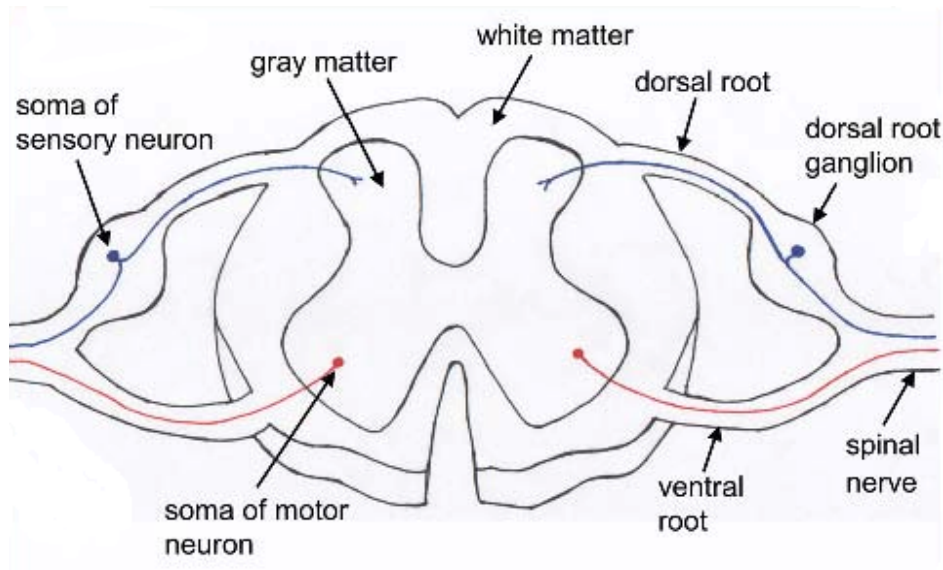


**Fig 2.7: Neuroanatomy of dorsal root ganglion showing sensory neurons passing through and reaching CNS.**

### 2.6.2 Entorhinal cortex slice culture

The entorhinal cortex is the main conduit between the hippocampus and the neocortex. In particular, the entorhinal cortex supplies the hippocampus with information from multiple senses. In addition, the entorhinal cortex also translates information from the hippocampus to the neocortex.

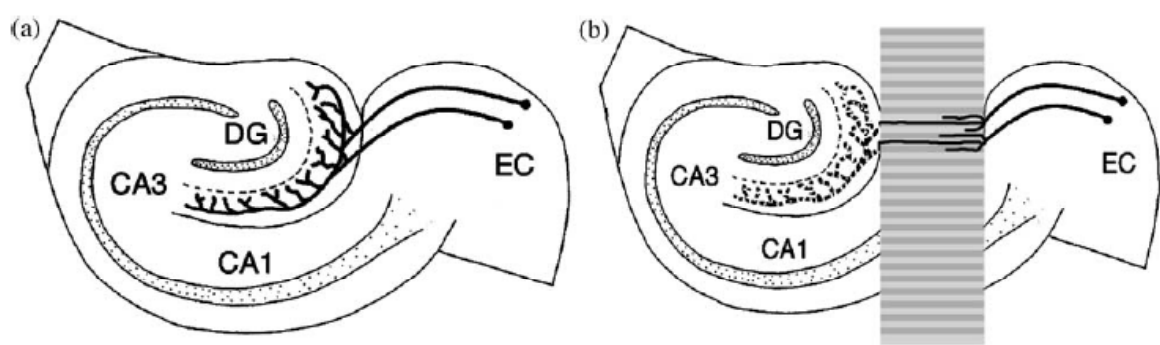


**Figure 2.8: schematic representation of axon projecting from Entorhinal cortex to dentate gyrus (a), axon regeneration and target reinnervation after lesion using ACH scaffolds (b).**

The entorhinal cortex acts to relay information to and from the hippocampus. It is through the entorhinal cortex that the hippocampus maintains interconnections with the neocortical multi-modal associations areas of the temporal, frontal, and parietal lobes. Axonal projections build the neuronal connections within the CNS. They can be destroyed either traumatic

lesions (e.g. spinal or head injury), but also by vascular insults and neurodegenerative diseases.

Most importantly, this connection develops and can be studied with the organotypic slice culture method avoiding or reducing the need for *in vivo* experiments. A second important reason is the specificity with which the entorhinal fibers terminate in the outer molecular layer of dentate gyrus. This makes the analysis of the specific re-innervation much easier.

### **2.6.3 Spinal cord slice culture**

The most important and most widely used CNS region for the study of axonal regeneration is the spinal cord, because it is clinically the most relevant due to the high prevalence and severe impact of spinal cord injury. So far, no slice culture model for the study of axonal regeneration in the spinal cord was available.

## References

- Aigner L, Arber S, Kapfhammer JP, Laux T, Schneider C, Botteri F, Brenner HR, Caroni P. Overexpression of the neural growth-associated protein GAP-43 induces nerve sprouting in the adult nervous system of transgenic mice. *Cell* 1995;83:269-78.
- Andac M, Plieva FM, Denizli A, Galaev IY, Mattiasson B. Poly(hydroxyethyl methacrylate)-based macroporous hydrogels with disulfide cross-linker. *Macromol Chem Phys* 2008;209:577-84.
- Avitabile T, Marano F, Castiglione F, Bucolo C, Cro M, Ambrosio L, et al. Biocompatibility and biodegradation of intravitreal hyaluronan implants in rabbits. *Biomaterials* 2001;22:195-200.
- Baier Leach J, Bivens KA, Patrick CW, Schmidt CE. Photocrosslinked hyaluronic acid hydrogels: Natural, biodegradable tissue engineering scaffolds. *Biotech Bioeng* 2003;82:587-9.
- Bailey SB, Eichler ME, Villadiego A, Rich KM. The influence of fibronectin and laminin during Schwann cell migration and peripheral nerve regeneration through silicon chambers. *J Neurocytol* 1993;22:176-84.
- Balgude AP, Yu X, Szymanski A, Bellamkonda RV. Agarose gel stiffness determines rate of DRG neurite extension in 3D cultures. *Biomaterials* 2001;22:1077-84.
- Bamber NI, Li H, Lu X, Oudega M, Aebischer P, Xu XM. Neurotrophins BDNF and NT-3 promote axonal re-entry into the distal host spinal cord through Schwann cell-seeded mini-channels. *Eur J Neurosci* 2001;13:257-68.
- Bechhold H. *Die Kolloide in Biologie und Medizin*. Dresden, Germany: Verlag Steinkopff; 1929.
- Becker TA, Kipke DR, Brandon T. Calcium alginate gel: A biocompatible and mechanically stable polymer for endovascular embolization. *J Biomed Mater Res* 2001;54:76-86.
- Belkas JS, Shoichet MS, Midha R. Peripheral nerve regeneration through guidance tubes. *Neurol Res* 2004;26:151-60.
- Bellamkonda R, Ranieri JP, Aebischer P. Laminin oligopeptide derivatized agarose gels allow three-dimensional neurite extension *in vitro*. *J Neurosci Res* 1995b;41:501-9.
- Bellamkonda R, Ranieri JP, Bouche N, Aebischer P. Hydrogel-based three-dimensional matrix for neural cells. *J Biomed Mater Res* 1995a;29:663-71.

- Benedetti L, Cortivo R, Berti T, Berti A, Pea F, Mazzo M, et al. Biocompatibility and biodegradation of different hyaluronan derivatives (Hyaff) implanted in rats. *Biomaterials* 1993;14:1154-60.
- Borkenhagen M, Clemence JF, Sigrist H, Aebischer P. Three-dimensional extracellular matrix engineering in the nervous system. *J Biomed Mater Res* 1998;40:392-400.
- Bracken MB, Shepard MJ, Collins WF, Holford TR, Young W, Baskin DS, Eisenberg HM, Flamm E, Leo-Summers L, Maroon J, et al. A randomized, controlled trial of methylprednisolone or naloxone in the treatment of acute spinal cord injury: results of the second national acute spinal cord injury study. *N Engl J Med* 1990;322:1405-11.
- Bunge MB. Bridging areas of injury in the spinal cord. *Neuroscientist* 2001;7:325-39.
- Burdick JA, Ward M, Liang E, Young MJ, Langer R. Stimulation of neurite outgrowth by neurotrophins delivered from degradable hydrogels. *Biomaterials* 2006;27:452-9.
- Buslov DK, Sushko NI, Tretinnikov ON. Study of thermal gelation of methylcellulose in water using FTIR-ATR spectroscopy. *J Appl Spectrosc* 2008;75:514-8.
- Campoccia D, Doherty P, Radice M, Brun P, Abatangelo G, Williams DF. Semisynthetic resorbable materials from hyaluronan esterification. *Biomaterials* 1998;19:2101-27.
- Chen YS, Hsieh CL, Tsai CC, Chen TH, Cheng WC, Hu CL, et al. Peripheral nerve regeneration using silicone rubber chambers filled with collagen, laminin and fibronectin. *Biomaterials* 2000;21:1541-7.
- Chow KS, Khor E, Wan ACA. Porous chitin matrices for tissue engineering: Fabrication and *in vitro* cytotoxic assessment. *J Polym Res* 2001;8:27-35.
- Chvatal SA, Kim YT, Bratt-Leal AM, Lee H, Bellamkonda RV. Spatial distribution and acute anti-inflammatory effects of Methylprednisolone after sustained local delivery to the contused spinal cord. *Biomaterials* 2008;29:1967-75.
- Ciardelli G, Chiono V. Materials for peripheral nerve regeneration. *Macromol Biosci* 2006;6:13-26.
- Crompton KE, Goud JD, Bellamkonda RV, Gengenbach TR, Finkelstein DI, Horne MK, et al. Polylysine-functionalised thermoresponsive chitosan hydrogel for neural tissue engineering. *Biomaterials* 2007;28:441-9.
- Cui FZ, Tian WM, Fan YW, Hou SP, Xu QY, Lee LS. Cerebrum repair with PHPMA hydrogel immobilized with neurite-promoting peptides in traumatic brain injury of adult rat model. *J Bioact Compat Polym* 2003;18:413-32.

- Cui FZ, Tian WM, Hou SP, Xu QY, Lee IS. Hyaluronic acid hydrogel immobilized with RGD peptides for brain tissue engineering. *J Mater Sci Mater Med* 2006;17:1393-401.
- Dalton PD, Flynn L, Shoichet MS. Manufacture of poly(2-hydroxyethyl methacrylate-co-methyl methacrylate) hydrogel tubes for use as nerve guidance channels. *Biomaterials* 2002;23:3843-51.
- de la Torre JC, Hill PK, Gonzalez-Carvajal M, Parker JC, Jr. Evaluation of transected spinal cord regeneration in the rat. *Exp Neurol* 1984;84:188-206.
- Dhoot NO, Tobias CA, Fischer I, Wheatley MA. Peptide-modified alginate surfaces as a growth permissive substrate for neurite outgrowth. *J Biomed Mater Res A* 2004;71:191-200.
- Dillon GP, Yu X, Sridharan A, Ranieri JP, Bellamkonda RV. The influence of physical structure and charge on neurite extension in a 3D hydrogel scaffold. *J Biomater Sci Polym Ed* 1998;9:1049-69.
- Dörfler HD. Grenzflächen und kolloid-disperse Systeme: Physik und Chemie Berlin Germany: Springer, 2002.
- Draget KI, Skjak-Braek G, Smidsrod O. Alginate based new materials. *Int J Biol Macromol* 1997;21:47-55.
- Dubey N, Letourneau PC, Tranquillo RT. Guided neurite elongation and schwann cell invasion into magnetically aligned collagen in simulated peripheral nerve regeneration. *Exp Neurol* 1999;158:338-50.
- Dubey N, Letourneau PC, Tranquillo RT. Neuronal contact guidance in magnetically aligned fibrin gels: effect of variation in gel mechano-structural properties. *Biomaterials* 2001;22:1065-75.
- Duconseille E, Woerly S, Kelche C, Will B, Cassel JC. Polymeric hydrogels placed into a fimbria-fornix lesion cavity promote fiber (re)growth: a morphological study in the rat. *Restor Neurol Neurosci* 1998;13:193-203.
- Ehrenfreund-Kleinman T, Golenser J, Domb AJ. Polysaccharide scaffolds for tissue engineering. In: Ma PE, J; editor. *Scaffolding in Tissue Engineering* Boca Raton, FL: CRC Press; 2006. p. 27-44.
- Fernandez-Cossio S, Leon-Mateos A, Sampedro FG, Oreja MT. Biocompatibility of agarose gel as a dermal filler: histologic evaluation of subcutaneous implants. *Plast Reconstr Surg* 2007;120:1161-9.

- Fitch MT, Silver J. Beyond the glial scar—cellular and molecular mechanisms by which glial cells contribute to CNS regenerative failure. In: Tuszynski MH, Kordower J, editors. *CNS Regeneration*. San Diego, CA: Academic Press; 1999. p 55-88.
- Flynn L, Dalton PD, Shoichet MS. Fiber templating of poly(2-hydroxyethyl methacrylate) for neural tissue engineering. *Biomaterials* 2003;24:4265-72.
- Freier T, Montenegro R, Shan Koh H, Shoichet MS. Chitin-based tubes for tissue engineering in the nervous system. *Biomaterials* 2005;26:4624-32.
- Friedman JA, Windebank AJ, Moore MJ, Spinner RJ, Currier BL, Yaszemski MJ. Biodegradable polymer grafts for surgical repair of the injured spinal cord. *Neurosurgery* 2002;51:742-52.
- Geoffrey CG, Matthew JC, Michael TL. *Annu Rev Med* 2007;58:299-312.
- Giannetti S, Lauretti L, Fernandez E, Salvinelli F, Tamburrini G, Pallini R. Acrylic hydrogel implants after spinal cord lesion in the adult rat. *Neurol Res* 2001;23:405-9.
- Grimpe B, Silver J. The extracellular matrix in axon regeneration. *Prog Brain Res* 2002;137:333-49.
- Gong HP, Zhong YH, Li JC, Gong YD, Zhao NM, Zhang XF. Studies on nerve cell affinity of chitosan-derived materials. *J Biomed Mater Res* 2000;52:285.
- Gonzalez AM, Berry M, Greenlees L, Logan A, Baird A. Matrix-mediated gene transfer to brain cortex and dorsal root ganglion neurones by retrograde axonal transport after dorsal column lesion. *J Gene Med* 2006;8:901-9.
- Gunn JW, Turner SD, Mann BK. Adhesive and mechanical properties of hydrogels influence neurite extension. *J Biomed Mater Res A* 2005;72:91-7.
- Gupta D, Tator CH, Shoichet MS. Fast-gelling injectable blend of hyaluronan and methylcellulose for intrathecal, localized delivery to the injured spinal cord. *Biomaterials* 2006;27:2370-9.
- Hashimoto T, Suzuki Y, Nakashima T, Tanihara M, Ide C. Peripheral nerve regeneration using non-tubular alginate gel crosslinked with covalent bonds. *J Mater Sci Mater Med* 2005;16:503-9.
- Horn EM, Beaumont M, Shu XZ, Harvey A, Prestwich GD, Horn KM, et al. Influence of cross-linked hyaluronic acid hydrogels on neurite outgrowth and recovery from spinal cord injury. *J Neurosurg Spine* 2007;6:133-40.



- Houweling DA, Lankhorst AJ, Gispén WH, Bar PR, Joosten EA. Collagen containing neurotrophin-3 (NT-3) attracts regrowing injured corticospinal axons in the adult rat spinal cord and promotes partial functional recovery. *Exp Neurol* 1998;153:49-59.
- Hudson TW, Evans GRD, Schmidt CE. Engineering strategies for peripheral nerve repair. *Clin Plast Surg* 1999;26:617-28.
- Hurtado A, Moon LD, Maquet V, Blits B, Jerome R, Oudega M. Poly (D,L-lactic acid) macroporous guidance scaffolds seeded with Schwann cells genetically modified to secrete a bi-functional neurotrophin implanted in the completely transected adult rat thoracic spinal cord. *Biomaterials* 2006;27:430-42.
- Ide C. Peripheral nerve regeneration. *Neurosci Res* 1996;25:101-21.
- Jain A, Kim YT, McKeon RJ, Bellamkonda RV. *In situ* gelling hydrogels for conformal repair of spinal cord defects, and local delivery of BDNF after spinal cord injury. *Biomaterials* 2006;27:497-504.
- Joosten EA, Bar PR, Gispén WH. Collagen implants and cortico-spinal axonal growth after mid-thoracic spinal cord lesion in the adult rat. *J Neurosci Res* 1995;41:481-90.
- Kataoka K, Suzuki Y, Kitada M, Hashimoto T, Chou H, Bai H, et al. Alginate enhances elongation of early regenerating axons in spinal cord of young rats. *Tissue Eng* 2004;10:493-504.
- Kataoka K, Suzuki Y, Kitada M, Ohnishi K, Suzuki K, Tanihara M, et al. Alginate, a bioresorbable material derived from brown seaweed, enhances elongation of amputated axons of spinal cord in infant rats. *J Biomed Mater Res* 2001;54:373-84.
- Khor E, Lim LY. Implantable applications of chitin and chitosan. *Biomaterials* 2003;24:2339-49.
- Klapka N, Müller HW. Collagen matrix in spinal cord injury. *J Neurotrauma* 2006;23:422-35.
- Kleinmann HK, McGarvey ML, Hassell JR, Star VL, Cannon FB, Laurie GW, et al. Basement membrane complexes with biological activity. *Biochem* 1986;25:312-8.
- Lee SM, Yune TY, Kim SJ, Park W, Lee YK, Kim YC, Oh YJ, Markelonis GJ, Oh TH. Minocycline reduces cell death and improves functional recovery after traumatic spinal cord injury in the rat. *J Neurotrauma* 2003;20:1017-27.
- Lesny P, De Croos J, Pradny M, Vacik J, Michalek J, Woerly S, et al. Polymer hydrogels usable for nervous tissue repair. *J Chem Neuroanat* 2002;23:243-7.
- Linda GG, Gail N. Tissue engineering-current challenges and expanding opportunities. *Science* 2002;295:1009-14.

- Livnat M, Peled E, Boss J, Seliktar D. In vivo degradation of semi-rigid polymeric films made of alginate and polyethylene glycol. *Isr J Chem* 2005;45:421-7.
- Loh NK, Woerly S, Bunt SM, Wilton SD, Harvey AR. The regrowth of axons within tissue defects in the CNS is promoted by implanted hydrogel matrices that contain BDNF and CNTF producing fibroblasts. *Exp Neurol* 2001;170:72-84.
- Mabilleau G, Moreau MF, Filmon R, Basle MF, Chappard D. Biodegradability of poly (2-hydroxyethyl methacrylate) in the presence of the J774.2 macrophage cell line. *Biomaterials* 2004;25:5155-62.
- Marchand R, Woerly S. Transected spinal cords grafted with *in situ* self-assembled collagen matrices. *Neurosci* 1990;35:45-60.
- Marchand R, Woerly S, Bertrand L, Valdes N. Evaluation of two cross-linked collagen gels implanted in the transected spinal cord. *Brain Res Bull* 1993;30:415-22.
- Midha R. Emerging techniques for nerve repair: nerve transfers and nerve guidance tubes. *Clin Neurosurg* 2006;53:185-90.
- Milella E, Barra G, Ramires PA, Leo G, Aversa P, Romito A. Poly(L-lactide)acid/alginate composite membranes for guided tissue regeneration. *J Biomed Mater Res* 2001;57:248-57.
- Mollers S, Heschel I, Damink LH, Schugner F, Deumens R, Muller B, et al. Cytocompatibility of a novel, longitudinally microstructured collagen scaffold intended for nerve tissue repair. *Tissue Eng Part A* 2009;15:461-72.
- Montheard JP, Chatzopoulos M, Chappard D. 2-hydroxyethylmethacrylate HEMA; chemical properties and applications in biomedical fields. *J Macromol Sci Macromol Rev* 1992;32:1-34.
- Mori M, Yamaguchi M, Sumitomo S, Takai Y. Hyaluronan-based biomaterials in tissue engineering. *Acta Histochem Cytochem* 2004;37:1-5.
- Mosahebi A, Simon M, Wiberg M, Terenghi G. A novel use of alginate hydrogel as Schwann cell matrix. *Tissue Eng* 2001;7:525-34.
- Novikova LN, Mosahebi A, Wiberg M, Terenghi G, Kellerth JO, Novikov LN. Alginate hydrogel and matrigel as potential cell carriers for neurotransplantation. *J Biomed Mater Res A* 2006;77:242-52.
- Orive G, Ponce S, Hernández RM, Gascón AR, Igartua M, Pedraz JL. Biocompatibility of microcapsules for cell immobilization elaborated with different type of alginates. *Biomaterials* 2002;23:3825-31.

- Potter W, Kalil RE, Kao WJ. Biomimetic material systems for neural progenitor cell-based therapy. *Front Biosci* 2008;13:806-21.
- Patist CM, Mulder MB, Gautier SE, Maquet V, Jerome R, Oudega M. Freeze-dried poly(D,L-lactic acid) macroporous guidance scaffolds impregnated with brain-derived neurotrophic factor in the transected adult rat thoracic spinal cord. *Biomaterials* 2004;25:1569-82.
- Piantino J, Burdick JA, Goldberg D, Langer R, Benowitz LI. An injectable, biodegradable hydrogel for trophic factor delivery enhances axonal rewiring and improves performance after spinal cord injury. *Exp Neurol* 2006;201:359-67.
- Plant GW, Chirila TV, Harvey AR. Implantation of collagen IV/poly(2-hydroxyethyl methacrylate) hydrogels containing Schwann cells into the lesioned rat optic tract. *Cell Transplant* 1998;7:381-91.
- Prang P, Muller R, Eljaouhari A, Heckmann K, Kunz W, Weber T, et al. The promotion of oriented axonal regrowth in the injured spinal cord by alginate-based anisotropic capillary hydrogels. *Biomaterials* 2006;27:3560-9.
- Raub CB, Suresh V, Krasieva T, Lyubovitsky J, Mih JD, Putnam AJ, et al. Noninvasive assessment of collagen gel microstructure and mechanics using multiphoton microscopy. *Biophys J* 2007;92:2212-22.
- Reed J, Walczak WJ, Petzold ON, Gimzewski JK. *In situ* mechanical interferometry of matrigel films. *Langmuir* 2009;25:36-9.
- Rees DA, Welsh EJ. Secondary and tertiary structure of polysaccharides in solutions and gels. *Angew Chem Int Edn* 1977;16:214-24.
- Reynolds B, Weiss S. Generation of neurons and astrocytes from isolated cells of the adult mammalian central nervous system. *Science* 1992;255:1707-10.
- Rochkind S, Shahar A, Amon M, Nevo Z. Transplantation of embryonal spinal cord nerve cells cultured on biodegradable microcarriers followed by low power laser irradiation for the treatment of traumatic paraplegia in rats. *Neurol Res* 2002;24:355-60.
- Sabra W, Deckwer WD. Alginate-a polysaccharide of industrial interest and diverse biological functions. In: Dimitru S, editor. *Polysaccharides: Structural diversity and functional versatility*. New York, NY: Marcel Dekker; 2005. p. 515-33.
- Sakiyama SE, Schense JC, Hubbell JA. Incorporation of heparin-binding peptides into fibrin gels enhances neurite extension: an example of designer matrices in tissue engineering. *Faseb J* 1999;13:2214-24.

- Schense JC, Hubbell JA. Three-dimensional migration of neurites is mediated by adhesion site density and affinity. *J Biol Chem* 2000;275:6813-8.
- Schmidt CE, Baier LJ. Neural tissue engineering: strategies for repair and regeneration. *Annu Rev Biomed Eng* 2003;5:293-347.
- Schwab ME. Repairing the injured spinal cord. *Science* 2002;295:1029-31.
- Shapiro L, Cohen S. Novel alginate sponges for cell culture and transplantation. *Biomaterials* 1997;18:583-90.
- Shoichet MS, Li RH, White ML, Winn SR. Stability of hydrogels used in cell encapsulation: An *in vitro* comparison of alginate and agarose. *Biotechnol Bioeng* 1996;50:374-81.
- Shoichet MS, Tator CH, Poon P, Kang C, Baumann MD. Intrathecal drug delivery strategy is safe and efficacious for localized delivery to the spinal cord. *Prog Brain Res* 2007;161:385-92.
- Sofroniew MV. Neural responses to axotomy. In: Tuszynski MH, Kordower J, editors. *CNS Regeneration*. San Diego, CA: Academic Press; 1999. p 3-26.
- Spilker MH, Yannas I, Hsu HP, Norregaard TV, Kostyk SK, Spector M. The effects of collagen-based implants on early healing of the adult rat spinal cord. *Tissue Eng* 1997;3:309-17.
- Stokols S, Sakamoto J, Breckon C, Holt T, Weiss J, Tuszynski MH. Templated agarose scaffolds support linear axonal regeneration. *Tissue Eng* 2006a;12:2777-87.
- Stokols S, Tuszynski MH. Freeze-dried agarose scaffolds with uniaxial channels stimulate and guide linear axonal growth following spinal cord injury. *Biomaterials* 2006b;27:443-51.
- Suzuki Y, Nishimura Y, Tanihara M, Suzuki K, Nakamura T, Shimizu Y, et al. Evaluation of a novel alginate gel dressing: cytotoxicity to fibroblasts *in vitro* and foreign-body reaction in pig skin *in vivo*. *J Biomed Mater Res* 1998;39:317-22.
- Suzuki K, Suzuki Y, Ohnishi K, Endo K, Tanihara M, Nishimura Y. Regeneration of transected spinal cord in young adult rats using freeze-dried alginate gel. *Neuroreport* 1999;10:2891-4.
- Tate MC, Shear DA, Hoffman SW, Stein DG, LaPlaca MC. Biocompatibility of methylcellulose-based constructs designed for intracerebral gelation following experimental traumatic brain injury. *Biomaterials* 2001;22:1113-23.
- Thiele H. Histolyse und Histogenese – Gewebe und ionotrope Gele – Prinzip einer Strukturbildung. Frankfurt, Germany: Akademische Verlagsgesellschaft; 1967.

- Thiele H, Andersen G. Iontrope Gele von Polyuronsäuren. 1. Bildung und Verhalten. Kolloid Z 1955a;140:76-102.
- Thiele H, Andersen G. Iontrope Gele von Polyuronsäuren. 2. Ordnungsgrad. Kolloid Z 1955b;142:5-24.
- Thiele H, Hallich K. Kapillarenstrukturen in ionotropen Gelen. Kolloid Z 1957;151:1-12.
- Thiele H, Hallich K. Über ionotrope Gele mit Kapillarstruktur. Z Naturforschg 1958; 13b:580-88.
- Thiele H, Micke H. Über Ionotropie. Kolloid Z 1950;117:144-53.
- Thonhoff JR, Lou DI, Jordan PM, Zhao X, Wu P. Compatibility of human fetal neural stem cells with hydrogel biomaterials *in vitro*. Brain Res 2008;1187:42-51.
- Thumbs J, Kohler H-H. Capillaries in alginate gels as an example of dissipative structure formation. Chem Phys 1996;208:9-24.
- Tian WM, Hou SP, Ma J, Zhang CL, Xu QY, Lee IS, et al. Hyaluronic acid-poly-D-lysine-based three-dimensional hydrogel for traumatic brain injury. Tissue Eng 2005;11:513-25.
- Tobias CA, Dhoot NO, Wheatley MA, Tessler A, Murray M, Fischer I. Grafting of encapsulated BDNF-producing fibroblasts into the injured spinal cord without immune suppression in adult rats. J Neurotrauma 2001;18:287-301.
- Tobias CA, Han SS, Shumsky JS, Kim D, Tumolo M, Dhoot NO, et al. Alginate encapsulated BDNF-producing fibroblast grafts permit recovery of function after spinal cord injury in the absence of immune suppression. J Neurotrauma 2005;22:138-56.
- Tsai EC, Dalton PD, Shoichet MS, Tator CH. Synthetic hydrogel guidance channels facilitate regeneration of adult rat brainstem motor axons after complete spinal cord transection. J Neurotrauma 2004;21:789-804.
- Tsai EC, Dalton PD, Shoichet MS, Tator CH. Matrix inclusion within synthetic hydrogel guidance channels improves specific supraspinal and local axonal regeneration after complete spinal cord transection. Biomaterials 2006;27:519-33.
- Vachoud L, Zydowicz N, Dormard A. Formation and characterization of physical chitin hydrogels. Carbohydr Res 1997;302:169-77.
- Valentini RF, Aebischer P, Winn SR, Galletti PM. Collagen- and laminin-containing gels impede peripheral nerve regeneration through semipermeable nerve guidance channels. Exp Neurol 1987;98:350-6.

- Wang A, Ao Q, Cao W, Yu M, He Q, Kong L, et al. Porous chitosan tubular scaffolds with knitted outer wall and controllable inner structure for nerve tissue engineering. *J Biomed Mater Res A* 2006;79:36-46.
- Wechsler S, Fehr D, Molenberg A, Raeber G, Schense JC, Weber FE. A novel, tissue occlusive poly(ethylene glycol) hydrogel material. *J Biomed Mater Res A*. 2008; 85:285-92.
- Wei YT, Tian WM, Yu X, Cui FZ, Hou SP, Xu QY, et al. Hyaluronic acid hydrogels with IKVAV peptides for tissue repair and axonal regeneration in an injured rat brain. *Biomed Mater* 2007;2:142-6.
- Weidner N, Blesch A. Perspectives for regenerative strategies following spinal cord injury. *Akt Neurol* 2002;29:223-8.
- Weng L, Gouldstone A, Wu Y, Chen W. Mechanically strong double network photocrosslinked hydrogels from N,N-dimethylacrylamide and glycidyl methacrylated hyaluronan. *Biomaterials* 2008;29:2153-63.
- Williams LR, Longo FM, Powell HC, Lundborg G, Varon S. Spatial-temporal progress of peripheral nerve regeneration within a silicone chamber: parameters for a bioassay. *J Comp Neurol*. 1983;218:460-70.
- Woerly S, Doan VD, Evans-Martin F, Paramore CG, Peduzzi JD. Spinal cord reconstruction using NeuroGel implants and functional recovery after chronic injury. *J Neurosci Res* 2001b;66:1187-97.
- Woerly S, Doan VD, Sosa N, de Vellis J, Espinosa A. Reconstruction of the transected cat spinal cord following NeuroGel implantation: axonal tracing, immunohistochemical and ultrastructural studies. *Int J Dev Neurosci* 2001a;19:63-83.
- Woerly S, Doan VD, Sosa N, de Vellis J, Espinosa-Jeffrey A. Prevention of gliotic scar formation by NeuroGel allows partial endogenous repair of transected cat spinal cord. *J Neurosci Res* 2004;75:262-72.
- Woerly S, Petrov P, Sykova E, Roitbak T, Simonova Z, Harvey AR. Neural tissue formation within porous hydrogels implanted in brain and spinal cord lesions: ultrastructural, immunohistochemical, and diffusion studies. *Tissue Eng* 1999;5:467-88.
- Woerly S, Pinet E, De Robertis L, Bousmina M, Laroche G, Roitback T, et al. Heterogeneous PHPMA hydrogels for tissue repair and axonal regeneration in the injured spinal cord. *J Biomater Sci Polym Ed* 1998;9:681-711.

- Woerly S, Pinet E, de Robertis L, Van Diep D, Bousmina M. Spinal cord repair with PHPMA hydrogel containing RGD peptides (NeuroGel). *Biomaterials* 2001c;22:1095-111.
- Wu S, Suzuki Y, Kitada M, Kitaura M, Kataoka K, Takahashi J, et al. Migration, integration, and differentiation of hippocampus-derived neurosphere cells after transplantation into injured rat spinal cord. *Neurosci Lett* 2001;312:173-6.
- Xu XM, Zhang SX, Li H, Aebischer P, Bunge MB. Regrowth of axons into the distal spinal cord through a Schwann-cell-seeded mini-channel implanted into hemisected adult rat spinal cord. *Eur J Neurosci* 1999;11:1723-40.
- Yoshii S, Oka M, Shima M, Taniguchi A, Taki Y, Akagi M. Restoration of function after spinal cord transection using a collagen bridge. *J Biomed Mater Res A* 2004;70:569-75.
- Yu LM, Kazazian K, Shoichet MS. Peptide surface modification of methacrylamide chitosan for neural tissue engineering applications. *J Biomed Mater Res A* 2007;82:243-55.
- Yu TT, Shoichet MS. Guided cell adhesion and outgrowth in peptide-modified channels for neural tissue engineering. *Biomaterials* 2005;26:1507-14.
- Yu X, Dillon GP, Bellamkonda RB. A laminin and nerve growth factor-laden three-dimensional scaffold for enhanced neurite extension. *Tissue Eng* 1999;5:291-304.
- Yuan Y, Zhang P, Yang Y, Wang X, Gu X. The interaction of Schwann cells with chitosan membranes and fibers *in vitro*. *Biomaterials* 2004;25:4273-8.
- Zan J, Chen H, Jiang G, Lin Y, Ding F. Preparation and properties of crosslinked chitosan thermosensitive hydrogel for injectable drug delivery systems. *J Appl Polym Sci* 2006;101:1892-8.
- Zielinski BA, Aebischer P. Chitosan as a matrix for mammalian cell encapsulation. *Biomaterials* 1994;15:1049-56.

# **Chapter 3**

## **Materials and methods**





### 3.1 Chemicals

#### 3.1.1 Hydrogel preparation and characterization:

Sodium alginate with an average molecular weight of 100,000 g/mol and a guluronic acid content of about 70% (Manugel DJX) was a friendly gift of International Specialty Products Global Technologies Deutschland GmbH (Germany). A second type of Sodium alginate with an average molecular weight of 75,000 g/mol and a guluronic acid content of about 60% commercialized as PRONOVA was bought from Novamatrix FMC biopolymer. Porcine skin gelatin was purchased from Fluka (Germany). Copper(II) nitrate trihydrate ( $\text{Cu}(\text{NO}_3)_2 \cdot 3\text{H}_2\text{O}$ ), strontium nitrate ( $\text{Sr}(\text{NO}_3)_2$ ), zinc nitrate tetrahydrate ( $\text{Zn}(\text{NO}_3)_2 \cdot 4\text{H}_2\text{O}$ ), sodium acetate, sodium hydroxide, sodium metaperiodate ( $\text{NaIO}_4$ ), sodium tetrahydridoborate ( $\text{NaBH}_4$ ), hydrochloric acid (37%), acetic acid (100%) and acetone were purchased in analytical grade from VWR International-Merck (Germany). Hexamethylene diisocyanate (HDI, >99%) was obtained from Sigma Life Science (Germany). For atomic emission spectroscopy standard ion solutions (TraceCert<sup>®</sup>:  $\text{Cu}^{2+}$ ,  $\text{Sr}^{2+}$ , and  $\text{Zn}^{2+}$ ) with a concentration of 1000 mg/L and decomposing acids (TraceSelect<sup>®</sup>), i.e., nitric acid ( $\text{HNO}_3$ ,  $\geq 69\%$ ) and perchloric acid ( $\text{HClO}_4$ , >70%), were bought from Fluka. Phosphate-buffered saline (PBS, 137 mmol/L NaCl, 2.7 mmol/L KCl, 10 mmol/L phosphate buffer, pH 7.4), ruthenium red ( $\geq 85\%$ ) and 4-amino-5-hydrazino-3-mercapto-1,2,4-triazole (Purpald<sup>®</sup>,  $\geq 97\%$ ) were also obtained from Fluka. A bicinchoninic acid protein assay (BCA) was bought from Sigma.

#### 3.1.2. Dorsal root ganglion cultures

Dulbecco's modified phosphate-buffered saline (PBS) (1X) was obtained from PAA Laboratories GmbH. Tris-buffered saline (TBS; pH 7.4) was prepared containing 1.3 mol/L NaCl, 0.0026 mol/L KCl purchased from Merck, 0.024 mol/L Tris base minimum 99.9% titration obtained from Sigma Aldrich. Dulbecco's modified eagle medium (DMEM), containing 5% glutamine and 0.5 % glucose, penicillin (10,000 U/ml)-streptomycin (10,000  $\mu\text{g/mL}$ ), 10% heat inactivated normal horse serum, 3 % donkey serum were purchased from PAN Biotech GmbH (Germany). Recombinant mouse nerve growth factor- $\beta$  (NGF- $\beta$ ) was obtained from R&D Systems GmbH (Germany). Paraformaldehyde (95%) was obtained from Aldrich, Agar, NaCl, HCl from VWR, Triton X-100 and Hoechst<sup>®</sup> dye from Sigma. The following primary antibodies were used for the DRG in vitro study. Mouse anti-GAP43 at

1/100, rabbit anti-p75 neurotrophin receptor at 1/2000, secondary antibodies: donkey anti-mouse (RHOX) and donkey anti-rabbit (FITC) were obtained from Chemicon-Millipore (Germany) at 1/1000.

### **3.1.3 Entorhinal cortex and spinal cord slice cultures**

Minimum essential medium (MEM) was obtained from Gibco (Germany) and supplemented with 2 mmol/L glutamax purchased from PAA Laboratories GmbH. The preparation medium was adjusted to pH 7.3.

The incubation medium contained 50% MEM, 25% basal medium eagle (BME), 2.5% HEPES buffer solution, 1.5% glucose, 1% glutamax all were purchased from Gibco and 1% sodium bicarbonate (7.5% solution) obtained from PAA Laboratories GmbH, (Germany), 25% heat-inactivated normal horse serum. The pH of the incubation medium was adjusted to 7.2.

The following antibodies were used for the entorhinohippocampal and spinal cord slice cultures. The primary antibody guinea pig anti-GFAP was obtained from Progen Biotechnik (Germany) and diluted at 1/1000. Mouse anti-GAP43 and rabbit anti-NF200 were used at 1/100 and 1/500, respectively. Mouse anti-NeuN was obtained from Chemicon-Millipore and used at 1/500. The secondary antibodies donkey anti-mouse (RHOX), donkey anti-guinea pig (FITC) and donkey anti-rabbit (FITC) were obtained from Chemicon-Millipore (Germany) at 1/1000. ProLong antifade kit was obtained from Molecular Probes.

### **3.1.4 *In vivo* experiments**

**3.1.4.1 Anesthetics:** Ketamine (62.5 mg/kg) and xylazine (3.175 mg/kg) were purchased from WDT (Germany), acepromazine (0.625 mg/kg) from Sanofi-Ceva (Germany) and dissolved in sterile 0.9% saline solution which was bought from Braun (Germany). Gel foam was also obtained from Braun (Germany).

#### **3.1.4.2 Perfusion and spinal cord tissue preparation**

Different solutions were used during perfusion and spinal cord tissue preparation. These solutions were 0.9 % saline solution, 4% paraformaldehyde (PFA), 30% sucrose, cryo protectant solution (CPS), 0.2 M phosphate buffer (pH 7.4) and tissue-Tek purchased from Sakura Finetek (NL). These solutions were prepared as follows:

Phosphate buffer solution: One liter of phosphate buffer solution contains 0.04 mol/L  $\text{NaH}_2\text{PO}_4 \cdot \text{H}_2\text{O}$ , 0.15 mol/L  $\text{Na}_2\text{HPO}_4 \cdot 7\text{H}_2\text{O}$  obtained from VWR (Germany).

4% paraformaldehyde: One liter of 4% PFA contains 40 g of paraformaldehyde prills obtained from Aldrich, 1 ml 10M NaOH obtained from VWR (Germany) and 500 ml phosphate buffer.

30% sucrose solution: One liter of solution contains 0.87 mol/L sucrose obtained from VWR (Germany), 400 ml phosphate buffer and 400 ml Millipore water.

Cryoprotectant solution: One liter of CPS solution contains 3.2 mol/L glycerin, 4.4 mol/L ethylene glycol obtained from VWR (Germany), 250 ml phosphate buffer and 250 ml Millipore water.

Nissl staining: For Nissl staining following chemicals were used: thionin and anhydrous chloroform (99%) were obtained from Sigma, absolute ethanol purchased from J. T. Baker, (Holland), 1M acetic acid, 1M NaOH, neoclear<sup>®</sup> and neomount<sup>®</sup> purchased from Merck, (Germany).

For all solution preparation de-ionised water used which was further purified with a Milli-Q<sup>®</sup> water purification system of Millipore (France); the purified water had a specific resistivity not lower than 18 M $\Omega$ :cm.

### **3.1.4.3 Animals**

*In vitro* experiments: For all *in vitro* experiments postnatal Wistar rats from in house breeding day 2-6 were used.

*In vivo* experiments: For all *in vivo* experiments adult female Fischer 344 rats (160-180 g) were used. All experiments were carried out in accordance with the institutional guidelines for animal care. All efforts were made to minimize the number of animals used. Animals had ad libitum access to food and water throughout the study. All surgical procedures were performed under anaesthesia.

## 3.2 Methods

### 3.2.1 Preparation of alginate-based capillary hydrogels

*Gel formation:* Sodium alginate was dissolved at a concentration of 20 g/L (2% w/w) in purified water. Optionally porcine skin gelatin was added to this solution at a concentration of 2 g/L (0.2% w/w). Electrolyte solutions ( $\text{Cu}(\text{NO}_3)_2$ ,  $\text{Sr}(\text{NO}_3)_2$ ,  $\text{Zn}(\text{NO}_3)_2$ ) were prepared at a concentration of 1 mol/L in purified water. All solutions were subsequently filtered through a Nalgene<sup>®</sup> vacuum filtration system equipped with a polyethersulfone membrane with a pore size of 0.2  $\mu\text{m}$  obtained by VWR International (Germany). 65 grams of alginate solution were poured into anodised cylindrical aluminium moulds (5.5 cm in diameter and 4 cm in height), covered by a glass lid, and allowed to stand for about 2 h; the alginate molecules should get close contact with the hydrophilic walls of the mould which is important for the stability during gel formation. Then the electrolyte solution was sprayed onto the alginate solution using a pump spray bottle (VWR) until the alginate was covered by a 5 mm thick layer of electrolyte solution (~10 mL); after several minutes another 10 mL of electrolyte solution were filled onto the alginate using a piston pipette. Moulds were covered by a lid and allowed to stand for at least one day until gel formation was finished. With the help of a spatula the metal alginate or metal gelatin/alginate gels were carefully removed from the aluminium moulds and immersed in sterile filtered water or 2 g/L gelatin solution, respectively, to remove excessive electrolyte; the water or gelatin solution was changed after at least 4 h for not less than 4 times.

*Gel cutting:* The obtained gel bodies were cut perpendicular to the longitudinal axis of the capillaries using a custom-made cutting machine. Gel bodies were mounted onto a slide, whose position in relation to the blade could be adjusted in a defined way. After removing the non-structured top layer of the gel (5 mm) one slice of 15 mm in thickness was cut from the gel cylinder.

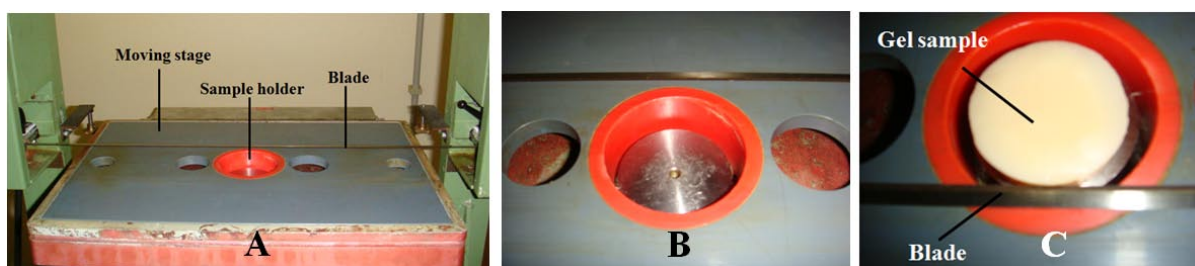


**Figure 3.1: Custom made cutting machine. Machine showing sample holder, cutting blade and moving stage (A), close up view of blade approaching towards sample holder (B), alginate gel in sample holder and blade cutting the gel (C).**

*Dehydration, crosslinking and ion exchange:* Gel slices were dehydrated by equilibrating in acetone/water mixtures of rising acetone content (25%, 50%, 75%) for a minimum of 4 h per step; then the gels were equilibrated in pure acetone and then in dry acetone twice for not less than 4 h per step; solutions are slightly agitated by stirring. Hexamethylene diisocyanate (HDI) was dissolved in dry acetone at a concentration of 0.1 mol/L and dehydrated acetone-soaked alginate gels were immersed in HDI solution for 4 h under slight stirring. Gels were removed from HDI solution and immersed in dry acetone for 5 min to remove HDI from the capillary lumens. Then the gel slices were put between two filter papers and dried in air for 10 min to remove acetone from the capillary lumens. The gels were immersed in sterile filtered water (with a load from the top because gels are swimming on the water interface) for 4 h under slight stirring. Then they were heated in water to 70°C for additional 2 h until carbon dioxide development stopped. After that, the gels were immersed in 1 mol/L hydrochloric acid solution (HCl) five times for at least 2 h under slight stirring to remove the crosslinking divalent cations. Finally, the gels were immersed in sterile filtered water for several times until the water reached a neutral pH. Gels were sterilised by incubation in 70% ethanol for 5 min and finally kept in sterile phosphate-buffered saline (PBS; pH 7.4).

### **3.2.1.1 Characterisation of alginate hydrogels**

*Pore structure:* Blocks of alginate hydrogels (5 mm x 5 mm x 15 mm) were cut from the gel cylinders using razor blades. Gel slices with 500  $\mu\text{m}$  in thickness were prepared from these blocks using a vibrating microtome VT1000 S of Leica (Germany). These thin slices were immersed in a 200 mg/L solution of ruthenium red in water for 1 h to enhance the contrast for light microscopy analysis (Figure 3.1). Images of the capillary structure were prepared using

a Eclipse E-400 light microscope from Nikon (Japan) in 50 to 200-fold magnification, a TK-1380-E Video Camera from JVC (Japan), and the Studio Quick Start software, version 8, from Pinnacle Systems Inc. (USA). Images were analysed by a self-made computer program regarding capillary diameter and capillary density. For each type of gel a minimum of 10 different images was used for structure characterization.

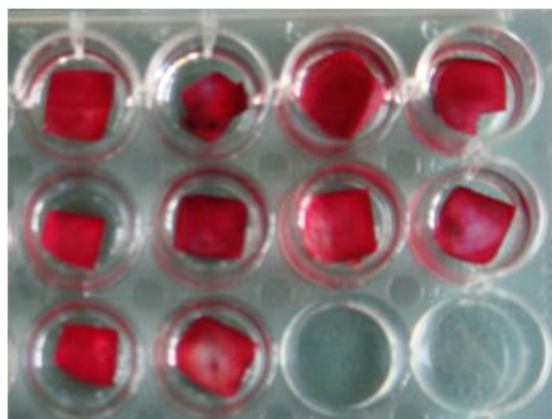


**Figure 3.2: Alginate gel slices in ruthenium red solution for pore structure analysis.**

*Ion exchange:* The efficacy of the ion exchange process was controlled by atomic emission spectroscopy. The gel cylinders were cut into slices of 2 mm in thickness using our custom-made cutting machine and then pieces of 10 mm in diameter were prepared using a hollow punch. The ion exchange process was performed 0 – 5 times by immersing the small gel specimens in 1 mol/L HCl solution for a minimum of 2 h per step. At the end, all gel samples were washed with water until a neutral pH was reached and dried by lyophilisation. The weight of each sample was measured using a MT-5 electronic microbalance of Mettler Toledo (Germany). The dried gel samples were individually placed in small porcelain cups and heated at 120°C after addition of 2 ml of ultra-pure concentrated HNO<sub>3</sub> until the liquid was completely vaporised. Then 2 ml of ultra-pure concentrated HClO<sub>4</sub> were added and the solution was heated again until the liquid was completely vaporised. The decomposition procedure using HClO<sub>4</sub> was repeated until a colourless remnant remained. This remnant was carefully dissolved in 0.5 mol/L ultra-pure HNO<sub>3</sub> solution and transferred into a calibrated 10-ml glass flask. The solutions obtained after alginate gel decomposition were analysed regarding their metal ion content by inductively coupled plasma atomic emission spectroscopy (ICP-AES) using a Spectroflame-EOP of Spectro Analytical Instruments GmbH

(Germany). Standard solutions were prepared within the concentration range 0.01 – 100 mg/L. The identified amount of the remaining cation was related to the weight of the dried gel sample (nmol cation / mg dried gel). A minimum of three specimens per type of cation and number of HCl washings was analysed.

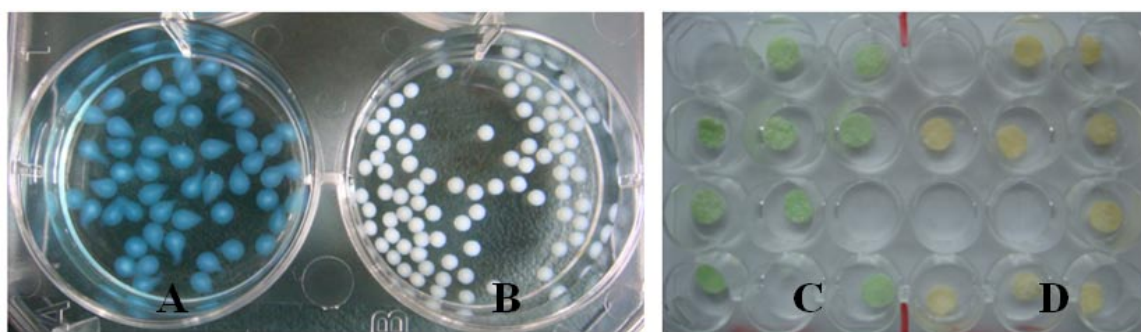


**Figure 3.3: Alginate gels in the form of beads (A, B) and slices (C, D) before (ion removal) HCl washing (A, C) and after (ion removal) HCl washings (B, D).**

*Stability testing:* Small gel slices of copper alginate with 2 mm in thickness and 10 mm in diameter have been used for stability testing. One group of the samples was crosslinked by HDI reaction, the other was not crosslinked. Copper ions were removed by HCl immersion from both groups and then the gel specimens were individually placed into the wells of 24-well culture plates (Nunc<sup>®</sup>) which were obtained from VWR. The samples were incubated in 2 ml of PBS solution at 37°C using a Cytoperm<sup>®</sup> incubator from Heraeus (Germany) and after 1, 3, 7, and 14 d the liquid was removed. Alginate dissolved from the gel samples was quantified using the Purpald<sup>®</sup>-assay after hydrolysis and oxidation of the carbohydrate moieties with NaIO<sub>4</sub> as described previously (Avigad G *et al.* 1983). For hydrolysis, 0.5 ml of 2 mol/L sodium hydroxide solution was added to 1.5 ml of the alginate containing supernatant, transferred into pressure-resistant Schott<sup>®</sup> screw cap glass vials (VWR) and heated at 75°C over night. The cooled hydrolysate was neutralised by adding 165 µl 6 mol/L HCl and mixed with 2.835 ml of a 0.1 mol/l acetic acid/sodium acetate buffer solution (pH 5.4) to give a sample volume of 5 ml. Then, 0.5 ml of this solution were transferred into the well of a 24-well culture plate and incubated after addition of 0.5 ml of a 30 mmol/L solution of NaIO<sub>4</sub> in acetic acid/sodium acetate buffer for 1 h in the dark at 20 °C. A 200 µl aliquot of



the oxidised alginate solution was transferred into a new well and incubated after addition of 300  $\mu$ l of a 0.1 mol/L Purpald<sup>®</sup> solution in 1 mol/L NaOH for 30 min at 20 °C. Finally, 500  $\mu$ l of a 0.1 mol/L NaBH<sub>4</sub> solution in 1 mol/L NaOH were added. The absorbance of the resulting solution was measured at 546 nm. As blanks, solutions consisting of NaIO<sub>4</sub>, Purpald<sup>®</sup>, and NaBH<sub>4</sub> without hydrolyzed alginate were used. A minimum of four gel samples per crosslinking condition and time point was used for stability testing.

*Gelatin content:* Small beads of copper alginate and copper gelatin/alginate were prepared by dropping 2% alginate solution into 1 mol/l Cu(NO<sub>3</sub>)<sub>2</sub> solution by the use of a burette. Beads were crosslinked with HDI and copper ions were removed with HCl as described above. Then, the beads were placed in different numbers into 2-mL Eppendorf<sup>®</sup> cups and incubated with 1.5 ml of the BCA protein assay working solution for 30 min at 40°C. The presence of the gelatin constituent was monitored by the development of a purple colour which was measured at 562 nm on a Lamda-18 UV/Vis spectrophotometer of Perkin Elmer Corp. (USA). Optical density was related to the number of beads and the dry weight which was determined after freeze drying.

### **3.2.2 In vitro model of regeneration: Isolation of dorsal root ganglia**

Dorsal root ganglia (DRG) were prepared from postnatal day 2-6 Wistar rats. Immediately after decapitation of the animals, the vertebral column was removed. Muscles and bones covering the spinal cord dorsally were removed, until the spinal cord surface and DRG located just outside of the spinal canal became visible. DRG were isolated from the cervical, thoracic, and lumbar region using a fine forceps and transferred into ice cold phosphate-buffered saline (PBS).

Gel samples were cut into defined dimensions (5mm x 5mm and capillary length 500  $\mu$ m) with a vibratome (Leica) and stored in 70% ethanol. Gel slices were washed twice with 0.1 mol/l PBS, first overnight and then for one hour. Finally they were equilibrated in incubation medium. As incubation medium we used Dulbecco's modified eagle medium supplemented with 100 U/ml penicillin, 100  $\mu$ g/ml streptomycin, 10% heat inactivated normal horse serum and 40 ng/ml NGF. The medium soaked gel slices were placed onto Millicell<sup>®</sup>-CM membranes (Millipore). Then, the isolated DRG were placed on top of the gels and incubated for 7 days in a humidified atmosphere with 5% CO<sub>2</sub> at 37°C. Medium and growth factors were changed in 2-day intervals during the incubation period.

Neurite outgrowth from DRG cultured on top of the pure anisotropic capillary hydrogels (pACH) and gelatin modified anisotropic capillary hydrogels (gACH) was performed for all types of alginate gels (pACH<sub>Cu,Sr,Zn</sub> and gACH<sub>Cu,Sr,Zn</sub>). We repeated this experiment three times using one gel per experiment for all type of alginate each time under same conditions and same sample sizes with 8-10 DRG on each gel.

### 3.2.2.1 Immunohistochemical analysis

After 7 days in culture with DRG gels were fixed in 4% paraformaldehyde in PBS for 2 h at room temperature. After embedding into agar gel (4%), hydrogels were cut parallel to the capillary orientation with the microtome. In case of small capillary diameters pACH<sub>Cu,Sr</sub> and gACH<sub>Cu,Sr</sub> the section thickness was adjusted at 80 µm, whereas gels with wider capillary diameters pACH<sub>Zn</sub> and gACH<sub>Zn</sub> sections were cut at 100 µm to avoid disintegration of these gels during the cutting process.

Double immunofluorescence techniques were performed to assess axon regrowth and Schwann cells migration into the capillary hydrogels. After washing the samples 3 x 5 min with tris-buffered saline (TBS; pH 7.4), non-specific antigens were blocked by incubating the sections for 2 h in a solution containing TBS, 0.1% Triton X-100 and 3% donkey serum. Then the sections were transferred into a solution of the respective primary antibody and incubated overnight at 4°C. The following primary antibodies were used: mouse anti-GAP43 for regenerating axons and rabbit anti-p75 neurotrophin receptor for Schwann cells. On the following day, the sections were washed 2 x 10 min with TBS and incubated with the secondary antibody solutions (donkey anti-mouse (RHOX) and donkey anti-rabbit (FITC), in TBS + 0.1% Triton) for 2 h. After one washing step thereafter the sections were counterstained with Hoechst<sup>®</sup> for 15 min. After one washing with TBS, the samples were mounted and coverslipped using the ProLong<sup>®</sup> Antifade Kit.

Confocal immunofluorescence microscopy (Leica TCS-NT, Germany) was performed at 250x magnification. an average of 40-50 scans through the z-axis of the section starting at the first scan containing specific fluorescence and ending at the last scan with detectable fluorescence were made and overlaid. Overlaid micrographs were used for quantification of axon length/density (GAP-43 immunoreactivity) and Schwann cell density (p75 low affinity NGF receptor immunoreactivity). We used three images per experiment for each condition, so a total of nine images for each condition were analysed out of three independent

experiments. Axon outgrowth was quantified by counting the number of fluorescent pixels using Scion Imaging freeware for Windows (Scion Corp.,USA). For axon length, the three longest axons per image were measured. Axon density and Schwann cell density were measured by two methods. First, the density per scaffold was measured by using defined square areas and secondly, the density per capillary volume was measured using exactly the areas determined by the different capillary diameters. For the first method, the defined square area had 120  $\mu\text{m}$  in length (150 pixel) and 80  $\mu\text{m}$  in width (100 pixel) resulting in 9600  $\mu\text{m}^2$  (15,000 pixel) area. For the second method, we quantified axon density and Schwann cell density within single capillaries for which we selected different areas depending on the varying capillary diameters.

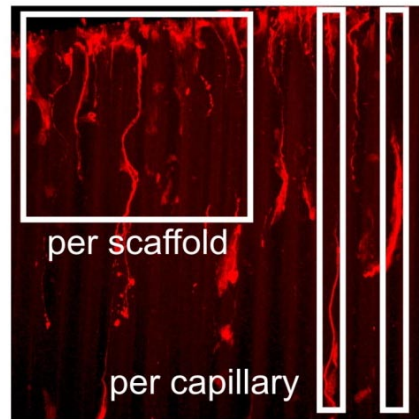


**Figure 3.4: Schematic drawing of methods used for quantification of signal density per scaffolds and density per capillary volume.**

The capillaries of the pACH<sub>Cu</sub> and gACH<sub>Cu</sub> had an area of  $\sim 5,000 \mu\text{m}^2$  (7,776 pixels) of pACH<sub>Sr</sub> and gACH<sub>Sr</sub>  $\sim 7,500 \mu\text{m}^2$  (11,664 pixels) and of pACH<sub>Zn</sub> and gACH<sub>Zn</sub>  $\sim 34,800 \mu\text{m}^2$  (54,460 pixels) respectively. To approximate the sampled areas in each condition, similar size the sampled areas in pACH<sub>Cu</sub>, gACH<sub>Cu</sub> and pACH<sub>Sr</sub>, gACH<sub>Sr</sub> conditons were adjusted to the average area of one pACH<sub>Zn</sub>, gACH<sub>Zn</sub>. Accordingly, 7 capillaries from pACH<sub>Cu</sub> and gACH<sub>Cu</sub> (total area is 54432 pixels, 972 pixels more than the area of pACH<sub>Zn</sub> and gACH<sub>Zn</sub>), and 5 capillaries from pACH<sub>Sr</sub> and gACH<sub>Sr</sub> (total area is 58320 pixels, 4860 pixels more than the area of pACH<sub>Zn</sub> and gACH<sub>Zn</sub>) were selected.

### **3.2.3 In vitro models: Central nervous system slice culture models**

#### **3.2.3.1 Entorhino-hippocampal slice culture**

Slice cultures were prepared from postnatal day 2-4 Wistar rat brain according to the previously published protocols (Stoppini L *et al.* 1991, Gahwiler BH *et al.* 1997). In brief, after decapitation of the animals, the hippocampus with the attached entorhinal cortex was dissected (Bilaterally) in ice-cold preparation medium and transverse slices of 400 µm were cut using a tissue chopper (McIlwain). Each postnatal rat brain yielded between 6 and 8 entorhino-hippocampal slices (per side). Slices were completely transected from the rhinal fissure to the hippocampal fissure using a sterile scalpel blade (Prang P *et al.* 2001). The isolated entorhinal cortex 4-6 slices were then transferred onto defined blocks of pACH and gACH which were already placed on millicell Millipore membranes which were immersed in incubation medium. After that, specimens were incubated for 7 days in incubation medium and humidified atmosphere with 5% CO<sub>2</sub> at 37°C. Incubation medium was changed every two days.

#### **3.2.3.2 Spinal cord slice culture**

Spinal cord slices were prepared from postnatal day 4-6 Wistar rats. After decapitation the complete vertebral column with surrounding muscle was removed and washed in ice cold PBS. The spinal cord was rapidly dissected out with fine scissors and transferred into ice cold preparation medium. The thoracic and lumbar spinal cord was used for further slice culture. Spinal slices of 400 µm were cut with the McIlwain tissue chopper and transferred onto defined alginate gel blocks. Up to 4-6 slices were kept on pACH and gACH blocks. Alginate blocks were already placed on millicell Millipore membranes in incubation medium. Filters were placed onto 1 ml of medium in a humidified incubator at 37°C with 5% CO<sub>2</sub> enriched atmosphere. Incubation medium was changed every two days.

#### **3.2.3.3 Morphological analysis of *in vitro* slice cultures**

The same procedure used to cut the gels after incubation for immunohistochemistry characterization. The gels had same thickness for each gel type maintained in DRG culture. The same procedure was followed for slice culture analysis. In short, the primary antibodies used for analysis of slice cultures were mouse anti-gap43, guinea pig anti-GFAP and rabbit anti-NF200. On the following day, sections were incubated with donkey anti-mouse, donkey

anti-rabbit (RHOX) and donkey anti-guinea pig (FITC) secondary antibodies. Additionally, sections were counterstained with Hoechst for 15 min. After one wash with TBS, sections were coverslipped using the ProLong<sup>®</sup> Antifade Kit. Axon and astroglia density were quantified in 3 images per condition and experiment; a total of 3 independent experiments for each condition were performed. Images were taken from those regions with highest immunoreactivity for axonal/astroglial marker with confocal laser microscopy same as above. Axon density and astrocyte cell density were measured by using the two methods which were described above for DRG culture. The capillary diameters of PRONOVA gels were different from those of the ISP gels used for DRG culture. Therefore, different sampling areas were selected. The capillaries of the pACH<sub>Ba</sub> and gACH<sub>Ba</sub> had an area of 5088 pixels (5088 x 7 capillaries = 35616 pixels), pACH<sub>Cu</sub> and gACH<sub>Cu</sub> had an area of 6784 pixels (6784 x 5 capillaries = 33920 pixels), of pACH<sub>Sr</sub> and gACH<sub>Sr</sub> had an area of 10176 pixels (10176 x 3 capillaries = 30528 pixels), and of pACH<sub>Zn</sub> and gACH<sub>Zn</sub> 33920 pixels, respectively.

### **3.2.4 Spinal cord injury *in vivo* model**

#### **3.2.4.1 Surgical procedures**

Spinal cord lesions were performed as previously described (Voremen M *et al.* 2003, Weidner N *et al.* 1999). Briefly, the dorsal columns containing the dorsal corticospinal tract and ascending proprioceptive projections were transected at cervical level C3 using a tungsten wire knife (David Kopf Instruments, USA). Immediately after injury, a dura incision was made along one half of previous wire knife transection. pACH and gACH blocks with standardized dimensions were inserted into the transection site. The orientation of the ACH capillaries followed the longitudinal axis of the spinal cord. The lesion/implantation site was covered with gel foam and antibiotic powder before readapting muscular layers and stapling the skin above the lesion.

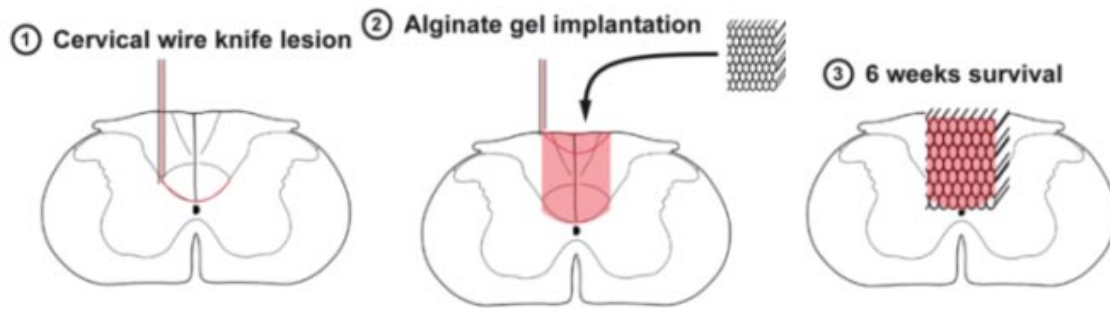


**Figure 3.5: Schematic drawing of spinal cord lesion using wire knife (1), implantation of alginate gel (2), integration of gel into lesion site (3).**

### **3.2.4.2 Processing of spinal cord tissue**

After perfusion of animals for 10 min with ice cold 0.9% saline and 15 min with fresh ice cold 4% PFA, spinal cord tissue was postfixed overnight in 4% PFA at 4°C. The following day spinal cords were transferred into 30% sucrose and kept for 3 days at 4°C before cutting the tissue embedded in Tissue-Tek (Sakura Finetek) on the cryostat (CM3000, Leica) at – 20°C. The tissue was cut on the cryostat and sections were collected in CPS. Every seventh section was collected separately on gelatin coated glass slides. Air dried sections were used for Nissl staining to see the integration of tissue. The sections were stored at 4°C till further use.

### **3.2.4.3 Nissl staining**

This method is used for the detection of nissl body in the cytoplasm of neurons on PFA fixed frozen sections. The nissl body will be stained purple-blue. This stain is commonly used for identifying the basic neuronal structure in brain or spinal cord tissue.

**Preparation of thionin:** To prepare 500 ml of thionin solution 18 ml 1M NaOH was added to the 100 ml of 1M acetic acid. The volume of 500 ml was made by addition of water. This solution was heated until steamy and then 1.25 g (0.01 mol) of thionin was added and boiled for 45 min afterwards cooled to room temperature and filtered into brown glass bottle. This solution can be stored at 37°C for 2-3 months.

**Nissl Staining procedure:** Tissue sections on gelatin coated slides were first washed in 1:2 chloroform/ethanol for 30 min and then rehydrated by immersion in ethanol/water mixture of

declining concentration of alcohol starting with 100% ethanol, over 95% to 70% to 50% ethanol for 2 min in each washing step and finally specimens were washed with distilled water for 5 min. This so called de-fating step reduced background fat staining. After that specimens were incubated in thionin solution for 30-40 seconds and quickly rinsed in distilled water about two times 10 dips each. Then the sections were dehydrated again from 50% ethanol over 70%, 95% to 100% ethanol 2 min for each step. After dehydration, sections were put in Neoclear<sup>®</sup> for 10 min and finally mounted with Neomount<sup>®</sup>.

#### **3.2.4.4 Morphological analysis of spinal cord tissue**

Double labelling immunofluorescence techniques were performed on 35 µm sagittal free-floating sections. The CPS stored sections were washed thrice with TBS 10 min each. The staining procedure was the same like in DRG and EC slice culture. In short, following primary antibodies were used: guinea pig anti-GFAP, rabbit anti-200 kD neurofilament (NF-200) and mouse anti-GAP-43. The following day, sections were incubated with secondary antibody solutions containing donkey anti-mouse (RHOX), donkey anti-rabbit (RHOX) or donkey anti-guinea pig (FITC) for 2h. Sections were counterstained with Hoechst for 15 min. After one wash with TBS, sections were mounted onto glass slides and cover-slipped with ProLong Antifade Kit.

#### **3.2.5 Statistical analysis**

All data were expressed as the medians including the 25-75% quartiles for alginate characterisation and mean standard deviation for DRG, EC slice culture, spinal cord slice culture, NPC differentiation and *in vivo* experiments. The statistical significance of differences was assessed by one-way analysis of variance (ANOVA) followed by Newman-Keuls post-hoc-test for comparison of axonal outgrowth in alginate hydrogels made with different cations. The statistical significance of axonal outgrowth in hydrogels with and without gelatin was assessed using the t-test followed by the nonparametric Mann-Whitney-U-Test (GraphPad, Prism 5 Software). Significance was accepted at a level of  $p < 0.05$ .

## References:

- Avigad G. A simple spectrophotometric determination of formaldehyde and other aldehydes: application to periodate-oxidized glycol systems. *Anal Biochem* 1983;134:499-504.
- Gahwiler BH, Capogna M, Debanne D, McKinney RA, Thompson SM. Organotypic slice culture: a technique has come of age. *Trends Neurosci* 1997;20:471-77.
- Pfeifer K, Vroemen M, Caioni M, Aigner L, Bogdahn U, Weidner N. *Reg Med* 2006;1: 255-66.
- Prang P, Del Turco D, Kapfhammer J. Regeneration of entorhinal fibers in mouse slice cultures is age dependant and can be stimulated by NT-4, GDNF and modulator of G-proteins and protein kinase C. *Exp Neurol* 2001;169:135-47.
- Stoppini L, Buchs PA, Muller DA. Simple method for organotypic cultures of nervous tissue. *J Neurosci Methods* 1991;37:173-82.
- Vroemen M, Aigner L, Winkler J, Weidner N. Adult neural progenitor cell graft survive after acute spinal cord injury and integrate along axonal pathways. *Eur J Neurosci* 2003;18:743-51.
- Weidner N, Grill RJ, Tuszynski MH. Elimination of basal lamina and the collagen “scar” after spinal cord injury fails to augment corticospinal tract regeneration. *Exp Neurol* 1999;160:40-50.





# **Chapter 4**

## **Results**



## 4.1 Structure of alginate-based capillary hydrogels

Oriented diffusion of divalent cations into sodium alginate solutions resulted in the formation of metal alginate hydrogels exhibiting a highly anisotropic structure of longitudinally aligned microchannels. These channels or capillaries were almost circular in cross-section and arranged in a more or less hexagonal fashion. Different cations caused the formation of hydrogels with varying capillary diameter and density. For ISP alginate, this is shown in Figure 4.1A. The diameters of the microchannels were about 10  $\mu\text{m}$  by using copper cations, 20  $\mu\text{m}$  by using strontium cations and about 54  $\mu\text{m}$  by using zinc cations, respectively (Figure 4.1B). The process of ionotropic gel formation was influenced when the starting sodium alginate solution was mixed with a gelatin constituent resulting in an alteration of the microchannel structure. When the gelatin content was chosen too high, e.g., 5 g/L gelatin in a 20 g/L sodium alginate solution, completely unstructured alginate-gelatin hydrogels were formed (data not shown). Addition of gelatin at a concentration of 2 g/L did not suppress capillary formation, but resulted in hydrogels with larger microchannel diameters compared to those made of pure alginate. The diameters of the microchannels were about 18  $\mu\text{m}$  by using copper cations, 28  $\mu\text{m}$  by using strontium cations and 77  $\mu\text{m}$  by using zinc cations, respectively (Figure 4.1B). The density of the microchannels within anisotropic capillary hydrogels varied between 27 and about 630 channels/ $\text{mm}^2$  depending on the crosslinking cation and the presence of gelatin (Figure 4.1C).

Results for Pronova alginate are shown in Figure 4.2A. The diameters of microchannels were about 11  $\mu\text{m}$  by using barium cations, 13  $\mu\text{m}$  by using copper cations, 26  $\mu\text{m}$  by using strontium cations, and 89  $\mu\text{m}$  by using zinc cations, respectively (Figure 4.2B). Addition of gelatin at a concentration of 2g/L did not suppress capillary formation, but microchannel diameter differs compared to those made of pure alginate. The diameter of microchannels were about 15  $\mu\text{m}$  by using barium cations, 14  $\mu\text{m}$  by using copper cations, 21  $\mu\text{m}$  by using strontium cations, and 85  $\mu\text{m}$  by using zinc cations, respectively. The density of the microchannels within anisotropic capillary hydrogels varied between 27 and about 915 channels/ $\text{mm}^2$  depending on the crosslinking cation and the presence of gelatin (Figure 4.2C).

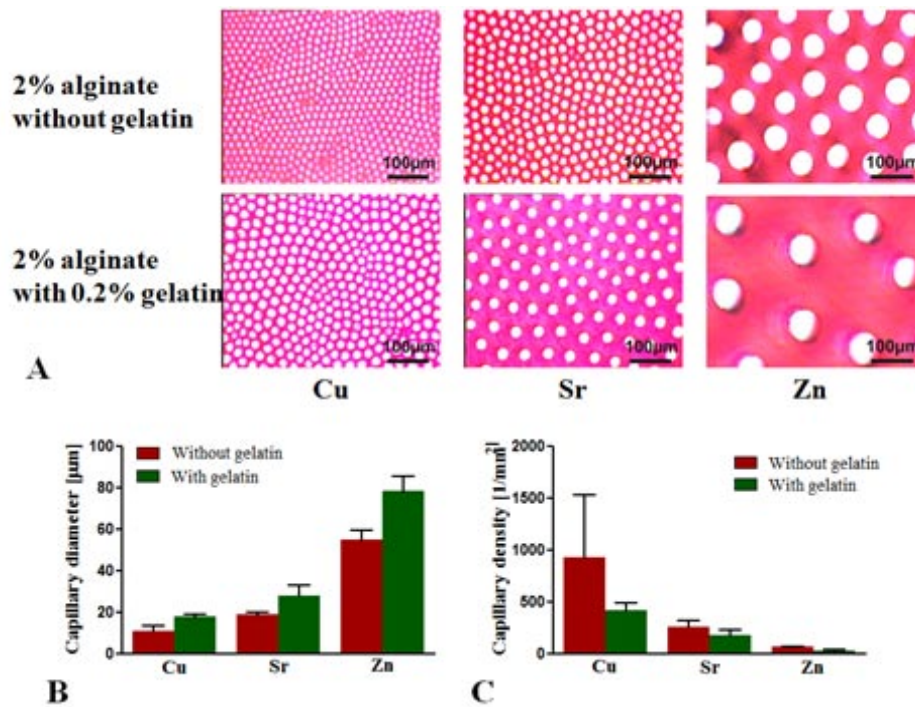


**Figure 4.1: ISP alginate:** Capillary structure of anisotropic alginate hydrogels depending on the metal cation used for ionotropic gel formation. Microscopy images of 2% alginate gels with and without gelatin modification (A), effect of metal ion on capillary diameter (B), and effect of metal ion on capillary density (C).

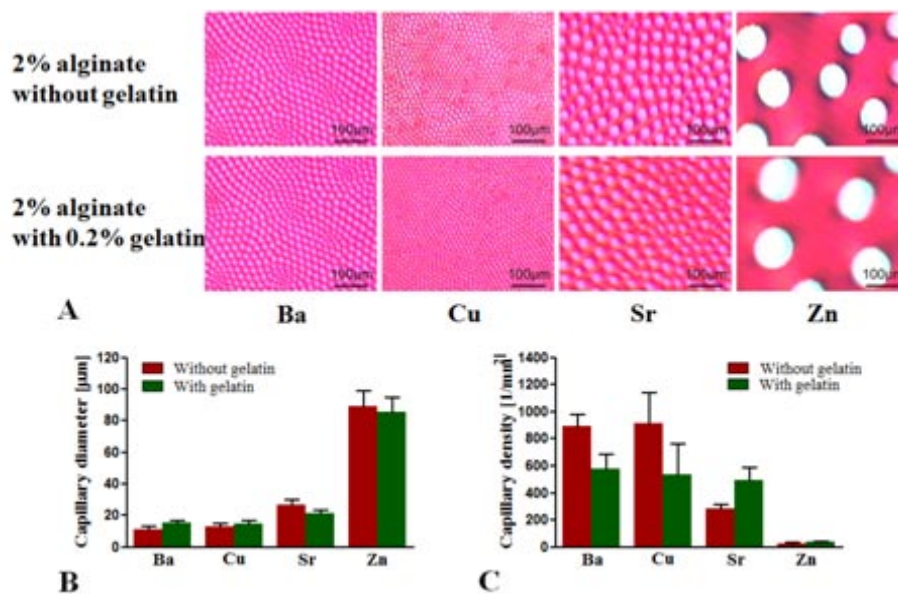


**Figure 4.2: Pronova alginate:** Capillary structure of anisotropic alginate hydrogels depending on the metal cation used for ionotropic gel formation. Microscopy images of 2% alginate gels with and without gelatin modification (A), effect of metal ion on capillary diameter (B), and effect of metal ion on capillary density (C).

### 4.1.1 Ion exchange

The cations we have used to generate anisotropic capillary hydrogels bare the possibility to behave either cytotoxic or to cause allergies. For application of these gels as biomaterials in the nervous tissue, it must first be ascertained whether the crosslinking metal cations have been quantitatively removed by an ion exchange process. We found that the application of 1 mol/l hydrochloric acid solution (HCl) is very effective in removing the crosslinking cations without destroying the structure of the capillary gels (Figure 4.3A), since protonated alginic acid is not soluble in water. As it was monitored by inductively coupled plasma atomic emission spectroscopy (ICP-AES), all types of cations were quantitatively removed requiring 4 times of HCl washing in the case of copper ions, 5 times for strontium and 6 times for zinc, respectively. The results shown here are from ISP alginate. (Figure 4.3B).

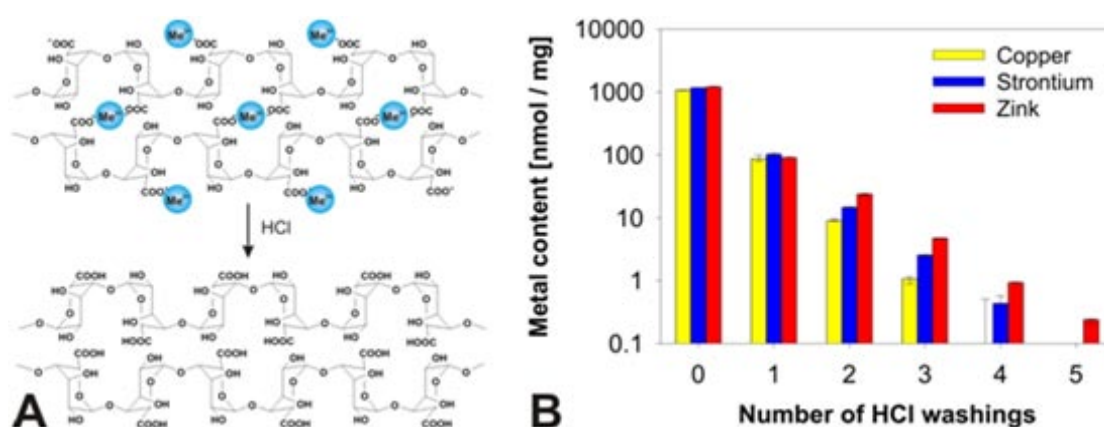


**Figure 4.3: Metal content in alginate hydrogels as determined by ICP-AES. Extraction of metal cations by HCl washing (A), metal content in alginate hydrogels after different numbers of HCl washings (B).**

### 4.1.2 Stabilisation of alginate-based capillary hydrogels

As soon as the gels got in contact with biological medium i.e., cell culture medium, PBS, or serum, the alginic acid dissolved, because monovalent cations, which were present in these liquids in high amounts, displaced the protons of the polyelectrolyte and formed water-soluble salts. Therefore, the anisotropic structure of the alginate gels was further stabilised by chemically crosslinking the hydroxyl groups of the carbohydrate chains via hexamethylene

diisocyanate (HDI). The application of water during the crosslinking reaction also allowed the formation of an interpenetrating network consisting of an aliphatic polyurea (Figure 4.4A). The diffuse reflection infrared fourier transform (DRIFT) spectra of unmodified alginate and HDI-crosslinked alginate are shown in (Figure 4.4B). Crosslinking with HDI caused the introduction of  $\text{CH}_2$ -groups ( $2850\text{ cm}^{-1}$  and  $2950\text{ cm}^{-1}$ ) and amide/urethane functionality at around  $1600\text{ cm}^{-1}$ . Therefore, IR can give a quantitative evidence for successful alginate crosslinking. This procedure yielded in still soft and flexible gels which clearly withstood the dissolution process during incubation in concentrated salt solution (PBS) for at least 14 days. (Figure 4.4C).

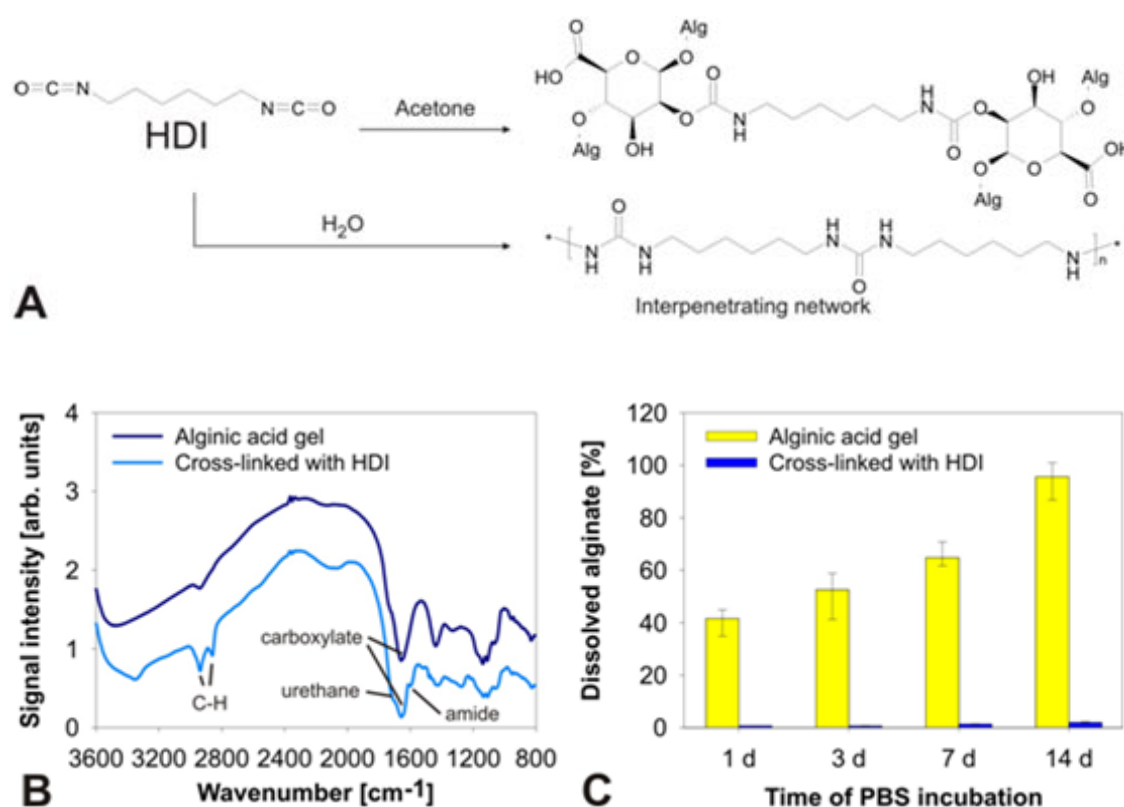


**Figure 4.4:** Strategy for crosslinking alginate molecules and stabilisation of the hydrogel capillary structure by applying HDI reaction (A), DRIFT spectrum shows characteristic peaks of amide and  $\text{CH}_2$  after crosslinking with HDI (B), degradation of alginate gel with and without crosslinking in PBS at different timepoints (C).

### 4.1.3 Determination of the gelatin constituent

Hydrogels which have been prepared from alginate-gelatin mixtures were analysed regarding their final gelatin content. Since it was not possible to quantify the amount of gelatin after gel crosslinking and ion exchange, we can only provide a semi-quantitative proof that at the end of the gel manufacturing process there is still a gelatin constituent detectable. By application of the unspecific BCA protein assay small hydrogel samples (beads) prepared from the purer Pronova alginate and also from ISP alginate have been characterised. It was seen that gels with gelatin resulted in outcome signals that were about 20 times higher than those obtained from gels without gelatin (Figure 4.5). Therefore, the presence of a detectable amount of gelatin was clearly demonstrated. The signal obtained from HDI-crosslinked gels was higher than that obtained from HDI-crosslinked and HCl-washed gels, thus indicating that during the ion exchange process either portions of the gelatin constituent became dissolved or chemical functions, which are active in the BCA assay, became altered.

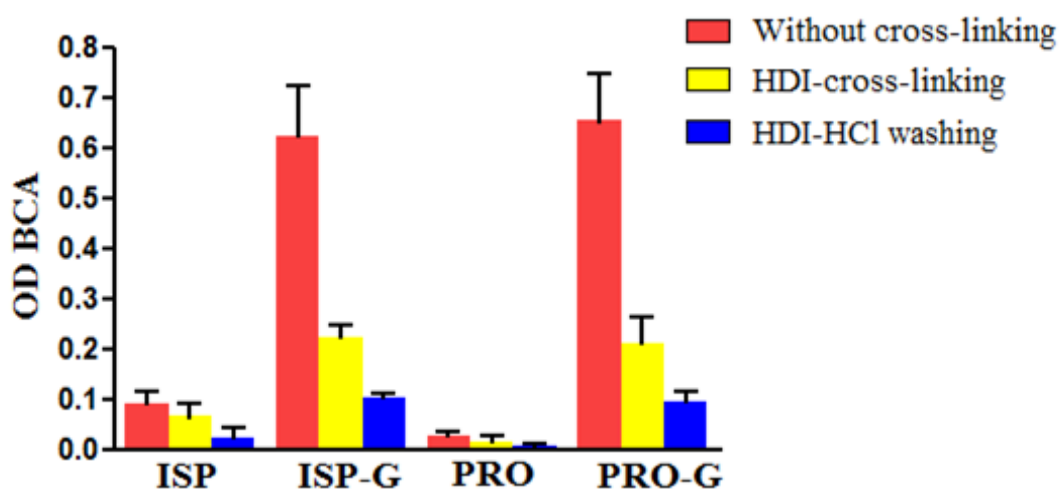


**Figure 4.5:** Gelatin content in alginate hydrogels determined by BCA assay. Gelatin content in ISP and Pronova alginate hydrogels without crosslinking, after HDI crosslinking and crosslinking and ion exchange.



## 4.2 Oriented outgrowth of DRG axons guided by anisotropic capillary hydrogels in vitro

To evaluate the permissiveness and the ability of anisotropic capillary hydrogels to support directed PNS axonal regrowth, dorsal root ganglia (DRG) were cultured on top of defined gel blocks for one week. The microchannels of the gels were oriented in such a way to allow direct transition of axons from the DRG into the anisotropic gel structure (Figure 4.6A). After 1 week, gels were examined immunohistochemically to characterise the axon outgrowth directed by the microchannel structure. Regenerating axons were visualised by detection of growth-associated protein 43 (GAP-43, Figure 4.6B) which is expressed at high levels in the growth cone during axonal regeneration. It can be clearly seen that the outgrowing axons follow the microchannel structure in an almost longitudinally oriented fashion. To assess if the microchannel structure allowed the migration of growth-supporting glial cells, i.e. Schwann cells, gel sections were stained for p75 low affinity nerve growth factor receptor (pNGFr) (Figure 4.6C) which is a surface marker for Schwann cells. Nuclear counter staining (Figure 4.6 E) from different section and not confocal image indicates that the hydrogels are densely packed with cells migrating in from the DRG. The merged image of Figure 4.6D provides an indication that axonal outgrowth into the microchannels is correlated to the presence of Schwann cells and that axons were frequently crossing the complete distance of the capillaries (500 $\mu$ m). The orientation of axons and cells decreases with increasing capillary diameter. Which we did not quantify, but can easily identified in the micrographs.

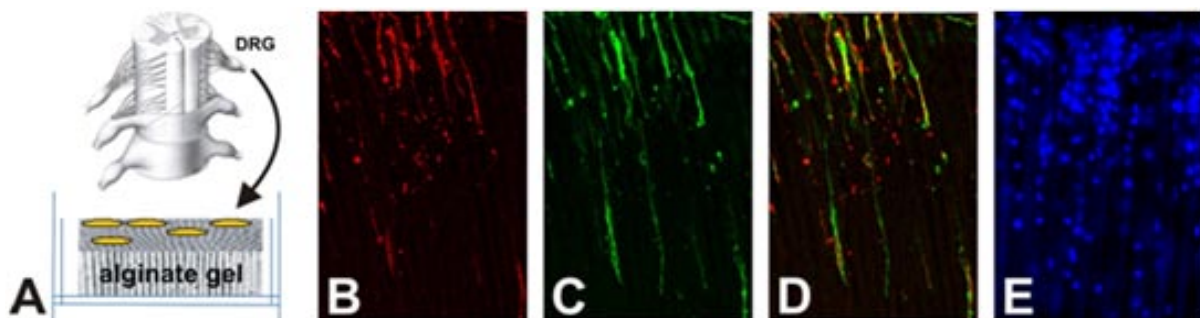


**Figure 4.6:** Neurite outgrowth from dorsal root ganglion culture into capillaries of alginate hydrogel. Isolation and culture of DRG *in vitro* on ACH gels (A), immunohistochemical analysis shows axon outgrowth (B) and Schwann cell migration (C), axons colocalized with Schwann cells (D), nuclear marker also shows cell migration into the capillary structure (E).

### 4.2.1 Influence of capillary diameter and gelatin constituent on axonal outgrowth

DRG were cultured on top of pure alginate hydrogel (pACH) or gelatin modified hydrogel (gACH) made with ISP alginate having a microchannel structure with capillary diameters varying between 10 and 77  $\mu\text{m}$ . From the confocal microscopy images of GAP-43 stained sections (Figure 4.8A) we quantified axon regeneration by determining the length of axon ingrowth into the hydrogels and axon density within the hydrogels. These parameters were correlated with the capillary diameter and the composition of the hydrogels.

Axon length was assessed by using nine sections from three individual experiments, whereby the three longest axons from each sample were selected. For the pACH no significant difference in the axon length depending on the capillary diameter was found (Fig.4.7A). In gACH (Figure 4.7B), hydrogels with wider capillaries (gACH<sub>Sr</sub>, gACH<sub>Zn</sub>) induced significantly longer axon ingrowth compared to gACH<sub>Cu</sub>. However, no significant difference was found between gACH<sub>Sr</sub> and gACH<sub>Zn</sub>. Pairwise comparison of pACH and gACH (Figure 4.7C) prepared by the same cation revealed no difference for the pACH<sub>Cu</sub> (325.38  $\mu\text{m}$ ) and gACH<sub>Cu</sub> (332.20  $\mu\text{m}$ ). In pACH<sub>Sr</sub> (341.73  $\mu\text{m}$ ) and gACH<sub>Sr</sub> (418.55  $\mu\text{m}$ ) and pACH<sub>Zn</sub> (345.90  $\mu\text{m}$ ) and gACH<sub>Zn</sub> (417.74  $\mu\text{m}$ ) the quantification of length of axon ingrowth was significantly increased in the gACH compared to pACH. The capillary size of the pACH and gACH changed from 11 to 18  $\mu\text{m}$  ( $\text{Cu}^{2+}$ ), from 19 to 27  $\mu\text{m}$  ( $\text{Sr}^{2+}$ ) and from 54 to 78  $\mu\text{m}$  ( $\text{Zn}^{2+}$ ), respectively.

To characterise the influence of the microchannel structure on the axon density we used two different methods (Figure 4.8B) to assess the axon specific immunoreactivity visualized with fluorescence and detected with laser confocal microscopy (Figure 4.8A). In the first method we defined a specific area of the hydrogel containing several individual capillaries and assessed the axon density per scaffold in terms of the percentage of positive pixels occupied with fluorescence immunoreactivity within this specific area. In the second method we defined the areas of single capillaries and assessed the axon density per capillary in terms of the percentage of positive pixels occupied with fluorescence immunoreactivity within these capillary areas. For method one, nine sections from three individual experiments were analysed and for method two the best 15 individual capillaries from these nine sections were used.

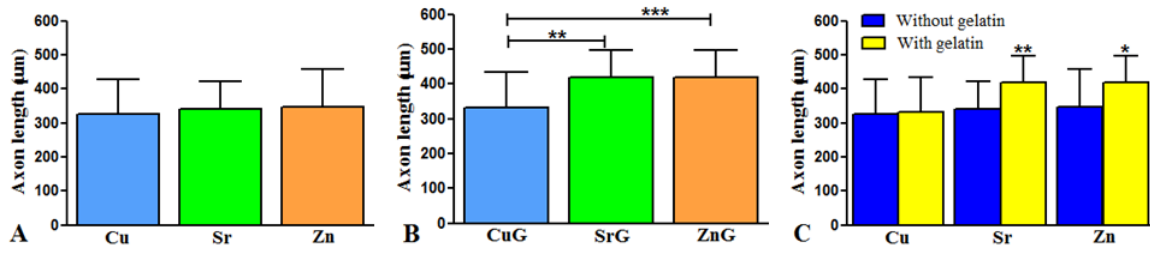


**Figure 4.7: Axon length from DRG within capillaries of ISP alginate hydrogels. Axon length determination on the basis of capillary diameter in pACH (A) and gACH with (B) and pair wise comparison between pACH and gACH with same cation (C). \* $p < 0.05$ , \*\* $p < 0.01$ , \*\*\* $p < 0.001$ .**

The axon density per scaffold increased with increasing diameter of the microchannels (Figure 4.8C,D). For the pACH significant differences were found between those made with pACH<sub>Cu</sub> (1364 pixels) and pACH<sub>Zn</sub> (2949 pixels) and those made with pACH<sub>Sr</sub> (1935 pixels) and pACH<sub>Zn</sub> (2949 pixels). The gACH displayed significant differences between gACH<sub>Cu</sub> (1313 pixels) and gACH<sub>Sr</sub> (2739 pixels) and also between gACH<sub>Cu</sub> and gACH<sub>Zn</sub> (3975 pixels). The presence of gelatin in hydrogels made with the same cations caused a slight but not significant increase in the axon density per scaffold for each cation examined.

The analysis of the axon density within single capillaries did not yield any difference comparing different microchannel diameter in pACH. Pairwise comparison between pACH and gACH did not reveal any differences (Figure 4.8E). In contrast, in gACH significantly higher axon density was found with larger microchannel diameters (gACH<sub>Sr</sub> (35%) and gACH<sub>Zn</sub> (38%) compared to those with the smallest capillaries (gACH<sub>Cu</sub>, (17%). No significant difference was found between gACH<sub>Sr</sub> and gACH<sub>Zn</sub>.

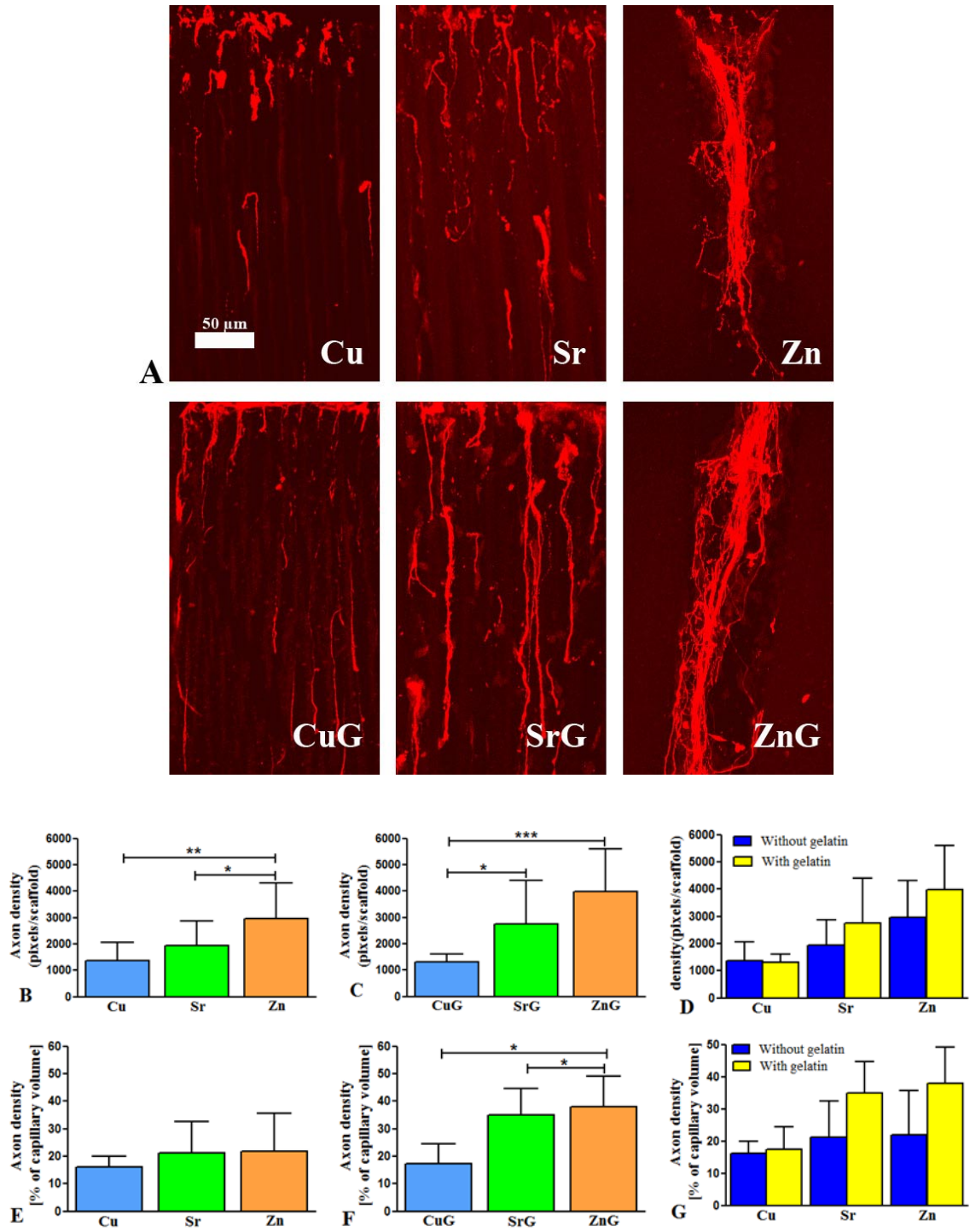


**Figure 4.8: DRG axon outgrowth into capillaries of alginate based hydrogels with different microchannel diameter. Immunohistochemical analysis of GAP-43 labelled axons (A), axon density per scaffold on the basis of the capillary diameter in pACH (B) and in gACH (C), pair wise comparison between pACH and gACH with same cation (D), percentage of axon density per capillary volume in pACH (E) and in gACH (F), pair wise comparison between pACH and gACH with same cation(G). \* $p < 0.05$ , \*\* $p < 0.01$ , \*\*\* $p < 0.001$ .**

#### 4.2.2 Influence of capillary diameter and gelatin constituent on Schwann cell migration

The migration of Schwann cells into the anisotropic capillary hydrogels was detected by p75<sup>lNGFr</sup> immunoreactivity (Figure 4.9A). The Schwann cell density within the microchannel structures was quantified in analogy to the quantification of axon density (Figure 4.8B). Paralleling findings of axon density, the Schwann cell density per scaffold increased with increasing microchannel diameter and gelatin modification. In pACH (Figure 4.9B) there were significant differences between gels made with pACH<sub>Cu</sub> (2290 pixels) and pACH<sub>Sr</sub> (3894 pixels) and also between pACH<sub>Cu</sub> (2290 pixels) and pACH<sub>Zn</sub> (4388 pixels). For gACH (Figure 4.9C) we found significant differences between gACH<sub>Cu</sub> (2384) and gACH<sub>Zn</sub> (5861 pixels) as well as between gACH<sub>Sr</sub> (3222 pixels) and gACH<sub>Zn</sub> (5861 pixels) (Figure 5.7B). No significant differences were found between pACH and gACH made with the same cation. Similar to the results of the axon density the analysis of the Schwann cell density within single capillaries showed almost no influence of the microchannel diameter and the gelatin constituent. For the pACH the Schwann cell density within single capillaries was almost the same showing no significant differences between the different microchannel diameters (Figure 4.9D). In the case of gACH we found a slight increase in Schwann cell density with increasing capillary diameter, whereby significant differences were found between gACH<sub>Cu</sub> (23%) and gACH<sub>Zn</sub> (31%) as well as between gACH<sub>Sr</sub> (25%) and gACH<sub>Zn</sub> (31%). No significant differences were found between pACH and gACH made with the same cation.

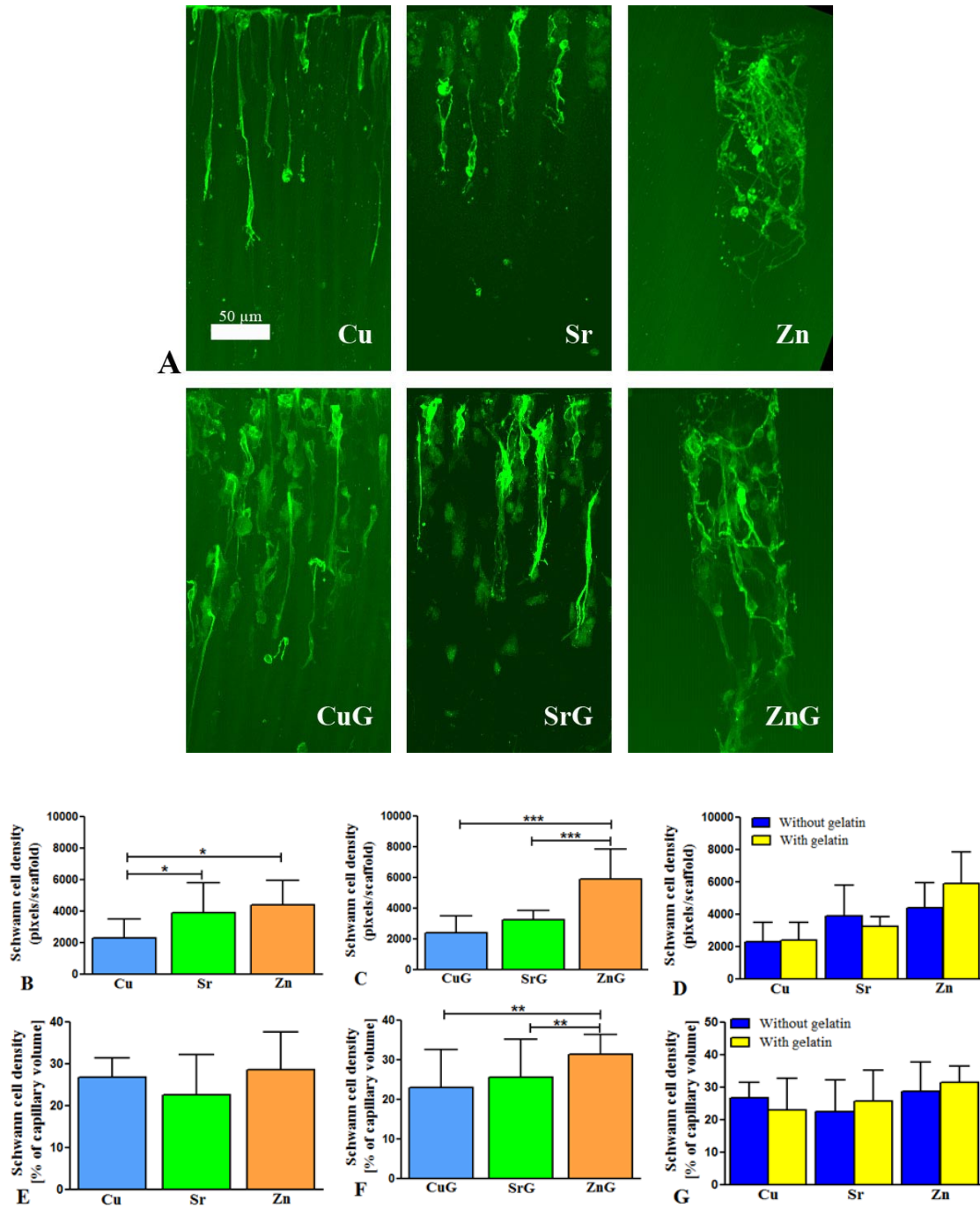


**Figure 4.9: Schwann cell migration from DRG explants into capillaries of alginate based hydrogels with different microchannel diameter. Immunohistochemical analysis of p75INGFr labelled Schwann cells (A), Schwann cell density per scaffold on the basis of the capillary diameter in pACH (B) and in gACH (C), pair wise comparison between pACH and gACH with same cation (D), percentage of Schwann cell density per capillary volume in pACH (E) and in gACH (F), pair wise comparison between pACH and gACH with same cation (G). \* $p < 0.05$ , \*\* $p < 0.01$ , \*\*\* $p < 0.001$ .**

### 4.3 Oriented outgrowth of entorhinal axons guided by anisotropic capillary hydrogels in vitro

Organotypic slice culture of rat brain entorhinal cortex (EC), an established tool to assess axonal regeneration in the CNS, was successfully adapted to the (Figure 4.10) method developed by Stoppini, Gahwiler (1991) EC with hippocampus was isolated from the brain. In contrast to former studies (Stoppini, Prang et al., 2006) EC separated selectively and cultured on top of the ACH gels made with ultra pure Pronova alginate to enhance the efficiency of axonal outgrowth. EC cultures prepared in this way maintained an excellent gross morphology, confirmed by immunostaining against NF-200 und Höchst counterstaining. Slices spontaneously attached to the filter supports and flattened over time to less than 100  $\mu\text{m}$  in thickness from the original 400  $\mu\text{m}$ .

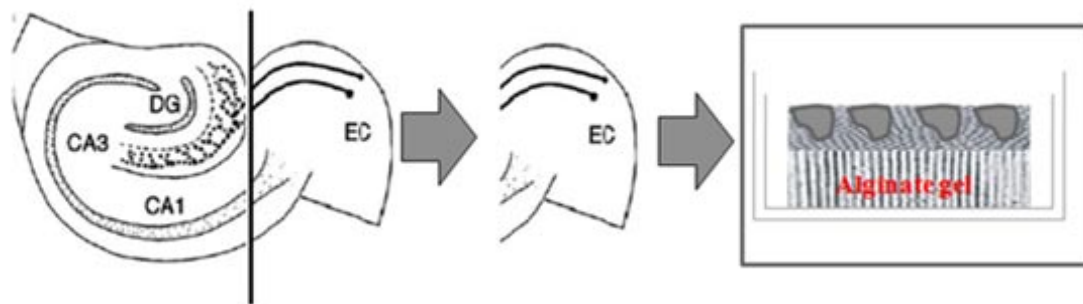


**Figure 4.10: Schematic drawing of the entorhino-hippocampal slices culture. Separated entorhinal cortex (EC) from hippocampus cultured on top of ACH scaffolds.**

To assess the permissiveness and the ability of ACH to direct axonal regrowth in the CNS neurite outgrowth from entorhinal cortex slice culture was investigated. Entorhinal cortex slices were placed on top of vertically oriented pACH and gACH to allow directed axon growth into the hydrogel capillaries. pACH and gACH maintained their capillary structure for the complete incubation period (1 week). Entorhinal axons were either identified by GAP-43 (Figure 4.11A) or NF-200 (Figure 4.12A) immunoreactivity. Axons regrew in a longitudinally oriented fashion seldom crossing the complete distance of the capillaries (300  $\mu\text{m}$ ). To prove if cell migration or cell support will help to enhance axon regeneration we assessed cell migration into ACH Astrocytes migrated into the capillaries of ACH scaffolds which was immunohistochemically detected by using GFAP marker (Figure 4.13A).



### 4.3.1 Influence of capillary diameter and gelatin constituent on axonal outgrowth

Entorhinal cortex slices were cultured on top of pACH or gACH having a microchannel structure with capillary diameters varying between 11 and 89  $\mu\text{m}$ . From the confocal microscopy images of GAP-43 and NF-200 stained sections (Figure 4.11A, 4.12A) we quantified axon outgrowth by analyzing the axon density, which was correlated with the capillary diameter and the composition of the hydrogels. Axon and cell density were assessed as described for the DRG in vitro assays.

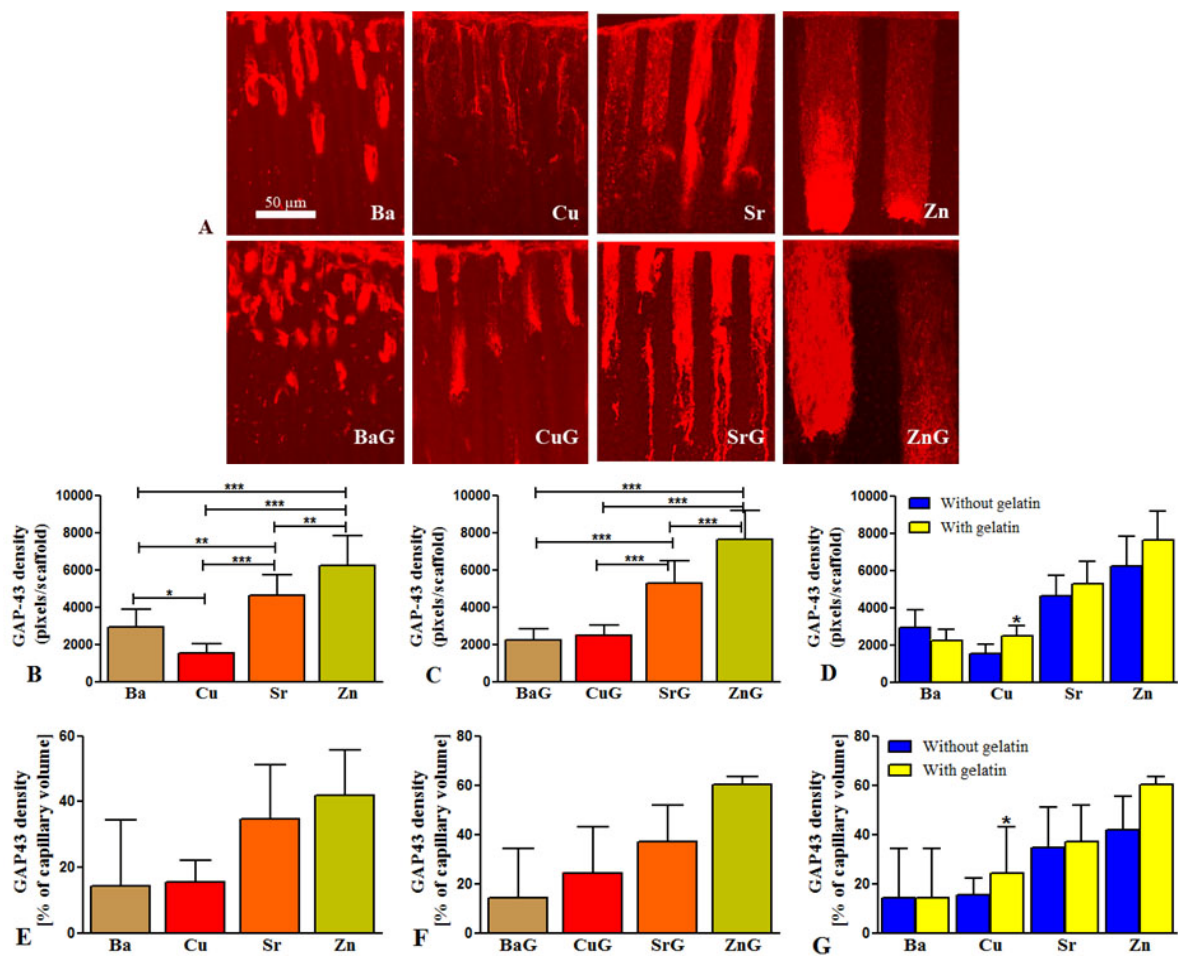


**Figure 4.11: Axon outgrowth from entorhinal cortex into ACH with different microchannel diameter. Micrograph with GAP-43 immunoreactive axons in different ACH (A), axon density per scaffold on the basis of the capillary diameter in pACH (B) and in gACH (C), pair wise comparison between pACH and gACH with same cation (D), percentage of GAP-43 immunoreactive axon density per capillary volume in pACH (E) and in gACH (F), pair wise comparison between pACH and gACH with same cation (G). \* $p < 0.05$ , \*\* $p < 0.01$ , \*\*\* $p < 0.001$ .**



The axon density per scaffold detected as GAP-43 immunoreactivity increased with increasing capillary diameter (Figure 4.11B,C). Interestingly, axon density was significantly higher in pACH<sub>Ba</sub> which consist of the smallest capillary diameters tested, compared to pACH<sub>Cu</sub>. We found significant differences between all groups i.e., pACH<sub>Ba</sub> (2913 pixels) and pACH<sub>Cu</sub> (1508 pixels), pACH<sub>Ba</sub> (2913 pixels) and pACH<sub>Sr</sub> (4615 pixels), pACH<sub>Ba</sub> (2913 pixels) and pACH<sub>Zn</sub> (6243 pixels), pACH<sub>Cu</sub> and pACH<sub>Sr</sub>, pACH<sub>Cu</sub> and pACH<sub>Zn</sub>, pACH<sub>Sr</sub> and pACH<sub>Zn</sub>. In gACH axon density per scaffolds increased with increasing capillary diameter. gACH showed significant differences between gACH<sub>Ba</sub> (2251 pixels) and gACH<sub>Zn</sub> (7629 pixels), gACH<sub>Ba</sub> (2251 pixels) and gACH<sub>Sr</sub> (5297 pixels), as well gACH<sub>Cu</sub> (2507 pixels) and gACH<sub>Zn</sub> (7629 pixels), and gACH<sub>Cu</sub> and gACH<sub>Sr</sub>. Also there was a significant difference between gACH<sub>Sr</sub> and gACH<sub>Zn</sub>. Pairwise comparison revealed only a difference in pACH<sub>Cu</sub> (1508 pixels) and gACH<sub>Cu</sub> (2507 pixels) prepared with same cation.

The analysis of axon density within single capillaries (Figure 4.11D) did not show any significant results for pACH and gACH. In connection with the capillary diameter, we found only significant differences between pACH<sub>Cu</sub> (15%) and gACH<sub>Cu</sub> (24%). However there was always the trend that gels with larger capillary diameter displayed increased axon density signals of GAP43 for both pACH and gACH.

Paralleling our findings with GAP-43 positive axons, the axon density determined by quantifying NF-200 immunoreactivity was enhanced with increasing capillary diameter (Figure 4.12A). In pACH (Figure 4.12B), significant differences in case of pACH<sub>Ba</sub> (3181 pixels) and pACH<sub>Zn</sub> (6368 pixels), pACH<sub>Cu</sub> (2160 pixels) and pACH<sub>Zn</sub> (6368 pixels), pACH<sub>Cu</sub> (2160 pixels) and pACH<sub>Sr</sub> (4167 pixels), and finally pACH<sub>Sr</sub> (4167 pixels) and pACH<sub>Zn</sub> (6368 pixels) were found. Again pACH<sub>Ba</sub> (3181 pixels) did not follow the rule, since axon density was higher than in pACH<sub>Cu</sub> (2160 pixels). The modified gACH (Figure 4.12C) showed significant differences between gACH<sub>Ba</sub> (2341 pixels) and gACH<sub>Zn</sub> (6976 pixels), gACH<sub>Ba</sub> (2341 pixels) and gACH<sub>Sr</sub> (6170 pixels), gACH<sub>Cu</sub> (2421 pixels) and gACH<sub>Zn</sub> (6976 pixels) and also between gACH<sub>Cu</sub> and gACH<sub>Sr</sub>. There is a significant difference on the basis of gelatin constituent between the gels pACH<sub>Ba</sub> (3181 pixels) and gACH<sub>Ba</sub> (2341 pixels) and pACH<sub>Sr</sub> (4167 pixels) and gACH<sub>Sr</sub> (6170 pixels).

The axon density of NF-200 within single capillaries (Figure 4.12D) did not show significant differences in any gel on the basis of the capillary diameter with pACH or gACH. There are

significant differences on the basis of the gelatin constituent between pACH<sub>Cu</sub> (20%) and gACH<sub>Cu</sub> (38%) and pACH<sub>Sr</sub> (33%) and gACH<sub>Sr</sub> (46%). Overall there is increased axon density with increasing capillary diameter.

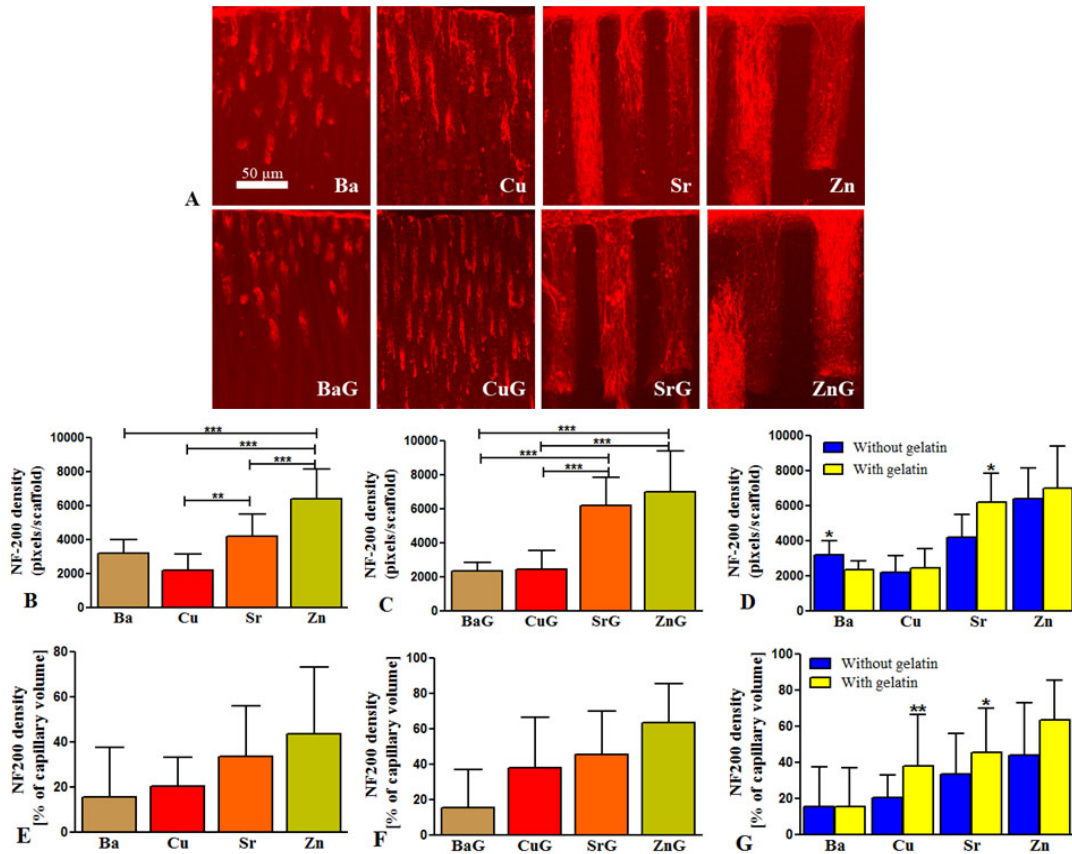


**Figure 4.12: Axon outgrowth from entorhinal cortex into ACH with different microchannel diameter. Micrograph with NF-200 immunoreactive axons in different ACH (A), axon density per scaffold on the basis of capillary diameter in pACH (B) and in gACH (C), pair wise comparison between pACH and gACH with same cation (D), percentage of NF-200 immunoreactive axon density per capillary volume in pACH (E) and in gACH (F), pair wise comparison between pACH and gACH with same cation (G). \*p < 0.05, \*\*p < 0.01, \*\*\*p < 0.001.**

#### 4.3.2 Influence of capillary diameter and gelatin constituent on astrocyte migration

The migration of astroglia into the ACH was assessed by quantifying GFAP expressing cells (Figure 4.13A). The astroglia density was measured per scaffolds on the basis of the capillary

diameter in pACH and gACH. pACH (Figure 4.13B) showed significant results between pACH<sub>Ba</sub> (2182 pixels) and pACH<sub>Zn</sub> (6315 pixels) and pACH<sub>Ba</sub> (2182 pixels) and pACH<sub>Sr</sub> (5061 pixels). There were also significant differences between pACH<sub>Cu</sub> (2303 pixels) and pACH<sub>Zn</sub> (6315 pixels) and pACH<sub>Cu</sub> and pACH<sub>Sr</sub>. Also significant results were found in case of pACH<sub>Sr</sub> and pACH<sub>Zn</sub>. In general, astrocyte density per scaffold was increased with increasing microchannel diameter of the gels.

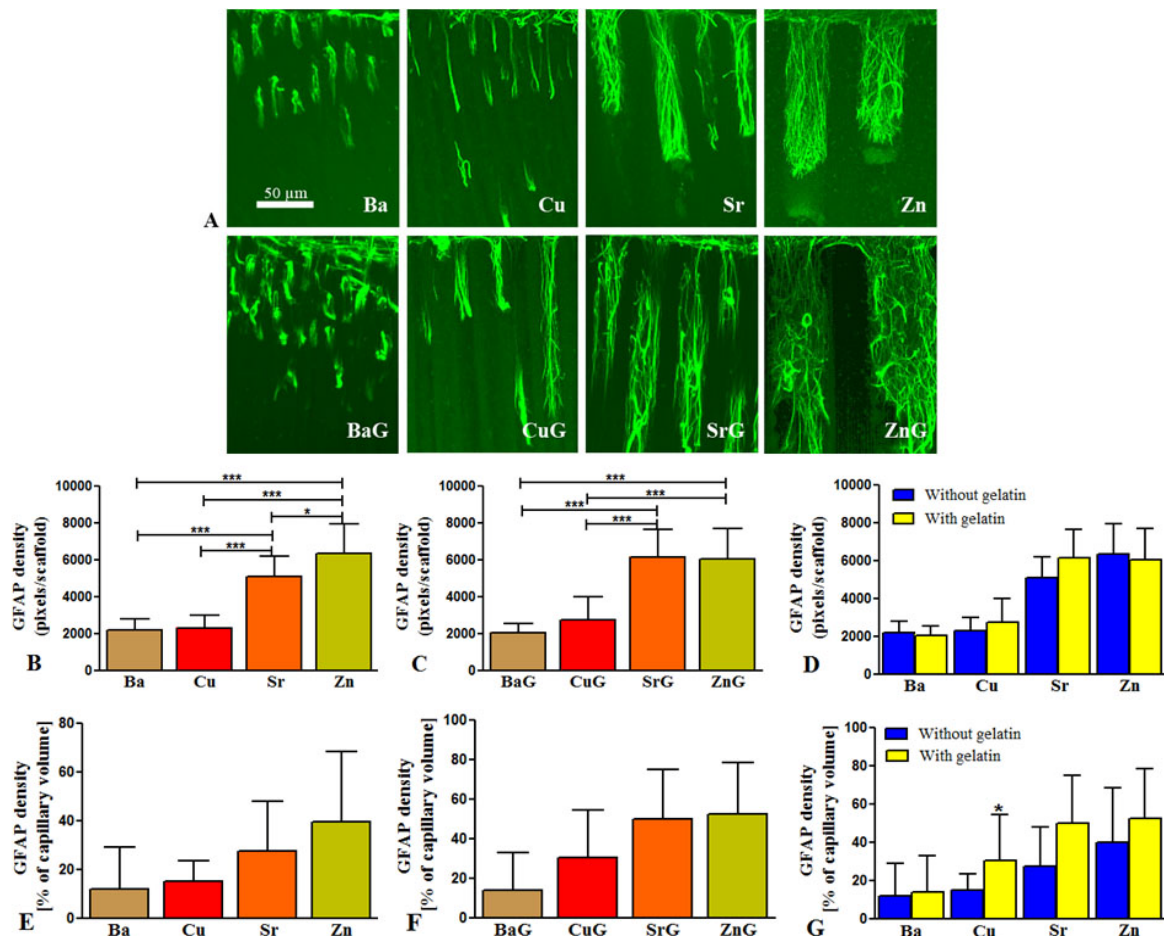


**Figure 4.13: Astrocyte migration from entorhinal cortex into ACH with different microchannel diameter. Immunohistochemical analysis of GFAP labelled astrocytes (A), astrocyte density per scaffold on the basis of capillary diameter in pACH (B) and in gACH (C), pair wise comparison between pACH and gACH with same cation (D), percentage of GFAP labelled astrocytes density per capillary volume in pACH (E) and in gACH (F), pair wise comparison between pACH and gACH with same cation (G). \*p < 0.05, \*\*\*p < 0.001.**

Astroglia density per scaffold on the basis of capillary diameter in gACH also showed significant results (Figure 4.13C). The density in gACH<sub>Ba</sub> was significantly lower than in gACH<sub>Cu</sub>, gACH<sub>Sr</sub> and gACH<sub>Zn</sub> gels with following probabilities: gACH<sub>Ba</sub> (2052 pixels) and gACH<sub>Sr</sub> (6153 pixels), gACH<sub>Ba</sub> (2052 pixels) and gACH<sub>Zn</sub> (6022 pixels). There were also significant differences between gACH<sub>Cu</sub> (2714 pixels) and gACH<sub>Sr</sub> (6153 pixels) and gACH<sub>Cu</sub> and gACH<sub>Zn</sub> and also between gACH<sub>Sr</sub> and gACH<sub>Zn</sub> (Figure 5.14B). There were no significant results found in pACH and gACH with same cation.

The astrocyte density within single capillaries was also assessed and the pACH and gACH showed the same trends with increasing astrocyte density in increasing capillary diameter (Figure 4.13D). There were no significant differences in any gel on the basis of the capillary diameter. On the basis of the gelatin constituent significant results were found for pACH<sub>Cu</sub> (15%) and gACH<sub>Cu</sub> (30%) with same cation.

#### **4.4 Oriented axonal outgrowth of spinal cord slice cultures into ACH**

Organotypic spinal cord slice cultures were successfully set up (Figure 4.14) using the interface method developed by Stoppini et al. Horizontal spinal cord slice cultures prepared in this way maintained an excellent gross morphology with the dorsal and ventral horns distinguishable from each other, facilitating the identification of neuronal populations. To confirm the preservation of the structure and to appraise the usefulness of this model, immunostaining was carried out for NeuN, NF-200, GFAP all are microscopic images not confocal. (Figure 4.15). Immunostaining with the marker NeuN confirmed that neurons readily survived and that there was acceptable preservation of neurons in the dorsal horn, especially the superficial area. In the ventral horn, however, there was an absence of staining particularly pertaining to the somatic motoneurons. Further analysis was performed with an antibody for axonal marker (NF-200) and astrocyte marker (GFAP) (Figure 4.15 A-H) (Hilton KJ *et al.* 2004).

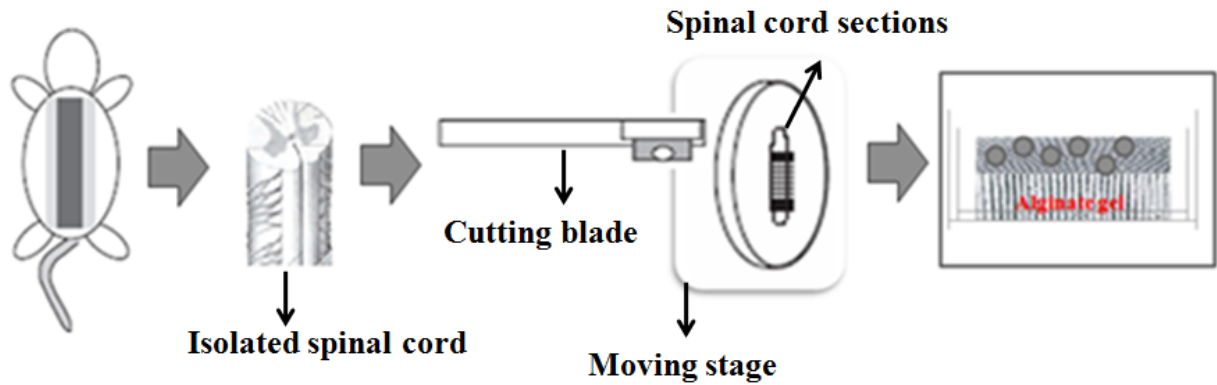


**Figure 4.14:** Schematic representation of spinal cord isolation, preparation and incubation of slice cultures *in vitro* on top of ACH gels.

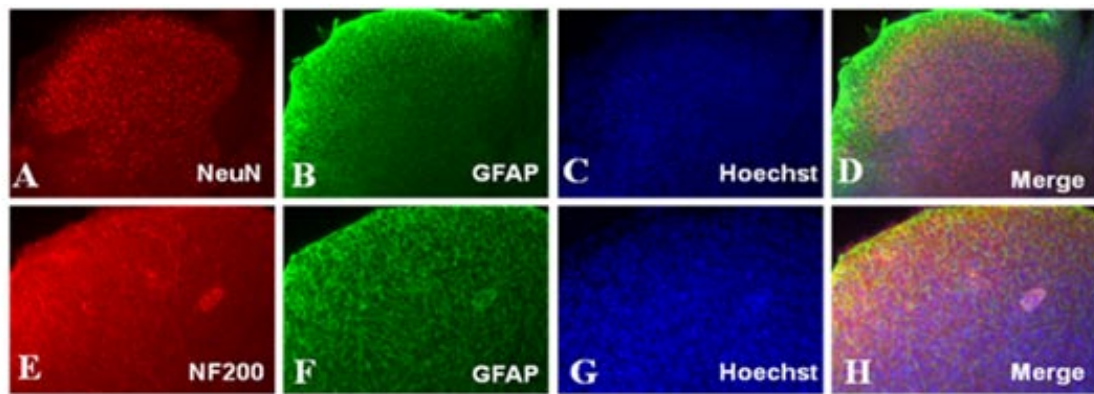


**Figure 4.15:** Morphology of spinal cord slice cultures *in vitro* after seven day in culture. NeuN (newborn neurons), GFAP (astrocytes), Hoechst (nucleus marker) and merge (A-D), NF-200 (axon marker), GFAP, Hoechst and merge (E-H).

#### 4.4.1 Influence of capillary diameter and gelatin constituent on axonal outgrowth from spinal cord slice cultures

Spinal cord slices were cultured on top of pACH or gACH having a microchannel structure with capillary diameters varying between 11 and 89  $\mu\text{m}$ . As previously, GAP-43 and NF-200 immunoreactive axons imaged with laser confocal microscopy (Figure 4.16A, 4.17A) were quantified to determine the axon density. Axon density was correlated with the capillary diameter and the composition of the ACH.

Axon density per scaffold quantified by analysis of GAP-43 positive axons within the ACH grew with increasing capillary diameter (Figure 4.16A). pACH showed significant results

(Figure 4.16B) on the basis of capillary diameter between pACH<sub>Ba</sub> (2839 pixels) and pACH<sub>Zn</sub> (11310 pixels), pACH<sub>Cu</sub> (3673 pixels) and pACH<sub>Zn</sub> (11310 pixels) and pACH<sub>Sr</sub> (3585 pixels) and pACH<sub>Zn</sub> (11310 pixels). gACH showed significant results (Figure 4.16C) on the basis of the capillary diameter between gACH<sub>Ba</sub> (3634 pixels) and gACH<sub>Zn</sub> (12568 pixels), gACH<sub>Cu</sub> (2903 pixels) and gACH<sub>Zn</sub> (12568 pixels) and gACH<sub>Sr</sub> (3891 pixels) and gACH<sub>Zn</sub> (12568 pixels). Pairwise comparison between pACH and gACH has no significant difference in any gel with same cation. The axon density within a single capillary (Figure 4.16D) showed no significant results.

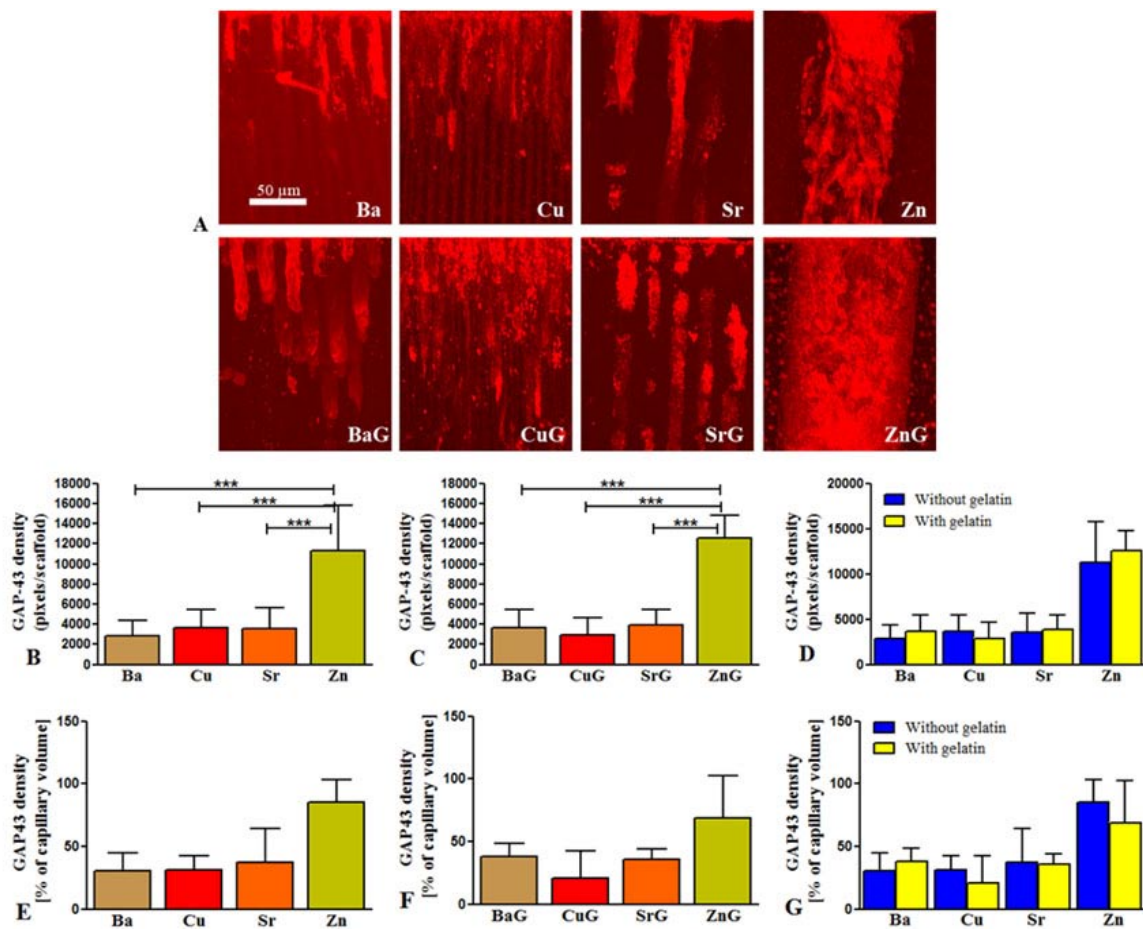


**Figure 4.16:** Axon outgrowth from spinal cord slice culture into ACH with different microchannel diameter. Micrographs of GAP-43 immunoreactive axons (A), axon density per scaffold on the basis of capillary diameter in pACH (B) and in gACH (C), pair wise comparison between pACH and gACH with same cation (D), percentage of GAP-43 positive axon density per capillary volume in pACH (E) and in gACH (F), pair wise comparison between pACH and gACH with same cation (G). \*\*\*p < 0.001.



The axon density per scaffold as determined by analysis of the NF-200 density in the ACH (Figure 4.17A) increased with increasing capillary diameter. pACH showed significant results (Figure 4.17B) on the basis of capillary diameter between pACH<sub>Ba</sub> (2252 pixels) and pACH<sub>Zn</sub> (5381 pixels) , pACH<sub>Cu</sub> (2748 pixels) and pACH<sub>Zn</sub> (5381 pixels) and pACH<sub>Sr</sub> (1965 pixels) and pACH<sub>Zn</sub> (5381 pixels) (Figure 4.17B). gACH showed significant results (Figure 4.17C) regarding capillary diameter between gACH<sub>Ba</sub> (2284 pixels) and gACH<sub>Zn</sub> (4775 pixels), gACH<sub>Cu</sub> (1855 pixels) and gACH<sub>Zn</sub> (4775 pixels), gACH<sub>Sr</sub> (1948 pixels) and gACH<sub>Zn</sub> (4775 pixels) (Figure 4.17C). Pairwise comparison between pACH and gACH with same cation had no significant differences.

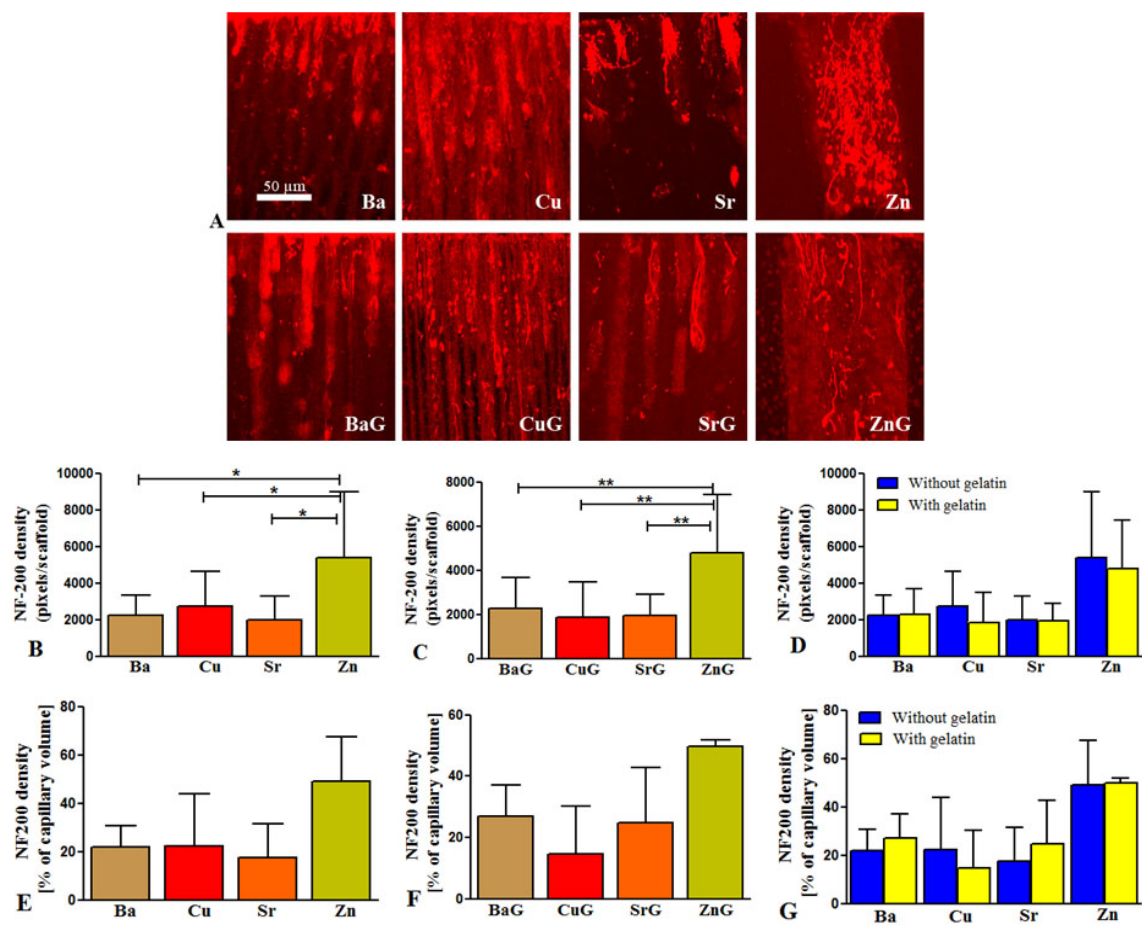


**Figure 4.17:** Axon outgrowth from spinal cord slice cultures into capillaries of ACH with different microchannel diameter. Micrographs of NF-200 immunoreactive axons (A), axon density per scaffold on the basis of capillary diameter in pACH (B) and in gACH (C), pair wise comparison between pACH and gACH with same cation (D), percentage of NF-200 positive axon density per capillary volume in pACH (E) and in gACH (F), pair wise comparison between pACH and gACH with same cation (G). \* $p < 0.05$ , \*\* $p < 0.01$ .

The axon density within single capillaries showed no significant differences (Figure 4.17D). Again, similar to the previous results the axon densities followed the trend to increase with increasing capillary diameter.

#### 4.4.2 Influence of capillary diameter and gelatin constituent on astroglia migration

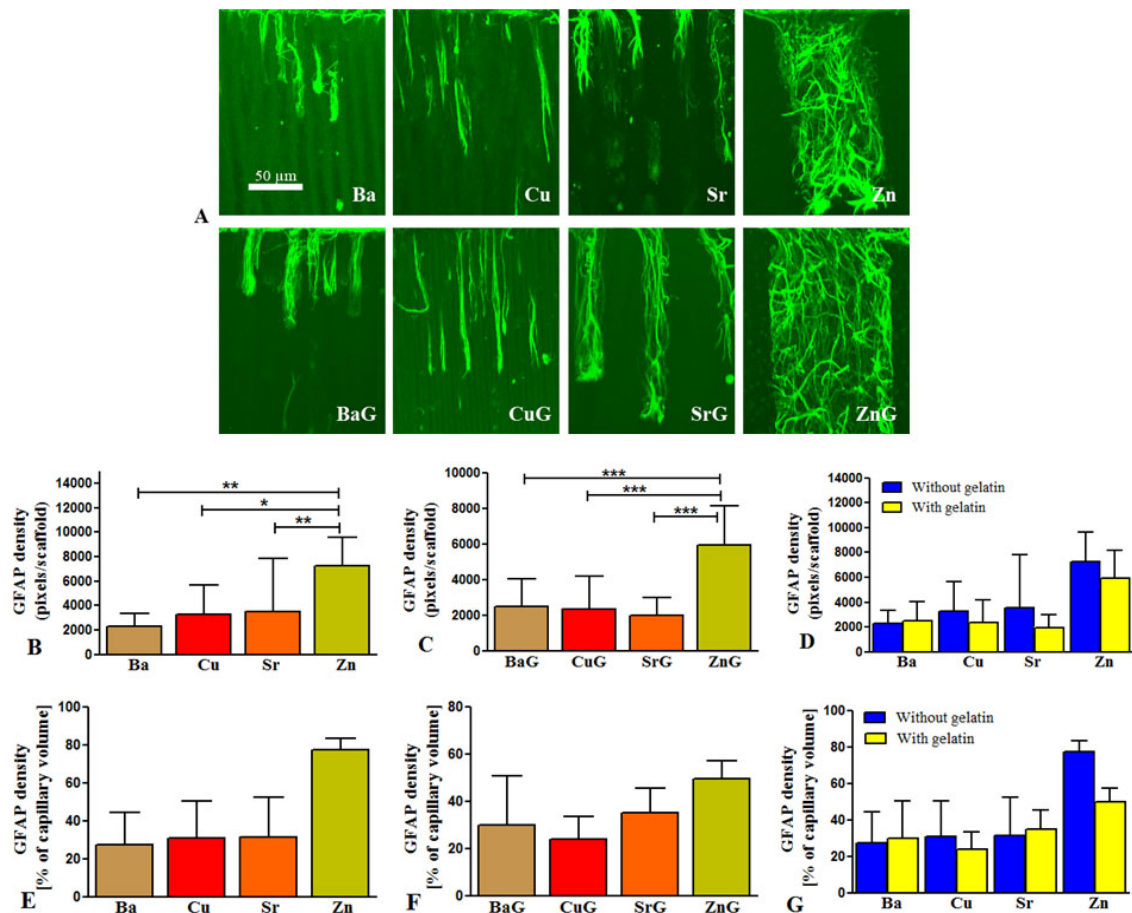


**Figure 4.18: Astroglia migration from spinal cord slice culture into ACH with different microchannel diameter. Micrographs of GFAP positive astrocytes (A), astrocyte density per scaffold on the basis of capillary diameter in pACH (B) and in gACH (C), pair wise comparison between pACH and gACH with same cation (D), percentage of GFAP positive astrocytes density per capillary volume in pACH (E) and in gACH (F), pair wise comparison between pACH and gACH with same cation (G). \* $p < 0.05$ , \*\* $p < 0.01$ , \*\*\* $p < 0.001$ .**

The migration of astroglia into ACH was revealed by labelling with the GFAP marker (Figure 4.18A). The astrocyte density was measured per scaffold on the basis of capillary



diameter in pACH and gACH. Alginate gels with wider capillaries showed an increased density of migrated astrocytes.

pACH (Figure 4.18B) showed significant results in pACH<sub>Ba</sub> (2306 pixels) and pACH<sub>Zn</sub> (7224 pixels), pACH<sub>Cu</sub> (3281 pixels) and pACH<sub>Zn</sub> (7224 pixels) and pACH<sub>Sr</sub> (3531 pixels) and pACH<sub>Zn</sub> (7224 pixels). gACH (Figure 4.18C) showed significant results between gACH<sub>Ba</sub> (2498 pixels) and gACH<sub>Zn</sub> (5934 pixels), gACH<sub>Cu</sub> (2352 pixels) and gACH<sub>Zn</sub> (5934 pixels) and gACH<sub>Sr</sub> (1967 pixels) and gACH<sub>Zn</sub> (5934 pixels) (Figure 4.18C). Pairwise comparison between pACH and gACH with same cation showed no significant results in any gel (Figure 4.18D). The astrocyte densities within capillaries showed no significant difference in case of pACH and gACH for different capillary diameter (Figure 4.18E,F). Pairwise comparison between pACH and gACH with same cation showed no significant results in any gel. (Figure 4.18G). Similar to the previous results density increases with increasing in capillary diameter.

#### **4.5 Anisotropic alginate-based gels enhance directed axon regrowth following spinal cord injury *in vivo***

The rats were anesthetized with an intramuscular injection with the UCSD anesthesia cocktail. The hairs on the back between the skull and the middle of the back removed generously. The skin was opened with medial incision starting at the end of the skull and ending approximately 1cm past the shoulder. The wound was opened by using the spreader with short teeth. A medial incision was made in the muscle layer, exposing the spinal process of C2 and C5. All tissue from C3 was removed to make sure that the forceps had an easy grip on C2. The ligament between C3 and C4 removed with the rongeurs. The spinal cord was exposed by removing about half of the bone arch of C3. The head of the rat mounted in the stereotaxic frame. The spinal column made horizontal by attaching the hemostatic forceps with large rounded tip to C5 and the forceps mounted in the holder arm. The tungsten wire knife mounted in the stereotaxic arm and position of the tip of the wire knife exactly 0.6mm to the left of the midline was adjusted. A small dura incision made and the tip of wire knife lowered 1.1mm below the surface of the dura. The wire from the wire knife extrudes 2.2mm and the knife holder raised in small steps. It was ensured that we axotomize all CST fibers by compressing the spinal cord tissue against the wire knife with a glass pipette until we able to saw the wire through the intact dura. The wire was retracted and the knife holder removed from the cord.

Immediately after the injury dura incision was made following one half of previous wire knife transaction. ACH gel blocks of standardised dimension were inserted into the transaction site. The orientation of the ACH capillaries followed the longitudinal axis of the spinal cord. The lesion/implantation site was covered with gel foam before readapting muscular layers and stapling the skin above the lesion.

Six weeks postoperatively, post-mortem histological evaluation (Nissl staining) showed that ACH scaffolds remained stable and maintained their microstructure. The overall GFAP immunoreactivity around the implant was increased.

#### 4.5.1 Integration of alginate gels

Six weeks postoperatively, post-mortem histological evaluation by Nissl staining showed that ACH scaffolds remained stable and maintained their microchannel structure. In most of the cases cyst like space surrounding the ACH more likely represent artifacts due to tissue shrinkage in the course of tissue processing (fixation and staining procedure). There is very less cyst formation around the ACH in all type of gels (Figure 4.19).

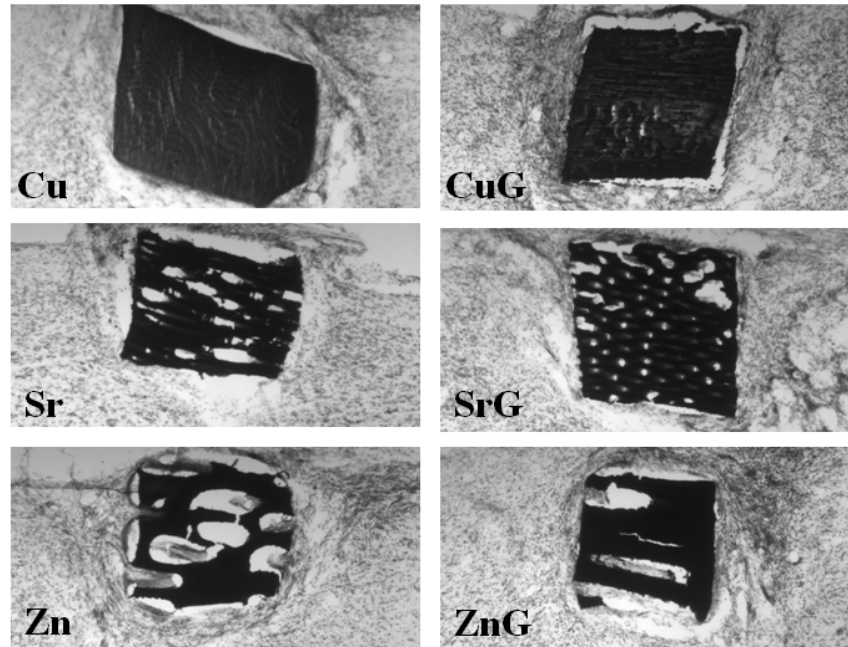


**Figure 4.19:** Nissl staining of sagittal sections of spinal cord from *in vivo* experiments shows all types of ACH scaffolds well integrated into lesion site

#### 4.5.2 Influence of capillary diameter and gelatin constituent on axonal outgrowth *in vivo*

ACH with capillary diameters varying between 11 and 89  $\mu\text{m}$  were implanted into spinal cord lesion. Six weeks after implantation axon density was determined by quantifying GAP-43 and NF-200 immunoreactive axons in pACH<sub>Cu,Sr,Zn</sub> and gACH<sub>Cu,Sr,Zn</sub> (Figure 4.20A, 4.21A). Axon density was quantified in the same fashion as described for all *in vitro* experiments. Thereafter, axon density was correlated with the capillary diameter and the gelatin constituent of the hydrogels.

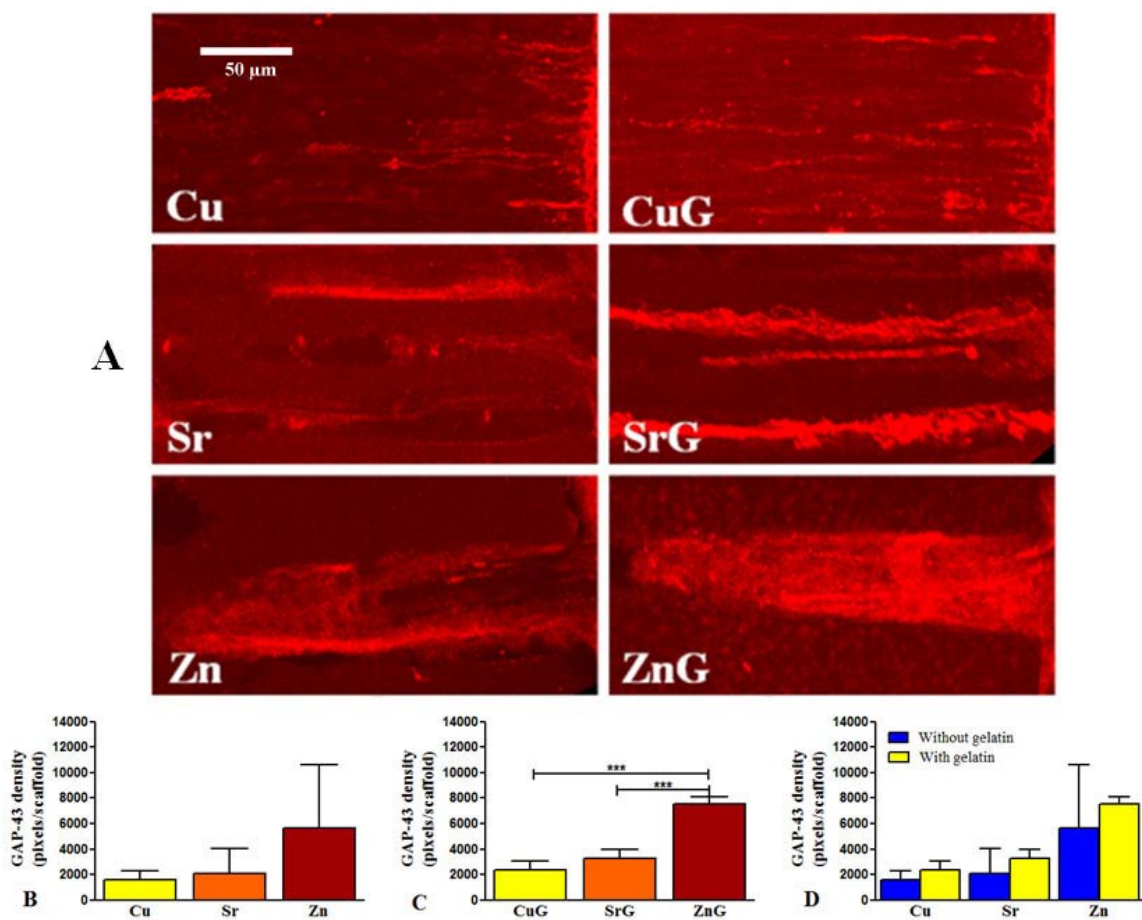


**Figure 4.20: Axon outgrowth from *in vivo* into ACH with different microchannel diameter. Micrographs of GAP-43 immunoreactive axons (A), axon density per scaffold on the basis of capillary diameter in pACH (B) and in gACH (C), pair wise comparison between pACH and gACH with same cation (D). \*\*\*p < 0.001.**

GAP-43 immunoreactive axonal representing regenerating axons grew robustly into pACH and gACH in a longitudinally oriented fashion (Figure 4.20A). Recapitulating *in vitro*

findings, axon density increased with wider capillary diameter. gACH have more signal than the pACH. We didn't find significant differences in pACH on the basis of capillary diameter. (Figure 4.20B), but we found significant results in gACH it showed significant differences between gACH<sub>Cu</sub> (2365 pixels) and gACH<sub>Zn</sub> (7547 pixels), gACH<sub>Sr</sub> (3265 pixels) and gACH<sub>Zn</sub> (7547 pixels) (Figure 4.20C). Pairwise comparison between pACH and gACH with same cation showed no significant results in any gel (Figure 4.20D).

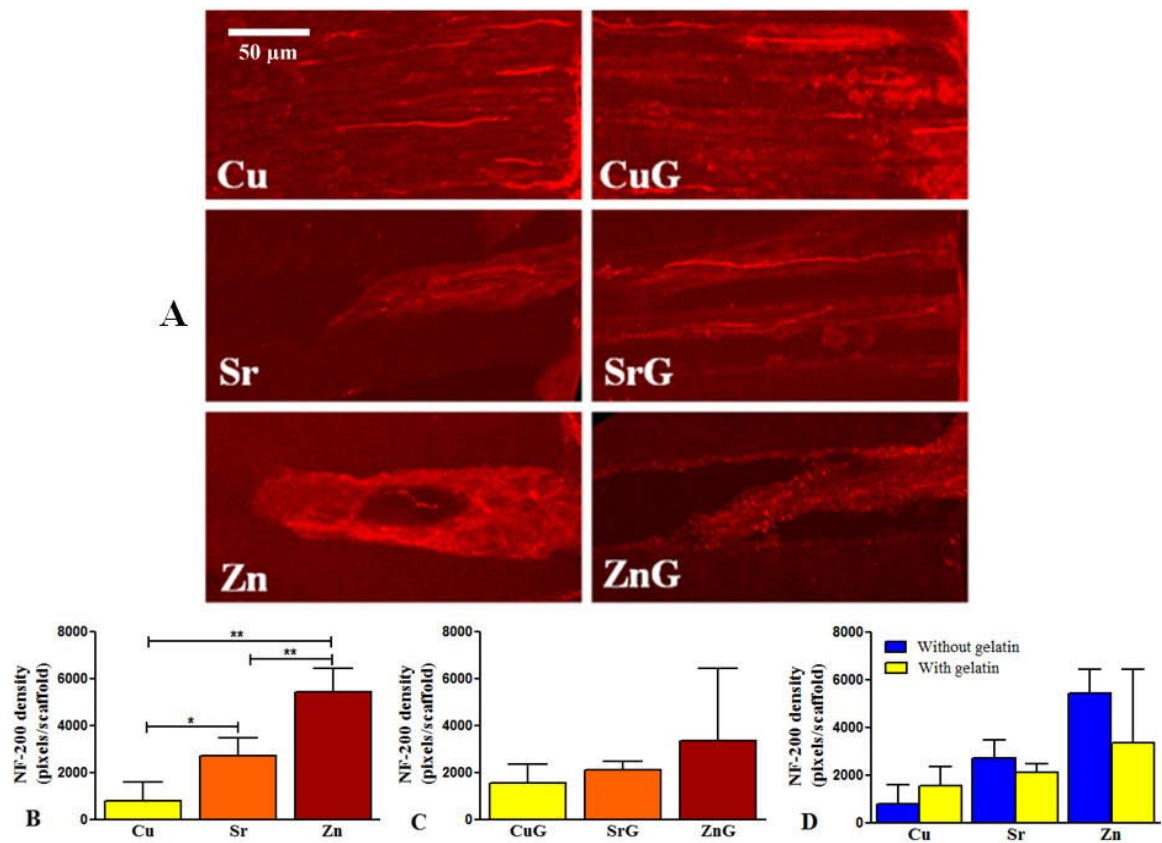


**Figure 4.21: Axon outgrowth from in vivo into ACH with different microchannel diameter. Micrographs of NF-200 immunoreactive axons (A), axon density per scaffold on the basis of capillary diameter in pACH (B) and in gACH (C), pair wise comparison between pACH and gACH with same cation (D). \* $p < 0.05$ , \*\* $p < 0.01$ .**

Axonal profiles immunoreactive for NF-200 were identified within ACH. As shown for GAP-43, NF-200 positive axon density increased with wider capillary diameter. (Figure 4.21A). pACH showed significant results between pACH<sub>Cu</sub> (796 pixels) and pACH<sub>Sr</sub> (2696 pixels), pACH<sub>Cu</sub> (796 pixels) and pACH<sub>Zn</sub> (5421 pixels) as well as pACH<sub>Sr</sub> (2696 pixels) and pACH<sub>Zn</sub> (5421 pixels) (Figure 4.21B). We didn't find significant results in gACH with

different capillary diameter (Figure 4.21C). Pair wise comparison between pACH and gACH with same cation did not reveal any significant differences. (Figure 4.21D).

**References:**

- Hilton KJ, Bateson AN, King AE. A model of organotypic rat spinal slice culture and biolistic transfection to elucidate factors that drive the preprotachykinin-A promoter. *Brain res rev* 2004;46:191-203.
- Prang P, Muller R, Eljaouhari A, Heckmann K, Kunz W, Weber T, et al. The promotion of oriented axonal regrowth in the injured spinal cord by alginate-based anisotropic capillary hydrogels. *Biomaterials* 2006;27:3560-9.



# **Chapter 5**

## **Discussion and Conclusion**





## 5.1 Discussion

The present work demonstrates that self-assembling anisotropic alginate-based capillary hydrogels represent a unique biopolymer scaffold, which combines several key features required for axonal regeneration after nerve injury in the CNS and PNS. They promote highly oriented axon regeneration within a three-dimensional structure raising the probability for appropriate target reinnervation. Furthermore, microchannel containing hydrogels provide support for the ingrowth and survival of glial cells such as SC or astrocytes thus increasing the capacity for axon regeneration. The uniqueness of the presented system is that the microchannel structure of the hydrogels could be varied very easily in terms of capillary diameter and density within relatively broad ranges. To our knowledge, such a feature could not be realized with any other microchannel containing system until today. We are sure that this speciality of our system will allow the adaption to a variety of clinical issues regarding regeneration in the peripheral or central nervous system.

The goal of the current work was to systematically analyze different ACH parameter (capillary diameter, introduction of cell adhesive gelatin) regarding directed axonal regeneration *in vitro* and *in vivo*. As a first step, capillary hydrogels were prepared from guluronic acid-rich types of alginate varying slightly in their molecular weight and purity grade i.e. food-grade alginate from ISP and ultra-pure alginate from Pronova. Using ISP alginate capillary diameters were varied between 10 and 54  $\mu\text{m}$  while using Pronova alginate capillary diameters were varied between 11 and 89  $\mu\text{m}$ . The different structures were obtained simply by the use of electrolyte solutions with different divalent cations for ionotropic gel formation. Most of the various anisotropic structures which have been created in three-dimensional scaffolds or hydrogels exhibited features in the size between 0.5 and 120  $\mu\text{m}$  (Flynn L *et al.* 2003, Wang A *et al.* 2006, Stokols S *et al.* 2006a, Mollers S *et al.* 2009). Unfortunately, in the most cases it was not possible to produce features of different but defined sizes with the same technology resulting in a lack of information on how the diameter of these features like fibres or channels influences the regeneration processes. It is known from the early work of Thiele *et al.* that the capillary diameter in anisotropic alginate gels depends on a variety of parameters like the concentration and the molecular composition of the alginate, the type and concentration of the gel-forming divalent cation as well as the presence of additional solutes like salts or sugars. The diameters of the capillaries usually increase as the concentration of the alginate solution decreases (Thiele H *et al.* 1967). The

capacity of different divalent cations to produce gels of varying order and capillary sizes was summarized by Thiele in the so-called ionotropic sequence (Thiele H *et al.* 1955, Thiele H *et al.* 1957). The capillary diameters obtained by him using the same cations which have been used in our work were as follows: 8-35  $\mu\text{m}$  ( $\text{Cu}^{2+}$ ) < 75-125  $\mu\text{m}$  ( $\text{Sr}^{2+}$ ) < 350  $\mu\text{m}$  ( $\text{Zn}^{2+}$ ) (Thiele H *et al.* 1957). The order of the series found by Thiele is the same as it was observed in the present study, however, the values for the capillary diameters differed significantly which might be explained by the different conditions of the alginate solution used within both studies. Both, the lower guluronic/mannuronic acid ratio of the starting alginate polymer and the lower concentration (10 g/L) of the alginate solution applied for gel formation might be reasons for the larger capillaries found by Thiele compared to the present work. The reason to employ alginate based anisotropic capillary hydrogels is that previous research findings on nerve repair strategies have demonstrated that in order to obtain significant regeneration of injured axons essential molecular and physical guidance cues are required. Physical guidance cues are longitudinal capillaries, micro and nanofibres or micro-sized grooves, whereas chemical cues are presented by adhesive matrix proteins, neurotrophic factors or growth supporting cells, which offer nutrient support, guidance and myelination of regenerating axons (Bellamkonda R *et al.* 1994, Belkas JS *et al.* 2004, Schmidt CE *et al.* 2003, Bellamkonda R *et al.* 2006, Fine EG *et al.* 2000). The addition of gelatin to the alginate solution resulted in the formation of larger capillaries which was also found for salts and other solutes (Thiele H *et al.* 1967). The addition of gelatin to the ISP alginate resulted into capillary diameters between 18 and 77  $\mu\text{m}$  while for Pronova alginate capillary diameters resulted between 14 and 85  $\mu\text{m}$ . The density of the microchannels within anisotropic capillary hydrogels for ISP alginate varied between 27 and about 630 channels/ $\text{mm}^2$  while for Pronova alginate it varied between 27 and about 915 channels/ $\text{mm}^2$ .

Covalent crosslinking of the alginate-based capillary hydrogels applying the aliphatic diisocyanate HDI did not affect the biocompatibility of the gels significantly since inflammatory responses or other signs of tissue damage were not found in our previous study after introducing the gels into rat spinal cord injuries (Prang P *et al.* 2006). By the *in vitro* testing of the present work we could further show that the stability against degradation and dissolution was drastically enhanced after HDI crosslinking compared to unmodified alginate gels. This prolonged stability of the hydrogels without altering their three-dimensional microchannel structure is a prerequisite for their successful application in nerve injury

therapies where regeneration is likely to take months and the physical stability of the employed guidance scaffold over such a period of time is very important. The divalent cations we have used to generate the anisotropic capillary hydrogels are suspected to elicit adverse effects after *in vivo* implantation. Therefore, we applied acidic washing solutions to the alginate hydrogels to exchange the crosslinking cations by protons which was found to be very effective by monitoring with atomic emission spectroscopy and also in earlier investigations of our group and others (Eljaouhari AA *et al.* 2006, Hassan RM *et al.* 1991). So, in summary, no adverse effects on the axon outgrowth experiments *in vitro* should be induced by the biomaterial.

A conventional method for identifying novel biomaterial-based guiding structures which can enhance axon outgrowth is to test the effects of these materials on primary neuronal cultures. The well-characterized dorsal root ganglion (DRG) outgrowth assay from PNS, entorhinal cortex slice culture and spinal cord slice culture from CNS was selected. Dorsal root ganglia are known for their abundance of adult neurons and Schwann cells. Three-dimensional microchannel containing hydrogels were prepared using food-grade ISP alginate created defined microchannel diameters of 10, 20 and 54  $\mu\text{m}$  for pure alginate gels (pACH) and of 18, 28 and 77  $\mu\text{m}$  for alginate-gelatin composite gels (gACH). Concerning the impact of the capillary diameter in our capillary hydrogels on axon regeneration in the DRG model we found a positive influence of wider pore diameters on axon length and density as well as on Schwann cell density. In the case of the smallest capillaries (20  $\mu\text{m}$ , ACH<sub>Cu</sub>), individual axons regrowing in a highly directed fashion were observed, whereas bundles of axons were frequently seen in ACH with the widest microchannels (55-80  $\mu\text{m}$ , ACH<sub>Zn</sub>). Individual axons did not regrow as oriented in ACH<sub>Zn</sub> compared to small capillary ACH<sub>Cu</sub>. Likely, compared to wider capillary diameter ACH small diameter ACH provide more mechanical guidance for Schwann cells migrating into the ACH, and consecutively ingrowing axons. Different strategies like Patterning the surface of polymer nerve guidance tubes (Miller C *et al.* 2001, Zhang N *et al.* 2005) compartmentation of tube lumens by thin polymer films (Clements IP *et al.* 2009) insertion of polymer filaments into tube lumens (Ribeiro-Resende VT *et al.* 2009, Schnell E *et al.* 2007) or creation of microchannels within (bio) polymer hydrogels (Bozkurt A *et al.* 2009, Sundback C *et al.* 2003, Sarig-Nadir O *et al.* 2009). All of which significantly enhance the surface area of guiding structures and to allow the ingrowth and adhesion of contact-mediated cells thus promoting endogenous nerve repair. In this way Schwann cells

can be activated to form longitudinally aligned columns resembling the natural Bands of Büngner which provide a suitable substrate for axonal regeneration by expressing adhesion molecules and diffusible growth factors (Bozkurt A *et al.* 2009, Ribeiro-Resende VT *et al.* 2009). DRG are commonly cultured on top of the test substrate for a certain period of time using DRG medium supplemented with nerve growth factor (Wong JW *et al.* 2008, Tucker BA *et al.* 2008). Since Schwann cells play a vital role in peripheral nerve regeneration after injury, the immunohistochemical analysis was centred on regrowing axons and Schwann cells, which migrated into the ACH capillaries. In line with numerous studies regrowing axons were always co-localised with Schwann cells within the capillaries suggesting that Schwann cells are required for successful axon regeneration through ACH (Bozkurt A *et al.* 2009, Ribeiro-Resende VT *et al.* 2009, Prang P *et al.* 2006, Zhang N *et al.* 2005).

Further *in vitro* assays derived from the central nervous system like spinal cord slice culture and entorhinal cortex slice culture. The slice cultures of spinal cord and entorhinal cortex were cultured on top of the ACH scaffolds *in vitro* to study CNS axon outgrowth and cell migration into the scaffolds. In our first study using gels with about 25µm in diameter we could present the proof of principle for target reinnervation of dissected axons from entorhinal cortex (Prang P *et al.* 2006). In the current work we demonstrated the effect of microchannel structure and gelatin modification on axon outgrowth and astrocyte migration into the capillary structure of our hydrogels. So far several research groups utilized slice culture lesion model systems to study regeneration or target reinnervation in the CNS (Bonnici B *et al.* 2008, Hilton KJ *et al.* 2004, Semino CE *et al.* 2004) but until now no biomaterial scaffolds have been used in any of these studies except our work (Prang P *et al.* 2006). In current work the CNS derived *in vitro* assays were used to test the different kinds of microchannel containing alginate hydrogels on their capacity to promote CNS cell migration and axon regeneration. The impact of the capillary diameter on axon regeneration was found to be significant in that wider pore diameters increased axon density as well as astrocyte density. Three-dimensional microchannel containing hydrogels were prepared using Pronova alginate created defined microchannel diameters of 11 for pACH<sub>Ba</sub>, 13 for pACH<sub>Cu</sub>, 26 for pACH<sub>Sr</sub> and 89 for pACH<sub>Zn</sub> µm for pure alginate gels (pACH) and of 15 for gACH<sub>Ba</sub>, 14 for gACH<sub>Cu</sub>, 21 for gACH<sub>Sr</sub> and 85 for gACH<sub>Zn</sub> µm for alginate-gelatin composite gels (gACH). Axon density and astrocyte density was enhanced with increased capillary diameter in pure alginate gels as well as in gelatin modified alginate gels.

Previous research findings on central nerve regeneration with slice culture models *in vitro* showed entorhinal-hippocampus interaction containing the entorhinal cortex, the perforant path, and the dentate gyrus. *In vitro* fluorescence labelling revealed that entorhinal neurons and single perforant fibres reach the outer molecular layer of the dentate gyrus (Kluge A *et al.* 1998). The formation of fibre connections between the entorhinal area and hippocampus was studied by using the extracellular and intracellular anterograde transport of biotin dextran (Li D *et al.* 1994). To study molecules involved in the regulation of sprouting after brain injury, *in vitro* model of collateral sprouting was established using entorhino-hippocampal slice culture from C57BL/6 mouse (Prang P *et al.* 2003). After CNS lesion or during neurodegenerative disease major challenges are reconstruction of neuronal circuits and the repair of axonal projections. In this direction proposed studies revealed that immature neuronal precursor cells could be used for the reconstruction of specific neuronal circuits (Radojevic V *et al.* 2004). The lesioned entorhinal-hippocampal pathway in slice culture facilitates regeneration when a synthetic peptide NEP1-40 was used. This peptide promoted axonal regeneration by blocking Nogo-66/NgR interaction and chondroitinase ABC which degrades chondroitin sulphate and promoting axon regeneration (Mingorance A *et al.* 2006). Axonal regeneration decreases with increasing maturation of central nervous system tissue and slice culture is the convenient tool. To enhance axonal regeneration in a complex microenvironment the use of neurotrophic factors and the modulation of intracellular signal transduction pathways could be useful (Prang P *et al.* 2001).

The use of organotypic slice cultures of the spinal cord to assess axonal growth and regeneration *in vitro* was also studied previously. Some of the studies in this direction are sagittal spinal cord slice culture model. In these cultures intrinsic spinal cord axons formed a strong fibre tract along the longitudinal axis of the slice. During the culture period axons get myelinated and forms synaptic contacts. After mechanical lesion in culture the regenerating axons crossing lesion site decreases with increasing maturation of culture (Bonnici B *et al.* 2008). The organotypic slice cultures of spinal cord showed viability over the period of 7 days. Preservation of neuron and their structure was demonstrated by using immunostaining marker such as NeuN and  $\beta$ -III tubulin (Hilton K *et al.* 2004). Slice culture model tested to study the roles of acidic fibroblast growth factor (aFGF) in axonal growth. It demonstrated that treatment with aFGF significantly increased the number of surviving neurons, axons stained for neurofilament immunostaining and Dil tracing crossed junction between two

pieces of spinal cord slices (Lee Yu-Shang *et al.* 2002). Immature astrocytes are able to support robust neurite outgrowth (Filous AR *et al.* 2010), this is observed in both the spinal cord slice culture and entorhinal cortex slice culture model. Therefore, both models derived from the central nervous system showed almost the same results as it was found for the DRG culture which stands as a model somewhere between the PNS and the CNS.

In comparison to the results obtained for two-dimensional microstructures, which have been prepared by photolithography and imprinting techniques showed the influence of structure size on axonal and Schwann cell orientation. In this context, it was found that linear grooves with depths of 300 nm and widths between 100 and 400 nm did not allow axons to grow within the grooves but on the ridge edges following the linear structure. From this study it can be concluded that structures in the submicron level are too small to allow axonal growth within the structure (Johansson F *et al.* 2006). Neurons cultivated on micropatterned substrate surfaces containing longitudinal grooves with depths between 2.5 and 69  $\mu\text{m}$  and widths between 50 and 350  $\mu\text{m}$  showed a clear behaviour in that the axons were following the grooves if they were deeper than 20  $\mu\text{m}$  and crossing the grooves if they were less deep than 11  $\mu\text{m}$ . The width of the tested groove structures did not influence the turning behaviour of the growing axons (Li N *et al.* 2005). In another study examining neurite orientation in microgrooves of 11  $\mu\text{m}$  in depth and 20-60  $\mu\text{m}$  in width strongest orientation was found in 20-30  $\mu\text{m}$  wide grooves. Axons grown in wider grooves exhibited a higher degree of bending (Mahoney MJ *et al.* 2005). Also for the alignment of Schwann cells the width of longitudinal microgrooves has been found as a key parameter in that widths smaller than 5  $\mu\text{m}$  and bigger than 10  $\mu\text{m}$  did not promote cell alignment in that way as it was found for grooves being 5-10  $\mu\text{m}$  wide (Bracken MB *et al.* 1990).

From the results cited above, several consistencies with our results can be found. Firstly, the structural features of the alginate-based capillary hydrogels were big enough to allow Schwann cell migration and axonal ingrowth. Secondly, the capillary sizes in the range of 20-35  $\mu\text{m}$  resulted in a higher degree of axonal orientation compared to larger capillary sizes. However, the structure of the cellular and axonal profiles found in the larger capillaries resembled the structure of a native nerve bundle much more closely.

Various studies were conducted to repair spinal cord injury *in vivo* by using different scaffolds. Many natural and artificial materials have been used in spinal cord injury repair.

The scaffolds used were made from natural polymer includes collagen or an alginate hydrogel. Alginate sponge made by freeze drying technique implanted into complete spinal cord transaction of infant or young rats stimulated the ingrowth of numerous myelinated and unmyelinated fibres; some of the axons were accompanied by astrocytic processes into hydrogels (Kataoka K *et al.* 2001, 2004, Suzuki K *et al.* 1999) as well as functional projections cross the gap and formed synaptic connections with host neurons on the other side (Suzuki Y *et al.* 2002) Self assembling collagen hydrogels prepared *in situ* by injection of fluid collagen solution into the mid-thoracic rat spinal cord lesion site allowed ingrowth of specifically labelled corticospinal axons and astroglial and microglial cells were also observed to invade the hydrogels (Joosten EA *et al.* 1995).

Hydrogels based on poly(2-hydroxyethyl methacrylate) (PHEMA) and poly N-(2-hydroxypropyl)-methacrylamide (PHPMA) belong to a group of synthetic biocompatible polymers, having various morphologies with and without modification were used for spinal cord repair. Modifying surface charge of the hydrogel using copolymer and polyelectrolyte enhances its mechanical properties. (Pradny M *et al.* 2005), another approach to improve axonal regeneration was studied to adjust the adhesion properties of the hydrogels. PHPMA hydrogels modified with an attached oligopeptide sequence (RGD) showed stronger adhesion to the host tissue and promoted the ingrowth of astrocytes and neurofilaments inside the hydrogel (Woerly S *et al.* 1995). Scaffold implantation combining with neurotrophic factors or stem cell treatment improved regeneration in spinal cord injury. PHPMA-RGD hydrogels modified with either brain derived neurotrophic factor (BDNF) or ciliary neurotrophic factor (CNTF) significantly increased the ingrowth of axons into the implant compared to unmodified hydrogels (Yu X *et al.* 1999, Loh NK *et al.* 2001). Hollow tubes of p(HEMA-MMA) with combination of various matrices and growth factor were implanted into the completely transected rat spinal cord and promoted axon growth into the tube. Astroglia surrounded the tube, but did not enter into it (Tsai EC *et al.* 2006). Poly(D,L-lactic acid) macroporous guidance scaffolds containing BDNF showed axon ingrowth and the survival of adjacent neurons in the rostral and caudal host spinal cord were increased but astroglia was not found to enter the scaffolds (Patist CM *et al.* 2004). Inhibition of astrogliosis and inflammation promotes spinal cord repair. Triptolide was shown to prevent astrocytes from reactive activation by blocking the JAK2/STAT3 pathway *in vitro* and *in vivo* (Su Z *et al.* 2010).



The implantation of alginate hydrogels into rat spinal cord defects *in vivo* showed the same effect on axon outgrowth as it was found in the *in vitro* tests in that microchannels of wider capillaries and microchannels with gelatin constituents showed enhanced axonal regeneration. Another finding was that astrocyte migration into ACH scaffolds was limited. Immunohistochemistry revealed that GAP-43 and NF-200 labelled axons were found in all type of microchannel scaffolds, but only very few GFAP processes were entered into the capillaries but mostly surrounded along the scaffolds. This finding about astrocytes didn't affect the axon ingrowth into the capillaries. Transplantation of astrocyte of developmentally immature phenotype promotes tissue sparing and axonal regeneration (White RE *et al.* 2008).

The influence of the presence of a gelatin constituent within the alginate hydrogels on axon regeneration was not so clear than the dependency on the capillary size. In most instances we found longer axons, a higher axon density and a higher Schwann cell density in hydrogels containing gelatin but this effect seemed to be more pronounced in gels exhibiting larger capillary diameters. We found the same effect of gelatin constituent on axon density and astrocyte density in slice culture systems. Since the addition of gelatin lead to an increase in the capillary diameter especially for gels made with zinc cations, it is not so clear if the positive influence is of biochemical origin due to the adhesion mediating properties of gelatin or if it is more a result of the larger capillary diameter. To answer this question, subsequent studies using hydrogels with microchannels of equal size, which will be modified with adhesion mediating molecules like gelatin or laminin after gel formation was finished, will be conducted. Further investigations regarding the influence of the capillary diameter on axonal regeneration in the central nervous system are also undertaken currently.

## **5.2 Conclusion**

Hydrogels are currently used in a wide range of biomedical applications because of their tissue-like mechanical and physicochemical properties. In our group we use a novel kind of alginate-based hydrogels containing linearly aligned capillaries of defined and variable sizes to promote axonal regeneration after nerve injury in a highly oriented fashion. We found robust ingrowth of peripheral nerve axons from dorsal root ganglia in all types of gels with capillary diameters ranging between 10 and 54  $\mu\text{m}$ . A higher degree of orientation but thinner axonal profiles were found in capillaries of 20-35  $\mu\text{m}$  in diameter, whereas a lower degree of orientation but larger axonal bundles were observed in capillaries of 55-80  $\mu\text{m}$  in diameter.

We also found robust ingrowth of central nerve axons from spinal cord slice culture and entorhinal cortex slice culture in all types of gels with capillary diameter of 11-89  $\mu\text{m}$ . Also the *in vivo* investigations showed axon outgrowth into all type of scaffolds. The adjustable properties of the alginate-based capillary hydrogels shown in the present study makes this system highly valuable to test axonal regeneration *in vitro* and *in vivo*, for example after modification with adhesion molecules, release systems for neurotrophic factors or certain cell populations, but it can also represent a clinically relevant regenerative strategy in order to elicit substantial functional recovery in patients suffering from nerve injury.

## References:

- Belkas JS, Shoichet MS, Midha R. Peripheral nerve regeneration through guidance tubes. *Neurol Res* 2004;26:151-60.
- Bellamkonda R, Aebischer P. Review: tissue engineering in the nervous system. *Biotech Bioeng* 1994;43:543-54.
- Bellamkonda RV. Peripheral nerve regeneration: an opinion on channels, scaffolds and anisotropy. *Biomaterials* 2006;27:3515-8.
- Bonnici B and Kapfhammer JP. Spontaneous regeneration of intrinsic spinal cord axons in a novel spinal cord slice culture model. *European Journal of Neuroscience* 2008;27:2483-92.
- Bozkurt A, Deumens R, Beckmann C, Olde Damink L, Schügner F, Heschel I, Sellhaus B, Weis J, Jahnen-Dechent W, Brook GA, Pallua N. *In vitro* cell alignment obtained with a Schwann cell enriched microstructured nerve guide with longitudinal guidance channels. *Biomaterials* 2009;30:169-79.
- Bracken MB, Shepard MJ, Collins WF, Holford TR, Young W, Baskin DS, Eisenberg HM, Flamm E, Leo-Summers L, Maroon J, et al. A randomized, controlled trial of methylprednisolone or naloxone in the treatment of acute spinal cord injury: results of the second national acute spinal cord injury study. *N Engl J Med* 1990;322:1405-11.
- Clements IP, Kim Y, English AW, Lu X, Chung A, Bellamkonda RV. Thin-film enhanced nerve guidance channels for peripheral nerve repair. *Biomaterials* 2009;30:3834-46.
- Eljaouhari AA, Müller R, Kellermeier M, Heckmann K, Kunz W. New anisotropic ceramic membranes from chemically fixed dissipative structures. *Langmuir* 2006;22:11353-9.
- Filous AR, Miller JH, Coulson-Thomas YM, Horn KP, Alilain WJ, Silver J. Immature astrocyte promotes CNS axonal regeneration when combined with chondroitinase ABC. *Dev Neurobiol* 2010;999A.
- Fine EG, Valentini RF, Aebischer P. Nerve Regeneration. In: Lanza RP, Langer R, Vacanti J, editors. *Principles of tissue engineering*. San Diego, CA: Academic Press; 2000. 785-97.
- Flynn L, Dalton PD, Shoichet MS. Fiber templating of poly(2-hydroxyethyl methacrylate) for neural tissue engineering. *Biomaterials* 2003;24:4265-72.
- Hassan RM. Alginate polyelectrolyte ionotropic gels. Part III. Kinetics of exchange of chelated divalent transition metal cations especially cobalt(II) and copper(II) by

- hydrogen ions in capillary ionotropic alginate polymembrane gels. *J Mater Sci* 1991;26:5806-10.
- Huang JH, Cullen DK, Browne KD, Groff R, Zhang J, Pfister BJ, Zager EL, Smith DH. Long-term survival and integration of transplanted engineered nervous tissue constructs promotes peripheral nerve regeneration. *Tissue Eng A* 2009;15:1677-85.
- Johansson F, Carlberg P, Danielsen N, Montelius L, Kanje M. Axonal outgrowth on nano-imprinted patterns. *Biomaterials* 2006;27:1251-8.
- Joosten EA, Bar PR, Gispén WH. Collagen implants and cortico-spinal axonal growth after mid-thoracic spinal cord lesion in the adult rat. *J Neurosci Res* 1995;41:481-90.
- Kataoka K, Suzuki Y, Kitada M, Hashimoto T, Chou H, Bai H, et al. Alginate enhances elongation of early regenerating axons in spinal cord of young rats. *Tissue Eng* 2004;10:493-504.
- Kataoka K, Suzuki Y, Kitada M, Ohnishi K, Suzuki K, Tanihara M, et al. Alginate, a bioresorbable material derived from brown seaweed, enhances elongation of amputated axons of spinal cord in infant rats. *J Biomed Mater Res* 2001;54:373-84.
- Kathryn JH, Alan NB, Anne E, King A. Model of organotypic rat spinal cord slice culture and biolistic transfection to elucidate factors that drive the preprotachykinin-A promoter. *Brain res rev* 2004;46:191-203.
- Kluge A, Hailer NP, Horvath TL, Bechmann I, Nitsch R. tracing of the entorhinal-hippocampal pathway *in vitro*. *Hippocampus* 1998;8:57-68.
- Lee Yu-Shang, Baratta J, Yu J, Lin VW, Robertson RT. aFGF promotes axonal growth in rat spinal cord organotypic slice co-cultures. *J Neurotrauma* 2002;19:357-67.
- Li D, Field PM, Yoshioka N, Raisman G. Axons regenerate with correct specificity in horizontal slice culture of the postnatal rat entorhino-hippocampal system. *EJN* 1994;6:1026-37.
- Li N, Folch A. Integration of topographical and biochemical cues by axons during growth on microfabricated 3-D substrates. *Exp Cell Res* 2005;311:307-16.
- Li X, Liu T, Song K, Yao L, Ge D, Bao C, Ma X, Cui Z. Culture of neural stem cells in calcium alginate beads. *Biotechnol. Prog.* 2006;22:1683-9.
- Loh NK, Woerly S, Bunt SM, Wilton SD, Harvey AR. The regrowth of axons within tissue defects in the CNS is promoted by implanted hydrogel matrices that contain BDNF and CNTF producing fibroblast. *Exp Neurol* 2001;170:72-84.

- Mahoney MJ, Chen RR, Tan J, Saltzman WM. The influence of microchannels on neurite outgrowth and architecture. *Biomaterials* 2005;26:771-8.
- Midha R. Emerging techniques for nerve repair: nerve transfers and nerve guidance tubes. *Clin Neurosurg* 2006;53:185-90.
- Miller C, Shanks H, Witt A, Rutkowski G, Mallapragada S. Oriented Schwann cell growth on micropatterned biodegradable polymer substrates. *Biomaterials* 2001;22:1263-9.
- Mingorance A, Sole M, Muneton V, Matrinez A, Nieto-Sampedro M, Soriano E, Antonio del Rio J. regeneration of lesioned entorhino-hippocampal axons *in vitro* by combined degeneration of inhibitory proteoglycans and blockade of Nogo-66/NgR signaling. *FASEB J* 2006;20:491-3.
- Mollers S, Heschel I, Damink LH, Schugner F, Deumens R, Muller B, et al. Cytocompatibility of a novel, longitudinally microstructured collagen scaffold intended for nerve tissue repair. *Tissue Eng Part A* 2009;15:461-72.
- Novikova LN, Pettersson J, Brohlin M, Wiberg M, Novikov LN. Biodegradable poly- $\beta$ -hydroxybutyrate scaffold seeded with Schwann cells to promote spinal cord repair. *Biomaterials* 2008;29:1198-1206.
- Olson H, Rooney G, Gross L, Nesbitt J, Galvin K, Knight A, Chen B, Yaszemski M, Winderbank A. Neural stem cell and Schwann cell loaded biodegradable polymer scaffolds support axonal regeneration in the transected spinal cord. *Tissue eng. A* 2009;15:1797-805.
- Pradny M, Lesny P, Smetana K, Vacik J, Slouf M, Michalek J, Sykova E. Macroporous hydrogels based on 2-hydroxyethyl methacrylate. Part II. Copolymers with positive and negative charges, polyelectrolyte complexes. *J Mater Sci Mater Med* 2005;16:767-73.
- Prang P, Del Turco D, Kapfhammer JP. Regeneration of entorhinal fibers in mouse slice cultures is age dependant and can be stimulated by NT-4, GDNF, and modulators of G-proteins and protein kinase C. *Exp neurol* 2001;169:135-47.
- Prang P, Del Turco D, Deller T. Association sprouting in the mouse fascia dentate after entorhinal lesion *in vitro*. *Brain res* 2003;978:205-12.
- Prang P, Muller R, Eljaouhari A, Heckmann K, Kunz W, Weber T, et al. The promotion of oriented axonal regrowth in the injured spinal cord by alginate-based anisotropic capillary hydrogels. *Biomaterials* 2006;27:3560-9.
- Patist CM, Mulder MB, Gautier SE, Maquet V, Jerome R, Oudega M. Freeze-dried poly(D,L-lactic acid) macroporous guidance scaffolds impregnated with brain-derived

- neurotrophic factor in the transected adult rat thoracic spinal cord. *Biomaterials* 2004;25:1569-82.
- Radojevic V, Kapfhammer JP. Repair of the entorhino-hippocampal projection *in vitro*. *Exp neurol* 2004;188:11-9
- Ribeiro-Resende VT, Koenig B, Nichterwitz S, Oberhoffer S, Schlosshauer B. Strategies for inducing the formation of bands of Büngner in peripheral nerve regeneration. *Biomaterials* 2009;30:5251-9.
- Sarig-Nadir O, Livnat N, Zajdman R, Shoham S, Seliktar D. Laser photoablation of guidance microchannels into hydrogels directs cell growth in three dimensions. *Biophys J* 2009;96:4743-52.
- Schmidt CE, Baier LJ. Neural tissue engineering: strategies for repair and regeneration. *Annu Rev Biomed Eng* 2003;5:293-347.
- Schnell E, Klinkhammer K, Balzer S, Brook G, Klee D, Dalton P, Mey J. Guidance of glial cell migration and axonal growth on electrospun nanofibers of poly- $\epsilon$ -caprolactone and a collagen/ poly- $\epsilon$ -caprolactone blend. *Biomaterials* 2007;28:3012-25.
- Shichinohe H, Kuroda S, Tsuji S, Yagamuchi S, Yano S, Lee J, Kobayashi H, Kikuchi S, Hida K, Iwasaki Y. Bone marrow stromal cells promote neurite extension in organotypic spinal cord slice: significance for cell transplantation therapy. *Neurorehabil neural repair* 2008;22:447-57.
- Stokols S, Tuszynski MH. Freeze-dried agarose scaffolds with uniaxial channels stimulate and guide linear axonal growth following spinal cord injury. *Biomaterials* 2006b;27:443-51.
- Su Z, Yuan Y, Cao L, Zhu Y, GAO I, Qiu Y, He C. Triptolide promotes spinal cord repair by inhibiting astrogliosis and inflammation. *Glia* 2010;58:901-15.
- Sundback C, Hadlock T, Cheney M, Vacanti J. Manufacture of porous polymer nerve conduits by a novel low-pressure injection molding process. *Biomaterials* 2003;24:819-30.
- Suzuki K, Suzuki Y, Ohnishi K, Endo K, Tanihara M, Nishimura Y. Regeneration of transected spinal cord in young adult rats using freeze dries alginate gel. *NeuroReport* 1999;10:2891-4.
- Suzuki Y, Kitaura M, Wu S, Kataoka K, Suzuki K, Endo K, Nishimura Y, Ide C. Electrophysiological and horseradish peroxidase-tracing studies of nerve regeneration through alginate-filled gap in adult rat spinal cord. *Neurosci Lett* 2002;318:121-4.

- Thiele H. Histolyse und Histogenese – Gewebe und ionotrope Gele – Prinzip einer Strukturbildung. Frankfurt, Germany: Akademische Verlagsgesellschaft; 1967.
- Thiele H, Andersen G. Ionotrope Gele von Polyuronsäuren. 2. Ordnungsgrad. *Kolloid Z* 1955;142:5-24.
- Thiele H, Hallich K. Kapillarenstrukturen in ionotropen Gelen. *Kolloid Z* 1957;151:1-12.
- Tsai EC, Dalton PD, Shoichet MS, Tator CH. Matrix inclusion within synthetic hydrogel guidance channels improves specific supraspinal and local axonal regeneration after complete spinal cord transection. *Biomaterials* 2006;27:519-33.
- Tsuji S, Kikuchi S, Shinpo K, Tashiro J, Kishimoto R, Yabe I, Yagamishi S, Takeuchi M, Sasaki H. Proteasome inhibition induces selective motor neuron death in organotypic slice cultures. *J Neurosci Res* 2005;82:443-51.
- Tucker BA, Mearow KM. Peripheral sensory axon growth: from receptor binding to cellular signaling. *Can J Neurol Sci* 2008;35:551-66.
- Wang A, Ao Q, Cao W, Yu M, He Q, Kong L, et al. Porous chitosan tubular scaffolds with knitted outer wall and controllable inner structure for nerve tissue engineering. *J Biomed Mater Res A* 2006;79:36-46.
- White RE, Jakeman LB. Don't fence me in: harnessing the beneficial roles of astrocytes for spinal cord repair. *Restor. Neurol Neurosci* 2008;26:197-214.
- Willenberg BJ, Hamazaki T, Meng F, Terada N, Batich C. Self-assembled copper-capillary alginate gel scaffolds with oligochitosan support embryonic stem cell growth. *J. Biomed. Mater. Res. Part A* 2006;79:440-50.
- Wong JWJ, Brastianos HC, Andersen RJ, O'Connor TP. A high-throughput screen to identify novel compounds to promote neurite outgrowth. *J Neurosci Meth* 2008;169:34-42.
- Woerly S, Laroche G, Marchand R, Pato J, Subr V, Ulbrich K. Intracerebral implantation of hydrogel coupled adhesion peptides: tissue reaction. *J Neural Transplant Plast* 1995;5:245-55.
- Yu X, Dillon GP, Bellamkonda RB. A laminin and nerve growth factor-laden three-dimensional scaffolds for enhanced neurite extension. *Tissue Eng* 1999;5:291-304.
- Zhang N, Zhang C, Wen X. Fabrication of semipermeable hollow fiber membranes with highly aligned texture for nerve guidance. *J Biomed Mater Res* 2005;75.

# **Appendix**





## List of Abbreviations

2D	Two dimensional
3D	Three dimensional
ACH	anisotropic capillary hydrogel
BBB	Basso, Beattie, Bresnahan locomotor scale
BCA	bicinchoninic acid-protein quantification assay
BSA	bovine serum albumin
BDNF	brain-derived neurotrophic factor
b-FGF	basic fibroblast growth factor
CNS	central nervous system
CNTF	ciliary derived neurotrophic factor
CPS	cryo protectant solution
DMEM	dulbecco's modified eagle medium
DP	degree of polymerization
DRIFT	diffuse reflection infrared fourier transform
DRG	dorsal root ganglion
EC	Entorhinal cortex
ECM	extracellular matrix
EDTA	Ethylenediamine tetraacetic acid
EGF	Epidermal growth factor
ELISA	enzyme-linked immunosorbent assay
ESC	embryonic stem cell
FCS	fetal calf serum
FGF	Fibroblast growth factor
FITC	Fluorescein isothiocyanate
FN	fibronectin
FTIR	Fourier-transformed infrared spectroscopy
FSGB	fish skin gelatine buffer
gACH	gelatin modified alginate hydrogel
gACHBa	gelatin modified barium alginate hydrogel
gACHCu	gelatin modified copper alginate hydrogel
gACHSr	gelatin modified strontium alginate hydrogel
gACHZn	gelatin modified zinc alginate hydrogel
GAP-43	growth associated protein 43
GFAP	glial fibrillary acidic protein
GLU	glutaraldehyde

GUA	guanidine
HDI	hexamethylene diisocyanate
HSA	human serum albumin
ICP-AES	inductively coupled plasma atomic emission spectroscopy
IGF	insulin-like growth factor
IKVAV	isoleucine-lysine-valine-alanine-valine
LA	Lactic acid
LN	Laminin
MBP	Myelin basic protein
MEM	Minimum essential medium
MSC	mesenchymal stem cells
NF	neurofilament
NGF	neural growth factor
NHS	N-hydroxysuccinimide
NPC	Neural progenitor cell
NT-3	Neurotrophin-3
PA	peptide amphiphile
pACH	pure alginate hydrogel
pACHBa	pure barium alginate hydrogel
pACHCu	pure copper alginate hydrogel
pACHSr	pure strontium alginate hydrogel
pACHZn	pure zinc alginate hydrogel
PBS	phosphate-buffered saline
PDL	poly-D-lysine
PE	polyethylene
PEG	poly(ethylene glycol)
PFA	paraformaldehyde
PGA	poly(glycolic acid)
pHEMA	poly(hydroxyethyl methacrylate)
pHPMA	poly[N-(2-hydroxypropyl) methacrylamide]
PLA	poly(lactic acid)
PLGA	poly(lactic-co-glycolic acid)
PNS	peripheral nervous system
PTFE	polytetrafluoroethylene
RGD	arginine-glycine-aspartic acid oligopeptide
RHOX	Rhodamine X

SVZ	sub ventricular zone
TBS	tris-buffered saline
TCPS	traditional tissue culture polystyrene
TGF- $\beta$	transforming growth factor $\beta$
YIGSR	tyrosine-isoleucine-glycine-serine-arginine (adhesion peptide)



# Curriculum vitae

## Personal information

**Name:** Kiran Chandrakantrao Pawar

**Date of birth:** 15 June 1980

**Place of birth:** Loha-Nanded

**Nationality:** Indian

**Marital status:** Single

## Education

**Since 04/2007** Doctoral researcher  
University of Regensburg

**2006-2003** Project Assistant-II  
National Chemical Laboratory (NCL) Pune, India.

**2002-2000** Master of science (M.Sc.) (Chemistry)  
S.R.T.M. University Nanded, India.

**2000-1997** Bachelor of science (B.Sc.)  
S.R.T.M. University Nanded, India.

## Academic Honors

1. 2007, “*Graduate Research Fellowship*” for Ph.D. from Bayerische Forschungsstiftung (BFS) Germany.
2. 2004, Qualified “*Graduate Aptitude Test in Engineering*” (GATE), conducted by Indian Institute of Technology (IIT) Delhi, India.
3. 2003, Qualified “*State Eligibility Test*” (SET) for Lectureship, conducted by the University of Pune, Government of Maharashtra, India.

## Publications

### Papers

1. Shubhangi Nair, **Kiran Pawar**, Jyoti Jog, Manohar Badiger. “Swelling and Mechanical Behavior of Modified Poly(vinyl alcohol)/Laponite Nanocomposite Membranes” *Journal of Applied Polymer Science*, **2007** Vol. 103, 2896-2903.
2. **Kiran Pawar**, Rainer Mueller, Massimiliano Caioni, Ulrich Boghdan, Werner Kunz, Norbert Weidner. “Influence of capillary diameter in alginate-based anisotropic capillary hydrogels on oriented axon regeneration and Schwann cell migration” (*Manuscript in Preparation*).
3. **Kiran Pawar**, Rainer Mueller, Peter Prang, Claudia Rotter, Norbert Weidner. “Anisotropic capillary hydrogel scaffolds guide Neurite migration from in vitro slice cultures and in vivo spinal cord lesion” (*Manuscript in Preparation*).

### Book chapter

1. Rainer Mueller, Irene Ferreira, **Kiran Pawar**, Norbert Weidner. Application of hydrogels to rewire the injured spinal cord. In: D.B. Stein, editor. Handbook of hydrogels: Properties, preparation and applications. Nova Science Publishers, Hauppauge, NY, in press.

### Citationable abstracts

1. Rainer Mueller, **Kiran Pawar**, Norbert Weidner. Oriented axon outgrowth from dorsal root ganglia guided by anisotropic capillary hydrogels. *Regenerative Medicine* 2009;4:122-3.
2. Rainer Mueller, **Kiran Pawar**, Norbert Weidner. Alginate-based anisotropic hydrogels as scaffolds for guided axon regeneration. *Tissue Engineering A* 2009;15:717-8.
3. Rainer Mueller, **Kiran Pawar**, Peter Prang, M. Kellermeier, Norbert Weidner. Anisotropic hydrogels with defined capillary diameters as guiding structures for directed axonal regrowth. *BIOmaterialien* 2007;8:163.

### Posters

1. Norbert Weidner, **Kiran Pawar**, Rainer Mueller, Massimiliano Caioni. Directed CNS axon regeneration through anisotropic alginate-based hydrogels. 6<sup>th</sup> FENS Forum of European Neuroscience. Geneva, Switzerland 2008.
2. Rainer Mueller, **Kiran Pawar**, Norbert Weidner. Alginate-based anisotropic hydrogels as scaffolds for guided axon regeneration. BioStar Congress 2008, 3<sup>rd</sup> Congress on Regenerative Biology and Medicine. Stuttgart, Germany 2008.
3. Irene Ferreira, **Kiran Pawar**, Rainer Mueller, Francisco Rivera, Massimiliano Caioni, Norbert Weidner. Combining alginate based anisotropic hydrogel and adult neural progenitor cells for spinal cord repair. 10<sup>th</sup> international congress on neural transplantation and repair. Freiburg, Germany 2008.





## Acknowledgement

This work was carried out from April 2007 until July 2010 in the Department of Neurology in collaboration with Department of Physical and Theoretical Chemistry of the University of Regensburg. I would like to thank all the people of these two departments.

First of all I would like to thank Prof. Dr. Ulrich Bogdahn and Prof. Dr. Werner Kunz for giving me the opportunity to work on this project under the supervision of their departments.

My warmest thanks are addressed to Prof. Dr. Norbert Weidner and Dr. Rainer Mueller. I had the great privilege to have both of them as my supervisors during my research activities and as source of encouragement to conduct my research. My special thanks to Massimiliano Caioni for teaching me all the techniques I used throughout my research work. I also thank Peter Prang for teaching me slice culture technique.

I like to thank my entire lab mates for their support and making my time in and outside the lab most enjoyable. I also like to thank Irene and Claudia for doing their thesis work with me and providing helpful contribution to my thesis. I like to thank Anu Singh for her initial help in Regensburg. Friends have always been my strength and it is delight to acknowledge all those who have been with me for various periods of time from NCL Pune and Regensburg Germany. I take this opportunity to acknowledge one and all.

I like to thank Bayerische Forschungsförderung (BFS) for giving me financial support.

The achievement made in my life was a dream of my parents, which came true. I am thankful to my parents (Mai, Kakaji) and my family for being always with me and giving me the right direction in my life. I am really inspired by my father, by his hard work and my loving mother, my brother Dr. Arun, sister-in-law Priyanka, Aditya and Arundhati (my nephew and niece) and my sisters and brothers-in-law. My special thanks to Lena for her mental support, love and understanding, which was very essential for the success of this thesis.



## **Declaration**

Herewith, I declare that I have made the present work on my own, and that I have only used the quoted utilities.

Regensburg

